THE
PHYSICAL REVIEW
A journal of experimental and theoretical physics established by E. L. Nichols in 1893

SECOND SERIES, VOL. 63, NOS. 1 AND 2 JANUARY 1 AND 15, 1943

The Relativistic Theory of Excited Spin States of the Proton and the Neutron

V. L. GINSBURG
P. N. Lebedev Physical Institute of the Academy of Sciences of U.S.S.R., Moscow, U.S.S.R.
(Received March 31, 1942)

The existing theory gives the cross section for the process of scattering of mesons by heavy particles (i.e., the protons and the neutrons), which increases with energy and is thus contradictory to experimental data as well as to a number of general principles. This increase must be explained as a result of the neglect of the reaction of the proper field of the particle's quasi-magnetic moment on the motion of this moment. If the proper field is taken into account in a quantum mechanical case, we are naturally led to the necessity of supposing that the proton and the neutron possess excited states of spin $\frac{3}{2}$ and even greater. In the present paper, the relativistic theory for the particle capable of being in the state with spin $\frac{1}{2}$ and the rest mass m_1, as well as in the state with spin $\frac{3}{2}$ and the rest mass $m_2 > m_1$ is developed. It is shown that the cross section for the scattering of light (of mesons) by the magnetic (by the quasi-magnetic) moment of such a particle increases at first with energy, as in the usual theory. However, for photons with energies $h\nu \gg (m_2 - m_1)c^2$ the cross section becomes constant (the recoil for the heavy particle being neglected). Therefore, the introduction of the higher spin states, which is adequate to account for the proper field of the particle's moment, offers the possibility of treating consistently the interaction of the magnetic moment with radiation by the usual perturbation theory methods.

1. INTRODUCTION

AS is well known, the cross section for the scattering of mesons by heavy particles (the protons and the neutrons), as calculated in the usual way, increases with energy indefinitely. Such an increase of the cross section, however, is contradictory to experimental data as well as to some very general principles of the theory.[1,2] This situation is due to the fact that the reaction of the proper field of the scattering particle on its motion is not taken into account in the usual quantum mechanical perturbation method. Consequently, the variation of the spin direction of the heavy particle, as well as the variation of its charge, takes place too freely, thus causing an unlimited increase of the scattering cross section.[3] Heisenberg emphasized[3] the occurrence of a similar situation in the classical theory of light scattering by the magnetic moment. In this case, the cross section at first increases as ν^2, ν being the frequency of the scattered radiation. The same result is obtained in a quantum theory of the type of the Pauli theory, in which

$$H = (p^2/2m) - \mu_0(\boldsymbol{\sigma}\mathbf{H})$$

is used for the energy operator, where the vector $\boldsymbol{\sigma}$ has the usual Pauli spin matrices as components. Finally, a cross section of a similar type results from a non-relativistic approximation of the light scattering by a particle which obeys the Dirac equation including a "true" magnetic

[1] W. Heisenberg, Reports of the Solvay Conference (1939).
[2] L. Landau, J. Phys. (U.S.S.R.) **2**, 485 (1940). *Editor's note:* See also H. J. Bhabha and H. C. Corben Proc. Roy. Soc. **A178**, 273 (1941); H. J. Bhabha, Proc. Roy. Soc. **A178**, 314 (1941).
[3] W. Heisenberg, Zeits. f. Physik **113**, 61 (1939).

moment:

$$\gamma_k\frac{\partial\psi}{\partial x_k}+\kappa\psi+\mu_0\frac{\gamma_i\gamma_k}{2i}F_{ik}\psi=0.$$

Here γ_i denotes the usual matrices of Dirac's theory and F_{ik} is the electromagnetic field tensor. It is exactly an equation of such a type that is used in the theory of the interaction of mesons with heavy particles (F_{ik} then being replaced by the corresponding meson field tensor).

If, however, the reaction of the magnetic moment proper field on the motion of this moment is taken into account in the classical theory, a constant value of the scattering cross section is obtained for high frequencies. This suggests the possibility of a similar account of the proper field in the quantum mechanics.

We shall begin the investigation of the problem with a more detailed consideration of the self-reaction of the moment in the classical theory.[4,5] Let us consider the motion of the moment of an uncharged, magnetized particle, its mass center being at rest. Let us assume the magnetization of the particle $\mathbf{M}=\boldsymbol{\mu}D(\mathbf{r})$, where $\boldsymbol{\mu}$ is the total magnetic moment and $D(\mathbf{r})$ the form factor ($\int D(\mathbf{r})dv=1$). The set of equations of motion runs as follows:

$$\frac{d\mathbf{s}}{dt}=[\boldsymbol{\mu}\mathbf{H}_{ext}]+\int[\boldsymbol{\mu}\mathbf{H}(\mathbf{r})]D(\mathbf{r})dv, \qquad (1)$$

$$\Box\mathbf{A}=-4\pi\ \mathrm{rot}\ \mathbf{M},\quad \mathrm{rot}\ \mathbf{A}=\mathbf{H},$$

$\mathbf{H}_{ext}$ is the external magnetic field, $\mathbf{s}$ is the angular momentum of the particle.

It is possible to eliminate the field $\mathbf{H}$ from Eq. (1) in the general case. If one neglects inessential terms,[4,5] the following equation for $\mathbf{s}$ results:

$$d\mathbf{s}/dt=[\boldsymbol{\mu}H_{ext}]-(4\nu_m/3\pi c^3)[\boldsymbol{\mu}(d^2\boldsymbol{\mu}/dt^2)]+(2/3c^3)[\boldsymbol{\mu}(d^3\boldsymbol{\mu}/dt^3)]. \qquad (2)$$

Here ν_m stands for the frequency which cuts off the Fourier spectrum of the proper field acting on the particle. Evidently, $\nu_m\sim c/r_0$, in which r_0 is the radius of the particle. Equation (2) should be supplemented by another one, which connects the vectors $\boldsymbol{\mu}$ and $\mathbf{s}$ with each other. We put, as usual, $\boldsymbol{\mu}=\kappa\mathbf{s}$. It will be seen later on that $\mathbf{s}$ subsequently ceases to play the part of the total angular momentum. The total angular momentum of the particle is the sum of the mechanical angular momentum $\mathbf{s}$ and of the angular momentum $(4\nu_m\kappa^2/3\pi c^3)[\mathbf{s}(d\mathbf{s}/dt)]$, the latter being of magnetic nature (see below). The term $\mathbf{R}=(2/3c^3)[\boldsymbol{\mu}(d^3\boldsymbol{\mu}/dt^3)]$ in Eq. (2) is dissipative and corresponds to the well-known radiation force $(2e^2/3c^3)(d^3\mathbf{r}/dt^3)$, which appears for the translatory motion of the charged particle. The term $\mathbf{L}=-(4\nu_m/3\pi c^3)[\boldsymbol{\mu}(d^2\boldsymbol{\mu}/dt^2)]$, which quantitatively exceeds $\mathbf{R}$ considerably (if $H\sim\cos\nu t$ then $R/L\sim\nu/\nu_m$), does not disturb the conservative character of the motion described by Eq. (2). This term alters essentially the equation of motion for the spin of the particle, as compared to that of which use is ordinarily made. In fact, the equation of motion for the spin is usually taken as

$$(d\mathbf{s}/dt)=\kappa[\mathbf{s}\mathbf{H}_{ext}] \qquad (3)$$

while, if the dissipative term is omitted, Eq. (2) gives:

$$(d\mathbf{s}/dt)=\kappa[\mathbf{s}\mathbf{H}_{ext}]-(4\nu_m\kappa^2/3\pi c^3)[\mathbf{s}(d^2\mathbf{s}/dt^2)]. \qquad (4)$$

Equation (4) is the intrinsic equation for the symmetrical spinning top. It reduces to Eq. (3) if $\mathbf{L}$ is neglected. It is precisely because of this neglect, characteristic of the usual theory of spin, that the angular momentum equals $\mathbf{s}$ and $\mathbf{s}^2=\mathrm{const}$. Equation (4) is equivalent to the set of equations

$$d\boldsymbol{\sigma}/dt=\kappa[\mathbf{s}\mathbf{H}_{ext}];\quad d\mathbf{s}/dt=-\alpha[\mathbf{s}\boldsymbol{\sigma}];\quad \alpha=3\pi c^3/4\nu_m\kappa^2 s^2. \qquad (5)$$

Hence, considering the case of the absence of the field, we may conclude that for the particle obeying Eq. (4) the total angular momentum is not $\mathbf{s}$ but $\mathbf{s}+(4\nu_m\kappa^2/3\pi c^3)[\mathbf{s}(d\mathbf{s}/dt)]$. It may be readily shown that in the presence of an external magnetic field the quantity σ^2 is not constant, and it is the quantity $\sigma^2-(2\kappa/\alpha)(\mathbf{sH})$ which is conserved. In the case of scattering of light, Eq. (3) leads to the cross section which increases as ν^2 (for detailed calculations see I). Of course, the

[4] V. L. Ginsburg, J. Phys. 5, 47 (1941).
[5] V. L. Ginsburg, Comptes rendus Acad. Sci. U.R.S.S. 31, 319 (1941). Further it is referred to as I.

same result may be obtained from Eq. (4), unless the term **L** ceases to be small. If, for example, we put $\kappa=e/mc$, $\nu_m=c/r_0=mc^3/e^2$, $\mu=\kappa h$ this term becomes of the same order as ds/dt when $\lambda=c/\nu\sim h/mc$. For the same suppositions concerning κ, ν_m, and μ, the term R becomes of the order of ds/dt only when $\lambda\sim e^2/mc^2$. If $\lambda\ll h/mc$ the cross section attains a constant value which is approximately r_0^2.

The above results show that the account of the proper field of the magnetic moment automatically leads to the substitution of Eq. (3) by Eq. (4), i.e., to the necessity of taking into account the variation of the angular momentum of the particle when it is in the field. Being inessential for low frequencies, this fact changes fundamentally the character of the motion for high frequencies of the perturbing force, as is clear if the scattering is considered as an example.

Going over to the quantum mechanics we conclude that the account of the proper field will be secured if Eq. (4), or the set of Eqs. (5) will be taken as the operator equation for the spin instead of Eq. (3), as is done in the Pauli theory. As is clear from the above considerations, in this case the spin of the particle will no longer be constant. On the contrary, the particle will be considered as a spinning top, and in the case of half-integral spin it will acquire the ability of being in the states with spins $\frac{1}{2}$, $\frac{3}{2}$, $\frac{5}{2}$, etc. Owing to the presence of the field, transitions between states of different spins must take place. Hence, the account of the proper field of the particles' moment, with no assumption *ad hoc*, leads to the conclusion that the elementary particles possess states with different spins. As should be expected, the quantum mechanical theory (see I), based on this supposition, results in the cutting off of the cross section for the scattering and therefore is adequate for the basic classical ideas. After obtaining these results, the author found out that the hypothesis of higher spin states had already been proposed by Heitler and developed by Heitler and Ma.[6] The vectors $\boldsymbol{\sigma}$ and **s**, introduced by these authors, satisfy Eqs. (5) if the natural substitution of $\{[\mathbf{s}\boldsymbol{\sigma}]-[\boldsymbol{\sigma}\mathbf{s}]\}\cdot\frac{1}{2}$ for $[\mathbf{s}\boldsymbol{\sigma}]$ is performed. These equations themselves may be obtained from the Hamiltonian

$$H=\tfrac{1}{2}\alpha\sigma^2-\kappa(\mathbf{sH})$$

if the commutation rules accepted by Heitler and Ma are used.

The above considerations as well as the Heitler and Ma theory are non-relativistic, and consequently can have only heuristic significance. Therefore, the theory of excited spin states asks for a relativistic formulation. The development of such a relativistic theory comprises the purpose of the present work.

It has already been pointed out in I that there are two ways possible. The first one is to attempt to generalize relativistically Eqs. (4) in the classical case and then perform the quantization (see I). The second way is to suppose, as seems natural, the excited states nearest to the fundamental state to be of the greatest importance and therefore to try to construct the Lagrange function for "the particle of variable spin" at once.

It is mainly the second possibility that the author has followed.[5,7] Accordingly the Lagrange function for a particle capable of being in the state with spin $\frac{1}{2}$ and the rest mass m_1 and in the state with spin $\frac{3}{2}$ and the rest mass $m_2>m_1$ will be given below.[8]

2. ON THE THEORY OF THE PARTICLE HAVING SPIN 3/2

The equations of the particle of spin $\frac{3}{2}$ must necessarily be used when constructing the theory of the "particle $\frac{1}{2}$–$\frac{3}{2}$." The theory of the particle of spin $\frac{3}{2}$ has been recently developed by Fierz and Pauli[9] in spinor form. The investigation and utilization of the equations for this particle are, however, considerably simplified if the wave functions are written in vector-bispinor form, as has been proposed by Ig. Tamm and A. Davydov.[10,11]

[6] W. Heitler, Nature **145**, 29 (1940); W. Heitler and S. T. Ma, Proc. Roy. Soc. **A176**, 368 (1940).

[7] V. L. Ginsburg, Comptes rendus Acad. Sci. U.R.S.S. **31**, 857 (1941); V. L. Ginsburg and P. E. Nemirovsky, J. Phys. (in press).

[8] Later on we refer to this particle as to the "particle $\frac{1}{2}$–$\frac{3}{2}$."

[9] M. Fierz and W. Pauli, Proc. Roy. Soc. **A173**, 211 (1939).

[10] The paper by Ig. Tamm and A. S. Davydov is not as yet published.

[11] V. L. Ginsburg, J. Phys. (1941, in press). It is referred to as II. *Editor's note:* See also W. Rarita and T. Schwinger, Phys. Rev. **60**, 61 (1941). In the following formula the spinor indices, which are usually dotted, will be written as bracketed indices.

In the absence of a field, the equations for the particle of spin $\frac{3}{2}$ have the form:[9]

$$p^{(\nu)\alpha}_{(\mu)} a_{\alpha\tau}^{(\mu)} = \kappa b_{\tau}^{(\nu)(\mu)},$$
$$p_{\alpha(\nu)} b_{\tau}^{(\nu)(\mu)} = \kappa a_{\alpha\tau}^{(\mu)}, \tag{6}$$

$$a_{\alpha\tau}^{(\mu)} = a_{\tau\alpha}^{(\mu)},$$
$$b_{\tau}^{(\nu)(\mu)} = b_{\tau}^{(\mu)(\nu)}, \tag{7}$$

$$p^{\alpha}_{(\mu)} a_{\alpha\tau}^{(\mu)} = 0, \quad p^{\tau}_{(\mu)} b_{\tau}^{(\mu)(\nu)} = 0. \tag{8}$$

Applying to Eq. (6) on the left the matrices $\sigma^{\alpha\tau}_{(\mu)}$ ($k=1, 2, 3, 4$) and contracting over spin indices τ and (μ) we get the equations in which the spinor indices are replaced by one vector index:

$$p^{(\nu)\alpha}_{(\nu)} a^{k}_{(\nu)} = \kappa b^{k(\nu)},$$
$$p_{\alpha(\nu)} b^{k(\nu)} = \kappa a^{k}_{\alpha}. \tag{9}$$

We see, moreover, that the Dirac Eq. (9) holds for each pair of vector components of the functions of the spin $\frac{3}{2}$ particle. Introducing the notations: $a_1{}^k = A_1{}^k$, $a_2{}^k = A_2{}^k$, $b^{k(1)} = A_3{}^k$, $b^{k(2)} = A_4{}^k$, we can write down Eqs. (9) in the usual form:

$$\gamma_k (\partial A^m / \partial x_k) + \kappa A^m = 0, \tag{10}$$

where

$$A^k = \begin{pmatrix} A_1{}^k \\ A_2{}^k \\ A_3{}^k \\ A_4{}^k \end{pmatrix}$$

and γ_k are the well-known Dirac matrices, operating on the spinor components of the vector-bispinor A^k. The symmetry conditions[7] may be written in the form

$$\gamma^k A^k = 0. \tag{11}$$

Because of the conditions of Eq. (11)

$$\gamma^m \gamma^k (\partial A^m / \partial x_k) = 2(\partial A^m / \partial x_m),$$

and therefore, applying to Eq. (10) the operator γ_m we obtain

$$\partial A^m / \partial x_m = 0. \tag{12}$$

Equation (12) is equivalent to Eqs. (8). For the adjoint functions[12] $A^{\dagger m} = A^{* m} \gamma^4$ we obtain:

$$[(\partial A^{\dagger m} / \partial x_k) \gamma_k] - \kappa A^{\dagger m} = 0, \tag{10'}$$
$$A^{\dagger m} \gamma^m = 0, \tag{11'}$$
$$\partial A^{\dagger m} / \partial x_m = 0. \tag{12'}$$

Equations (10) and (12) may be obtained also from a variation principle.[9,11] The corresponding Lagrange function is

$$L_{3/2} = A^{\dagger m} \gamma_k \frac{\partial A^m}{\partial x_k} + \kappa A^{\dagger m} A^m - i\left(A^{\dagger m} \frac{\partial C}{\partial x_m} - \frac{\partial C^\dagger}{\partial x_m} A^m \right) - \tfrac{3}{2} C^\dagger \gamma^k \frac{\partial C}{\partial x_k} + 3\kappa C^\dagger C. \tag{13}$$

Here C is a bispinor (or undor of the first rank). Variation of (13) with respect to $A^{\dagger m}$ with the subsidiary condition (11'), as well as with respect to $C^\dagger$, gives

$$\gamma_k \frac{\partial A^m}{\partial x_k} + \kappa A^m - \tfrac{1}{2} \gamma^m \frac{\partial A^k}{\partial x_k} - i \frac{\partial C}{\partial x_m} + \frac{i}{4} \gamma^m \gamma^k \frac{\partial C}{\partial x_k} = 0, \tag{14}$$
$$\gamma_k \frac{\partial C}{\partial x_k} - 2\kappa C + \tfrac{2}{3} i \frac{\partial A^k}{\partial x_k} = 0.$$

As may be shown (very similar calculations are given below), it follows from Eqs. (14) that

$$C = 0. \tag{15}$$

Therefore, these equations are equivalent to Eqs. (10) and (12). The external field may be introduced in the function (13) and in Eqs. (14) in the usual manner. In the presence of the field the quantity C is no longer equal to zero.

The current vector is:

$$s_k = ei\{A^{\dagger m} \gamma_k A^m - \tfrac{3}{2} C^\dagger \gamma_k C - i(A^{\dagger k} C + C^\dagger A^k)\}$$

$$\rho = \frac{s_0}{e} = \frac{s_4}{ie} = \{A^{* m} A^m - \tfrac{3}{2} C^* C + (A^{* 0} \gamma^4 C + C^* \gamma^4 A^0)\}. \tag{16}$$

[12] One should keep in mind that the fourth component is taken to be imaginary ($x_4 = ict$) and therefore $A^{*\alpha} = \bar{A}^\alpha (\alpha = 1, 2, 3)$, $A^{* 4} = -\bar{A}^4$, where $\bar{A}^m$ is the complex conjugate to A^m.

In the presence of the field the energy-momentum tensor is:

$$T_{ik}=\hbar cA^{\dagger m}\gamma_k\frac{\partial A^m}{\partial x_i}. \tag{17}$$

Further details may be found in II, where the conservation laws, the form of the proper functions, the perturbation theory for the case of presence of the field, and other problems are treated. Only a few simple results made use of below will be given here.

Introducing matrices $\alpha_k=i\gamma_4\gamma_k$, $\beta=\gamma_4$ and substituting iA^0 for A^4 we obtain Eqs. (10)–(12) in the form:

$$\begin{aligned}
&i\hbar(\partial A^m/\partial t)=HA^m,\\
&\boldsymbol{\alpha}\mathbf{A}=A^0,\\
&\operatorname{div}\mathbf{A}+(1/c)(\partial A^0/\partial t)=0,\\
&H=c(\mathbf{p}\boldsymbol{\alpha})+mc^2\beta,\quad p=-i\hbar\nabla,\\
&\mathbf{A}=(A^1,A^2,A^3).
\end{aligned} \tag{18}$$

The eigenfunctions of the particle of spin $\frac{3}{2}$ when at rest are as follows (for the general case see in II):

(1) The energy $W=\kappa\hbar c$, the spin component along Z axis for different states equals $\pm\frac{3}{2}$, $\pm\frac{1}{2}$

$$\begin{aligned}
&A^1_{3/2}=\frac{1}{\sqrt{2}}\begin{pmatrix}1\\0\\0\\0\end{pmatrix};\quad A^2_{3/2}=\frac{1}{\sqrt{2}}\begin{pmatrix}i\\0\\0\\0\end{pmatrix};\quad A^3_{3/2}=0;\\
&A^1_{-3/2}=\frac{1}{\sqrt{2}}\begin{pmatrix}0\\1\\0\\0\end{pmatrix};\quad A^2_{-3/2}=\frac{1}{\sqrt{2}}\begin{pmatrix}0\\-i\\0\\0\end{pmatrix};\quad A^3_{-3/2}=0;\\
&A^1_{1/2}=\frac{1}{\sqrt{6}}\begin{pmatrix}0\\1\\0\\0\end{pmatrix};\quad A^2_{1/2}=\frac{1}{\sqrt{6}}\begin{pmatrix}0\\i\\0\\0\end{pmatrix};\quad A^3_{1/2}=\frac{1}{\sqrt{6}}\begin{pmatrix}-2\\0\\0\\0\end{pmatrix};\\
&A_{-1/2}=\frac{1}{\sqrt{6}}\begin{pmatrix}1\\0\\0\\0\end{pmatrix};\quad A^2_{-1/2}=\frac{1}{\sqrt{6}}\begin{pmatrix}-i\\0\\0\\0\end{pmatrix};\quad A^3_{-1/2}=\frac{1}{\sqrt{6}}\begin{pmatrix}0\\2\\0\\0\end{pmatrix}.
\end{aligned} \tag{19}$$

According to Eq. (18) the fourth component of A^k for the particle at rest vanishes. The functions (19) are normalized by means of the condition

$$A_\alpha{}^{*m}A_\beta{}^m=\delta_{\alpha\beta}. \tag{19'}$$

The indices $\pm\frac{3}{2}$ and $\pm\frac{1}{2}$ designate the value of the projection of spin on Z axis in the given state.

(2) The energy $W=-\hbar c\kappa$

$$\begin{aligned}
&A^1_{3/2}=\frac{1}{\sqrt{2}}\begin{pmatrix}0\\0\\1\\0\end{pmatrix};\quad A^2_{3/2}=\frac{1}{\sqrt{2}}\begin{pmatrix}0\\0\\i\\0\end{pmatrix};\quad A^3_{3/2}=A^3_{-3/2}=0;\\
&A^1_{-3/2}=\frac{1}{\sqrt{2}}\begin{pmatrix}0\\0\\0\\1\end{pmatrix};\quad A^2_{-3/2}=\frac{1}{\sqrt{2}}\begin{pmatrix}0\\0\\0\\-i\end{pmatrix};\quad A^1_{1/2}=\frac{1}{\sqrt{6}}\begin{pmatrix}0\\0\\0\\1\end{pmatrix};\quad A^2_{1/2}=\frac{1}{\sqrt{6}}\begin{pmatrix}0\\0\\0\\i\end{pmatrix};\\
&A^3_{1/2}=\frac{1}{\sqrt{6}}\begin{pmatrix}0\\0\\-2\\0\end{pmatrix};\quad A^1_{-1/2}=\frac{1}{\sqrt{6}}\begin{pmatrix}0\\0\\1\\0\end{pmatrix};\quad A^2_{-1/2}=\frac{1}{\sqrt{6}}\begin{pmatrix}0\\0\\-i\\0\end{pmatrix};\quad A^3_{-1/2}=\frac{1}{\sqrt{6}}\begin{pmatrix}0\\0\\0\\2\end{pmatrix}.
\end{aligned} \tag{20}$$

3. WAVE EQUATIONS FOR "THE PARTICLE 1/2–3/2"

It seems natural to try to form the Lagrange function for "the particle $\frac{1}{2}$–$\frac{3}{2}$" by means of connecting, in some relativistically invariant manner, the Lagrange functions of particles of spins $\frac{1}{2}$ and $\frac{3}{2}$. For the spin $\frac{1}{2}$ the Lagrange function is:

$$L_{1/2}=\psi^\dagger\gamma_k(\partial\psi/\partial x_k)+k\psi^\dagger\psi. \tag{21}$$

If no new terms connecting the quantities A^k and C with each other are introduced, the most general expression of this kind is [see Eqs. (13) and (21)]

$$\begin{aligned}L=L_{3/2}+L_{1/2}+\alpha C^\dagger\psi+\alpha^*\psi^\dagger C\\ +\beta C^\dagger\gamma_k(\partial\psi/\partial x_k)+\beta^*\psi^\dagger\gamma_k(\partial C/\partial x_k)\\ +\epsilon A^{\dagger m}(\partial\psi/\partial x_m)+\epsilon^*(\partial\psi^\dagger/\partial x_m)A^m.\end{aligned} \tag{22}$$

Variation of this function with respect to A^m [the condition (11′) being kept in mind], and with respect to $C^\dagger$ and $\psi^\dagger$ gives:

$$\begin{aligned}&\gamma_k(\partial A^m/\partial x_k)+\kappa A^m-\tfrac{1}{2}\gamma_m(\partial A^k/\partial x_k)\\ &\quad-i(\partial C/\partial x_m)+(i/4)\gamma_m\gamma_k(\partial C/\partial x_k)\\ &\quad+\epsilon(\partial\psi/\partial x_m)-(\epsilon/4)\gamma_m\gamma_k(\partial\psi/\partial x_k)=0,\\ &\gamma_k(\partial C/\partial x_k)-2\kappa C+\tfrac{2}{3}i(\partial A^k/\partial x_k)\\ &\quad-\tfrac{2}{3}\alpha\psi-\tfrac{2}{3}\beta\gamma_k(\partial\psi/\partial x_k)=0,\\ &\gamma_k(\partial\psi/\partial x_k)+k\psi+\alpha^*C\\ &\quad+\beta^*\gamma_k(\partial C/\partial x_k)-\epsilon^*(\partial A^k/\partial x_k)=0.\end{aligned} \tag{23}$$

Operating on the first of these equations by the operator $\partial/\partial x_m$ and on the second one by $\gamma_m(\partial/\partial x_m)$, one obtains an equation which, after multiplying by some easily found factors and their mutual addition gives

$$\frac{\partial A^m}{\partial x_m}-\tfrac{2}{3}i\gamma_m\frac{\partial C}{\partial x_m}-\frac{\alpha i}{2\kappa}\gamma_m\frac{\partial\psi}{\partial x_m}+\left(\frac{3\epsilon}{2\kappa}-\frac{\beta i}{2\kappa}\right)\Box\psi=0.$$

Combining this equation with the second of Eqs. (23) we are led to the conclusion that

$$\begin{aligned}6\kappa C+2\alpha\psi+\left(2\beta+\frac{\alpha}{\kappa}\right)\gamma_k\frac{\partial\psi}{\partial x_k}\\ +\left(\frac{3i\epsilon}{2\kappa}+\frac{\beta}{\kappa}\right)\Box\psi=0.\end{aligned} \tag{24}$$

If Eq. (22) had not contained the function ψ, i.e., if we had dealt with a particle having spin $\frac{3}{2}$, Eq. (15) would immediately follow from Eq. (24), as must necessarily be. If we put $2\beta+(\alpha/\kappa)=(3i\epsilon/2\kappa)+(\beta/\kappa)=0$, Eqs. (23) split up into two independent equations describing the particles with spins $\frac{1}{2}$ and $\frac{3}{2}$. In the general case Eqs. (23), besides the solutions corresponding to spin $\frac{3}{2}$, have several solutions corresponding to states with spin $\frac{1}{2}$ and different values of the rest mass. This result may be easily understood. In fact, the total number of components of the functions A^m, ψ, and C is 24. Condition (10) reduces this number to 20. On the other hand "the particle $\frac{1}{2}$–$\frac{3}{2}$" must be described by a function with 12 components. Therefore, Eqs. (23) will describe such a particle if 8 subsidiary conditions will follow from these equations.[9,13] This is the case if we put $\beta=\epsilon=0$. It is just such a variant of the theory which is possibly not unique that will be treated below. Here, comparing Eqs. (24) and (23_3) we have

$$C=\alpha a\psi,\quad a=(k-2\kappa)/(6\kappa^2-\alpha\alpha^*). \tag{25}$$

By making use of Eqs. (23_2), (23_3), and (25) one may readily see that

$$\begin{aligned}\frac{\partial A^m}{\partial x_m}=-i\delta\psi,\\ \delta=\alpha\left(\frac{b}{2\kappa}+\tfrac{3}{2}ab\right)=\alpha(3\kappa a+1+\tfrac{3}{2}ab),\end{aligned} \tag{26}$$

where

$$b=k+\alpha\alpha^*a. \tag{27}$$

Eliminating C and $\partial A^k/\partial x_k$ from Eqs. (23) with $\beta=\epsilon=0$ by means of Eqs. (25)–(27) we get finally:

$$\begin{aligned}&\gamma_k(\partial A^m/\partial x_k)+\kappa A^m+i(g/\hbar c)\gamma_m\psi\\ &\qquad-i\alpha a(\partial\psi/\partial x_m)=0,\\ &\gamma_k(\partial\psi/\partial x_k)+b\psi=0,\\ &\qquad g=(\hbar c/4)[(b/\kappa)+2ab]\alpha.\end{aligned} \tag{28}$$

The general expressions for the current four-vector, the energy-momentum tensor, and the

[13] In the case of the particle of spin $\frac{3}{2}$ such conditions are found in Eqs. (11) and (12).

angular momentum tensor will not be given here. They are easily found by the usual methods from Eq. (22). In the absence of a field which was assumed above, and by taking into account Eq. (25) we obtain for the particle density and the energy density:

$$\rho=\frac{s^4}{ie}=\{A^{*m}A^m+(1-\tfrac{3}{2}\alpha\alpha^*a^2)\psi^*\psi + a(\alpha A^{*0}\gamma_4\psi+\alpha^*\psi^*\gamma_4 A^0)\}. \quad (29)$$

$$-T_{44}=ih\left\{A^{*m}\frac{\partial A^m}{\partial t}+(1-\tfrac{3}{2}\alpha\alpha^*a^2)\psi^\dagger\frac{\partial\psi}{\partial t} + a\left(\alpha A^{*0}\gamma_4\frac{\partial\psi}{\partial t}-\alpha^*\frac{\partial\psi^*}{\partial t}\gamma_4 A^0\right)\right\}. \quad (30)$$

The set of Eqs. (28) may be solved without difficulty. One group of solutions, corresponding to spin $\frac{3}{2}$, results from Eq. (28) if ψ is put equal to zero. In this case the equations for A^m coincide with the equations for the particle having spin $\frac{3}{2}$. The second group of solutions which corresponds to spin $\frac{1}{2}$[14] results if $\psi\neq 0$. Here ψ must be determined from Eq. (28_2) and subsequently A^m may be found by means of Eqs. (28_1). The rest mass in the state with spin $\frac{3}{2}$ is $m_2=|\kappa|\hbar/c$, while in the state with spin $\frac{1}{2}$ $m_1=|b|\hbar/c$. The moduli of κ and b are taken since both signs are possible.

Keeping in mind the future application to the theory of the proton-neutron, it seems natural to consider m_1 as a quantity of the same order as m_2, and therefore to put for the "excitation energy"

$$\Delta=(m_2-m_1)c^2\ll m_1c^2\sim m_2c^2. \quad (31)$$

The cutting off for the process of scattering must take place for energies of the photon (or meson) of order $h\nu\sim\Delta$.[5,6] Therefore owing to Eq. (31) we may, in a preliminary investigation, in order to clarify the general character of the energy dependance of the cross section, consider the case of $h\nu<m_1c^2$. Evidently, it is then permissible to neglect the proton recoil and to assume the heavy particle as being at rest. The non-relativistic approximation, resulting therefrom, corresponds to the non-relativistic theory of Heitler and Ma and of the present author.[5] There is, however, a fundamental difference of principle, since the fulfillment of the requirements put forward by relativity is obvious in the present theory.

Equations (20)–(28) are more suitable to handle if they are written in the following form[15]

$$\begin{aligned} ih(\partial\mathbf{A}/\partial t)&=\{c(\boldsymbol{\alpha}\mathbf{p})+\kappa hc\beta\}\mathbf{A} + \{g\boldsymbol{\alpha}+\alpha a\beta\mathbf{p}\}\psi,\\ ih(\partial A^0/\partial t)&=\{c(\boldsymbol{\alpha}\mathbf{p})+\kappa hc\beta\}A^0 + \{g+\alpha a ih(\partial/\partial t)\}\psi,\\ ih(\partial\psi/\partial t)&=\{c(\boldsymbol{\alpha}\mathbf{p})+bhc\beta\}\psi,\\ \operatorname{div}\mathbf{A}+(1/c)(\partial A^0/\partial t)&=-i\delta\psi,\quad \boldsymbol{\alpha}\mathbf{A}=A^0. \end{aligned} \quad (32)$$

Let us find the eigenfunctions of the particle at rest. For $\psi=0$ these functions were already written down in Section 2. There was given a set of formulae (19) which corresponds to the mass $\kappa\hbar/c$, while set (20) corresponds to the mass $-\kappa\hbar/c$.

The solutions of Eqs. (32) describing the state with spin $\frac{1}{2}$ are:[16]

(1) The energy $W=bhc$

$$\begin{aligned} &\psi_+=u\begin{pmatrix}1\\0\\0\\0\end{pmatrix};\quad A_+^0=\frac{\delta}{b}\psi_+;\quad A_+^1=\frac{\delta u}{3b}\begin{pmatrix}0\\0\\0\\1\end{pmatrix};\quad A_+^2=\frac{\delta u}{3b}\begin{pmatrix}0\\0\\0\\i\end{pmatrix};\quad A_+^3=\frac{\delta u}{3b}\begin{pmatrix}0\\0\\1\\0\end{pmatrix};\\ &\psi_-=u\begin{pmatrix}0\\1\\0\\0\end{pmatrix};\quad A_-^0=\frac{\delta}{b}\psi_-;\quad A_-^1=\frac{\delta u}{3b}\begin{pmatrix}0\\0\\1\\0\end{pmatrix};\quad A_-^2=\frac{\delta u}{3b}\begin{pmatrix}0\\0\\-i\\0\end{pmatrix};\quad A_-^3=\frac{\delta u}{3b}\begin{pmatrix}0\\0\\0\\-1\end{pmatrix}. \end{aligned} \quad (33)$$

[14] This is clear from the investigation of the expression for the tensor of angular momentum density. We do not write it here explicitly.

[15] $\boldsymbol{\alpha}$ and β are Dirac matrices. It should be borne in mind that the letter α also designates the constant included everywhere. However, it is hardly possible to confuse the α_x matrices with this constant.

[16] When performing the calculations the relation $hc\delta(b+\kappa)/g=3$ may be useful.

(2) The energy $W=-b\hbar c$

$$\psi_+=u\begin{pmatrix}0\\0\\1\\0\end{pmatrix};\quad A_+{}^0=-\frac{\delta}{b}\psi_+;\quad A_+{}^1=-\frac{\delta u}{3b}\begin{pmatrix}1\\0\\0\\0\end{pmatrix};\quad A_+{}^2=-\frac{\delta u}{3b}\begin{pmatrix}-i\\0\\0\\0\end{pmatrix};\quad A_+{}^3=-\frac{\delta u}{3b}\begin{pmatrix}0\\-1\\0\\0\end{pmatrix};$$

$$\psi_-=u\begin{pmatrix}0\\0\\0\\1\end{pmatrix};\quad A_-{}^0=-\frac{\delta}{b}\psi_-;\quad A_-{}^1=-\frac{\delta u}{3b}\begin{pmatrix}0\\1\\0\\0\end{pmatrix};\quad A_-{}^2=-\frac{\delta u}{3b}\begin{pmatrix}0\\i\\0\\0\end{pmatrix};\quad A_-{}^3=-\frac{\delta u}{3b}\begin{pmatrix}1\\0\\0\\0\end{pmatrix}. \tag{34}$$

Here the index + designates the functions describing the state with spin projection on the Z axis equal to $\frac{1}{2}$, the index − corresponds to the projection $-\frac{1}{2}$. The functions (33) and (34) are normalized by means of the condition $\rho=1$ [see Eq. (29)]. They are mutually orthogonal. From the normalization condition we have:

$$|u|^2=\frac{6\kappa^2}{6\kappa^2-\alpha\alpha^*}.$$

Therefore the inequality

$$6\kappa^2>\alpha\alpha^* \tag{35}$$

must necessarily hold. If this inequality were not to hold, ρ could not be normalized with a determined sign. The particle in the state with spin $\frac{1}{2}$ could then have another sign of the charge than in the state with spin $\frac{3}{2}$.

Condition (35) being fulfilled, the total charge of the field under investigation is always definite, which is necessary for quantization of the theory in accordance with the Pauli principle. The energy, on the contrary, is not definite, as happens in all cases of half-integral spin.

4. INTERACTION WITH A FIELD. THE PERTURBATION THEORY

The whole theory has been formulated in the Lagrange form and therefore the generalization for the case of the presence of a field may be readily performed. Indeed, inclusion of the interaction with an electromagnetic field, consistent with the requirements of gauge invariance, is secured by changing $\partial/\partial x_k$ in Eqs. (22) or (23) into $\pi_k=(\partial/\partial x_k)-(ei/\hbar c)\phi_k$, ϕ_k is the field potential. However, we are mostly interested [see (38)] in the case when the equations include terms depending on the field strength explicitly, i.e., terms containing the tensor $F_{ik}=(\partial\phi_k/\partial x_i)-(\partial\phi_i/\partial x_k)$. The interaction with any field, with the meson field for instance, is described by the introduction of the corresponding relativistically invariant terms into the Lagrange function. If the terms of Eqs. (23_1)–(23_3), containing the field variables, are designated by V_m, U, and W, respectively, the equations acquire the form ($\beta=\epsilon=0$!):

$$\begin{aligned}
&\gamma_k\frac{\partial A^m}{\partial x_k}+\kappa A^m-\tfrac{1}{2}\gamma_m\frac{\partial A^k}{\partial x_k}-i\frac{\partial C}{\partial x_m}\\
&\qquad+\frac{i}{4}\gamma_m\gamma_k\frac{\partial C}{\partial x_k}+V_m=0,\\
&\gamma_k\frac{\partial C}{\partial x_k}-2\kappa C+\tfrac{2}{3}i\frac{\partial A^k}{\partial x_k}-\tfrac{2}{3}\alpha\psi+U=0,\\
&\gamma_k\frac{\partial\psi}{\partial x_k}+k\psi+\alpha^*C+W=0.
\end{aligned} \tag{36}$$

In the force free case, when $V_m=U=W=0$, the conditions (25) and (26) hold. It seems therefore natural to introduce instead of c the quantity

$$D=C-\alpha a\psi. \tag{37}$$

In the absence of a field $D=0$. When a field is present we obtain, reproducing the calculations that led us to Eq. (25),

$$D=\frac{1}{6\kappa^2-\alpha\alpha^*}\left\{\alpha W+3\kappa U+\tfrac{2}{3}\gamma_k\frac{\partial U}{\partial x_k}-2i\frac{\partial V_m}{\partial x_m}\right\}. \tag{38}$$

Instead of (26) we have:

$$\frac{\partial A^k}{\partial x_k}=-i\delta\psi+\tfrac{2}{3}i\left\{U-\alpha aW+\gamma_k\frac{\partial D}{\partial x_k}-(2\kappa+\alpha\alpha^*aD)\right\}. \tag{39}$$

This equation corresponds to the Eq. (36_2).

Equations (36_1) and (36_3) acquire the form:

$$\gamma_k(\partial A^m/\partial x_k)+\kappa A^m+(ig/\hbar c)\gamma_m\psi$$
$$-i\alpha a(\partial\psi/\partial x_m)-i(\partial D/\partial x_m)$$
$$-(i/2)\gamma_m\gamma_k(\partial D/\partial x_k)+(i/2)(3\kappa+\alpha\alpha^* a)\gamma_m D \quad (40)$$
$$+V_m-\tfrac{3}{4}i\gamma_m U+(i/2)\alpha a\gamma_m W=0,$$
$$\gamma_k(\partial\psi/\partial x_k)+b\psi+\alpha^* D+W=0.$$

In the absence of a field these equations give Eqs. (28), which was to be expected. Keeping in mind the future application to the radiative processes we shall develop here the non-stationary perturbation theory for the set of Eqs. (38)–(40). Similarly to the case of spin $\frac{3}{2}$ some difficulties are encountered in this way.[11] For example, for the particle at rest in the state with spin $\frac{3}{2}$ $A^4=0$ always holds (see Section 2). Therefore, expanding the wave function of the particle at rest in a field into the functions of the non-perturbed problem we always obtain for the fourth component the zero value. This, however, cannot be the case. In fact, for the state with spin $\frac{3}{2}$, when a field is present, $\partial A^k/\partial x_k\neq 0$ [see (39)]. However, it follows from Eqs. (38), (39) that $\partial A^k/\partial x_k$ and $A^4=iA^0$ are small quantities of the first order of magnitude. Because of this circumstance, as may be shown, in the perturbation theory assuming V_m, U, and W to be small, the development of the wave function in a series of eigenfunctions of unperturbed problems is still possible. We put therefore

$$A^m=\sum_n b_{n\mathrm{II}}(t)A^m_{n\mathrm{II}}(\mathbf{x},t)+\sum_n b_{n\mathrm{I}}(t)\,A^m_{n\mathrm{I}}(\mathbf{x},t),$$
$$\psi=\sum_n b_{n\mathrm{I}}(t)\,\psi_{n\mathrm{I}}(\mathbf{x},t), \quad (41)$$

where $A^m_{n\mathrm{II}}$ are the solutions of the unperturbed problem which correspond to the state with spin $\frac{3}{2}$, and $(A^m_{n\mathrm{I}},\psi_{n\mathrm{I}})$ are those corresponding to the state with spin $\frac{1}{2}$.

Keeping in mind the future applications we confine ourselves to the case of the particle at rest and we neglect the recoil. Let us introduce Eq. (41) into Eq. (46). Multiplying the expressions arising thus by $A^{\dagger m}_{n\mathrm{II}}$ or by $A^{\dagger m}_{n\mathrm{I}}$ and by $\psi_{n\mathrm{I}}$, respectively, summing with respect to m and making use of Eqs. (11′), (19), (19′), and (33)–(34) we get:

$$i\hbar(db_{n\mathrm{II}}/dt)=\hbar c(A^{\dagger m}_{n\mathrm{II}}V_m), \quad (42)$$

and

$$\frac{db_{n\mathrm{I}}}{dx_4}\{(A^{*m}_{n\mathrm{I}}A^m_{n\mathrm{I}})-i\alpha a(A^{\dagger 4}_{n\mathrm{I}}\psi_{n\mathrm{I}})\}$$
$$-i\left(A^{\dagger 4}_{n\mathrm{I}}\frac{\partial D}{\partial x_4}\right)+(A^{\dagger m}_{n\mathrm{I}}V_m)=0,$$
$$\frac{db_{n\mathrm{I}}}{dx_4}(\psi^\dagger_{n\mathrm{I}}\psi_{n\mathrm{I}})+\alpha^*(\psi^*_{n\mathrm{I}}D)+(\psi^*_{n\mathrm{I}}W)=0,$$
$$\frac{db_{n\mathrm{I}}}{dx_4}\{\tfrac{3}{2}i(A^{*4}_{n\mathrm{I}}A^4_{n\mathrm{I}})+\alpha a(A^{\dagger 4}_{n\mathrm{I}}\psi_{n\mathrm{I}})\}$$
$$+\left(A^{\dagger 4}_{n\mathrm{I}}\frac{\partial D}{\partial x_4}\right)-2\kappa(A^{*4}_{n\mathrm{I}}D)+(A^{*4}_{n\mathrm{I}}U)=0.$$

The last of these equations is obtained from Eq. (36_2) or (39) after multiplying by $A^{*4}_{n\mathrm{I}}$. Now, taking into account the properties of functions (33)–(34), we eliminate the quantity D and obtain:

$$i\hbar\eta\frac{db_{n\mathrm{I}}}{dt}=\hbar c(A^{*m}_{n\mathrm{I}}V_m)$$
$$+i\hbar c(A^{*4}_{n\mathrm{I}}U)+\frac{2\kappa i\hbar c}{\alpha^*}(A^{*4}_{n\mathrm{I}}W),$$
$$\eta=-\frac{2\kappa\delta^*}{\alpha^* b}|u|^2=-\frac{6\kappa^2}{6\kappa^2-\alpha\alpha^*}(1+3a\kappa). \quad (43)$$

It may be easily seen that the probabilities of transitions from state I into state II and vice versa are not equal to each other when η is not equal to unity. In contrast to the usual cases, in the theory developed here the principle of detailed balance does not follow from the equations of motion.* This circumstance seems to be very interesting and requires additional investigations. In order to secure the validity of the principle of detailed balance which seems to be necessary, the requirement $\eta=1$ must be fulfilled. This requirement reduces the number of alternative constants involved in the theory. We shall assume below that $b>0$ and, therefore, $m_1=b\hbar/c$. From the condition $\eta=1$ we get for $|\alpha|^2$:

$$|\alpha|^2=6\kappa^2$$

or

$$|\alpha|^2=6\kappa^2+3\kappa b. \quad (44)$$

* *Editor's note:* See note added at end of paper.

The unavoidable condition (35) is satisfied only if the case (44) is assumed, and if, moreover, the negative value of κ is chosen, this choice being at our disposal. In the theory of the proton the mass m_1 for the ground state is known, and the single new constant involved in the theory is the mass m_2 of the particle in the excited state. In fact

$$b=m_1c/\hbar, \quad \kappa=-m_2c/\hbar, \quad m_2>m_1>0, \qquad |\alpha|^2=(3c^2/\hbar^2)(2m_2^2-m_2m_1). \tag{45}$$

The remaining constants introduced above [see Eqs. (25)–(27)] are:

$$|u|^2=-2\kappa/b=2m_2/m_1, \qquad a=\frac{b-2\kappa}{6\kappa^2}=\frac{\hbar(m_1+2m_2)}{6m_2^2c}, \qquad \left|\frac{\delta}{b}\right|^2=\left|\frac{\alpha b}{4\kappa^2}\right|^2=\frac{3m_1^2}{2m_2^2}\left(1-\frac{m_1}{2m_2}\right). \tag{46}$$

5. THE SCATTERING CROSS SECTION

Now we go over to the calculation of the cross section for the scattering of light by the "particle $\frac{1}{2}$–$\frac{3}{2}$." As is clear from what has been said in Section 1, we are interested in the interaction energy terms involving F_{ik}. These are, for example,

$$A^{\dagger m}\frac{\gamma_i\gamma_k}{2i}A^mF_{ik}, \quad \psi^\dagger\frac{\gamma_i\gamma_k}{2i}\psi F_{ik}, \quad i(\psi^\dagger\gamma^iA^k+A^{\dagger k}\gamma^i\psi)F_{ik},$$

$$A^{\dagger m}\frac{\gamma_i\gamma_m}{2i}A^kF_{ik}=\frac{2}{i}A^{\dagger i}A^kF_{ik}, \text{ etc.}$$

In distinction to the Dirac theory we introduce also the terms containing $\partial F_{ik}/\partial x_m$. A fuller analysis of all the possible interactions of the particle with different tensor fields encounters no difficulties. However, it would go beyond the limits of the present article. Here we should like only to establish the theory of excited states and to prove that this automatically prevents the unlimited increase of the scattering cross section due to the magnetic moment. Because of the complete similarity of this case to the case of scattering of, for example, vector mesons by the quasi-magnetic moment of the heavy particle, no special investigation of the latter case is necessary. When the mesons are charged it is only essential to introduce[6,17] the neutron-proton states with the charges $-e$ and $2e$ in order to obtain a constant scattering cross section for high frequencies. Let us now, therefore, as an example, consider the light scattering by a neutron-proton, the interaction energy being assumed as

$$\frac{\mu_1}{\hbar c}A^{\dagger m}\frac{\gamma_i\gamma_k}{2i}A^mF_{ik}+\frac{\mu_2}{\hbar c}\psi^\dagger\frac{\gamma_i\gamma_k}{2i}\psi F_{ik}. \tag{47}$$

The cross section for the elastic scattering of light having the frequency ν is

$$\sigma=\frac{2\pi}{\hbar c}\frac{\nu^2d\Omega}{(2\pi)^3c^3\hbar}|H|^2,$$

$$H=\sum\left\{\frac{v^{\mathrm{I}}_{n'0}v^{\mathrm{I}}_{kn'}}{h\nu}-\frac{v^{\mathrm{I}}_{n''0}v^{\mathrm{I}}_{kn''}}{h\nu}+\frac{v^{\mathrm{II}}_{m'0}v^{\mathrm{II}}_{km'}}{h\nu-\Delta}-\frac{v^{\mathrm{II}}_{m''0}v^{\mathrm{II}}_{km''}}{h\nu+\Delta}\right\}, \tag{48}$$

where v_{ik} are the matrix elements of the interaction energy. The index I denotes the transitions between states with spin $\frac{1}{2}$, the index II, those for which in the intermediate states the spin equals $\frac{3}{2}$. The particle is assumed to be at rest, and the excitation energy is put equal to $\Delta=(m_2-m_1)c^2$. The eigenfunctions of the initial and the final states are determined according to Eq. (33), the eigenfunctions of the intermediate states with spin $\frac{3}{2}$ are given by Eqs. (20). Here we have $\kappa<0$ and therefore $W=-\hbar c\kappa=m_2c^2>0$.

For the sake of definitiveness, as the initial state the state $(\psi_+^{\mathrm{I}}, A_+^{m\mathrm{I}})$ [see Eq. (33)] will be taken. The magnetic field of the light wave we shall assume to be directed along the Z axis. The unit vector along this direction will be denoted by $\mathbf{e}_0$. From the usual quantization of the electromagnetic field one readily shows that the matrix element of the magnetic field strength for a one-photon transition is

$$(1|\mathbf{H}|0)=(2\pi\hbar\nu)^{\frac{1}{2}}\mathbf{e},$$

where the inessential phase factor has not been written out. Omitting the simple calculations of

[17] Similarly to the higher spin-excited states the "higher" charge states must evidently be considered as a natural consequence of the reaction of the heavy particle proper charged field. *Editor's note:* See also H. J. Bhabha, Phys. Rev. **59**, 100 (1941).

the matrix elements for the interaction energy we shall give here only the final result.

For the process involving no change in spin direction, i.e., if the final state coincides with the initial state (ψ_+^{I}, A_+^{mI}):

$$|H|^2=B^2\frac{16\Delta^2 e_z^2}{\{(h\nu)^2-\Delta^2\}^2}, \qquad (49)$$

$$B^2=(8/27)^2\pi^2h^2\mu_1^4\left|\delta u/b\right|^4\nu^2.$$

Here e_z denotes the Z component of the magnetic field of the scattered wave ($|e|=1$). The formula (49) is a result only of transitions to the intermediate states with spin $\frac{3}{2}$.

For the process involving a change of the spin direction, i.e., when the final state is the one which is denoted by $(\psi_-^{I}A_-^{mI})$, connecting the values of the constants μ_1 and μ_2 by the assumption

$$\frac{4}{27}\mu_1^2\left|\frac{\delta u}{b}\right|^2=\left\{\mu_2|u|^2-\frac{10}{9}\mu_1\left|\frac{\delta u}{b}\right|^2\right\}^2,$$

we have:

$$|H|^2=B^2\left\{\frac{2}{h\nu}-\frac{1}{h\nu-\Delta}-\frac{1}{h\nu+\Delta}\right\}^2(e_x^2+e_y^2)$$

$$=\frac{4B^2\Delta^4}{(h\nu)^2\{(h\nu)^2-\Delta^2\}^2}. \qquad (50)$$

The total cross section is found by summing over the final state, i.e., by adding the results of the substitution of Eqs. (49) and (50) in Eq. (48). If $h\nu\ll\Delta$, only the first term in the brackets [in Eq. (50)] is of importance, and we obtain, as usual, for the light scattering by a magnetic moment a cross section, which increases with the frequency:

$$\sigma=\text{const.}\ \nu^2.$$

If, on the contrary, $h\nu\gg\Delta$, the part of the cross section which is not connected with a change of the spin direction, approaches a constant value independent of the frequency.

The cross section which is connected with a change of the spin direction decreases at high frequencies as $1/\nu^2$, this decrease being in full accordance with classical arguments. In fact, the change of moment direction must necessarily be hampered, if the reaction of the proper field is taken into account.

In the above calculations the heavy particle has been assumed to be at rest, this being permissible if $h\nu<m_1c^2$. If the recoil of the heavy particle were taken into account, the scattering cross section when $h\nu\gg\Delta$ would evidently decrease with the energy, probably as $1/\nu$.

It seems hardly advisable to perform any fuller calculations of the scattering cross section in different cases which are distinguished by the assumptions concerning the interaction energy, by the neglect or the inclusion of recoil, etc. before the connection with the theory of nuclear forces is established. Therefore, the purpose of further investigation is to consider the nuclear forces within the bounds of the relativistic theory developed above. In order to do this, the interaction with various meson fields must be included in the equations. Here various possibilities arise. Independently of this problem however, the above results seem to make the hypothesis of excited proton states very probable.

Unlimited growth of the cross section results also when the light scattering by the meson with spin 1 is calculated. This result is explained apparently as in the case of the scattering by a proton, by the neglect of the proper field of the meson magnetic moment.[4,5,18] According to this point of view it seems to be of interest to consider the particle capable of occupying states with spin 1 and rest mass m_1 and with spin 2 and the rest mass $m_2>m_1$. One may believe that the cross section for the light scattering by such a "particle 1–2" for high energies will not increase with the energy. However, since in this case the cross section must be calculated with the motion of the particle taken into account, some difficulties may be encountered.

In conclusion I wish to express my sincere gratitude to Professor Ig. Tamm for his encouragement and advice.

ADDED NOTE

In the above article it was erroneously concluded that for the particle transitions ($\frac{1}{2}\rightleftarrows\frac{3}{2}$) the principle of detailed balance does not hold. The erroneousness of this conclusion follows from the

[18] In distinction to the case of a proton, no terms including F_{ik} are introduced. Therefore, that part of the scattering which is connected with the magnetic moment becomes noticeable only at high energies. At low energies the scattering by the meson charge predominates.

fact that the fundamental equations of the theory [Eqs. (36)] are invariant with respect to the change of the sign of time. Meanwhile Eq. (43), which was derived by the perturbation method and indeed led to the above conclusion concerning the lack of symmetry of transition, does not actually follow from the Eq. (39) since the development (41) is not complete. As a matter of fact, for the unperturbed system in the state of spin $\frac{3}{2}$ we have $\psi=0$. However, in the presence of the field even in this state $\psi\neq 0$, while the development (41) does not take into account that part of the function ψ which in the presence of the field corresponds to the state of spin $\frac{3}{2}$.

Therefore the formula (43) is wrong, while the relations (44)–(46) are not necessary. The whole general theory, of course, remains unchanged. The fundamental result of the paper—the cutting off of the cross section for the scattering of light by the particle's moment—also remains valid. This is easily shown by the evaluation of the cross section for the scattering by means of the correspondence principle instead of the incorrect perturbation theory, as was done in Section 5. Thus the result of Section 5 remains true, i.e., the cross section for the scattering, which in the beginning increases as the square of the photon energy, ceases to depend on energy for $E\gg\Delta$.

I should like also to point out the following: In order to avoid the change of the number of independent functions describing the particle $(\frac{1}{2}-\frac{3}{2})$ when the field is put on, it suffices that the right-hand side of Eq. (38) involves no time derivatives of A^m, D, and ψ. This requirement restricts to some extent the choice for the expression of the energy of interaction of the particle with the field. The usual interaction with the electromagnetic field, expressible by means of potentials, satisfies this requirement. The interaction described by Eq. (47) does not satisfy it. It is, however, very easy to find another type of interaction energy which does and which moreover leads to the cutting off of the cross section as well.

The equations for the particle capable of being in the states of spins 1 and 2, mentioned at the end of the paper, have been recently obtained and investigated. The calculation of the scattering of light by the particle (1–2) in the relativistic case, which is only of interest according to the arguments given at the end of the paper, turns out to be very cumbersome, although not very difficult and has not yet been performed.

JANUARY 1 AND 15, 1943 PHYSICAL REVIEW VOLUME 63

High Centrifugal Fields and Radioactive Decay

SIMON FREED, A. H. JAFFEY, AND M. L. SCHULTZ
George Herbert Jones Laboratory, University of Chicago, Chicago, Illinois

(Received October 6, 1942)

Previous experiments to detect some influence on the decay process of a naturally radioactive substance by means of centrifugal fields (20,000 g) had yielded no effect within 0.1 percent. It seemed of value to re-examine such a possibility in view of the high centrifugal fields (order of 1,000,000 g) now available, the new types of decay processes in artificial radioactivity, and the non-electromagnetic forces now recognized as operating in atomic nuclei. Except for fission an example of each type of radioactive decay was investigated. Two methods were employed, one of which made use of a toroidal tube counter surrounding the spinning rotor. An ionization chamber furnished a precision of several tenths of a percent and the counter allowed a precision of several percent. No definite effect was found. However, in Br^{80} where a transition occurs between isomers by emission of gamma-rays rather than the usual transformation within the nucleus involving charged particles, there was some sign of systematic deviation from the accepted half-lives in a centrifugal field of 632,000 g but it may be within the total experimental error.

MANY experiments, very diverse in character, have all failed to effect any measurable change in the decay processes of naturally radioactive substances.[1] The discovery of artificial radioactivity throughout the periodic system, the appearance of new types of nuclear transformations and the new basic particles, the neutron and the positron, have brought to the fore the need of attempting once again to influence the decay processes and thus to link

[1] F. W. Kohlrausch, "Radioaktivität," *Handbuch der Experimental Physik* (Leipzig, 1928), Vol. 15, p. 669.

these phenomena with the main body of physics and chemistry.

Such experiments now seem especially timely because of the failure of electromagnetic theory to account for results in scattering experiments where the interactions of proton-proton and neutron-proton (particles unlike in charge but of about the same mass)[2] are of the same magnitude. Hence non-electromagnetic forces, still very obscure, are now entertained as operative in the structure and properties of atomic nuclei. Also not clear is the importance of the theory of relativity in intra-nuclear dynamics although extreme concentration of matter and intensity of the fields are accepted as present in nuclei. Because of the equivalence of gravitational and accelerational fields and the availability of very high centrifugal fields these investigations were undertaken to determine what influence fields of about 500,000 g to 1,000,000 g have on the radioactive intensity at a given instant and on the rate of its decay in substances which represent every radioactive decay process now known except fission.

Rutherford and Compton, and Compton[3] had found that centrifugal fields about 20,000 g did not affect the intensity of the gamma-radiation from a radon bulb by as much as 0.1 percent. Effects due to centrifugal fields are hardly to be expected on grounds of energy alone since the potential energy due to rotation, in the present experiments, is only of the order of 0.1 ev whereas nuclear transformations are attended by energy changes of the order of 10^6 ev. What was sought was a response to a particular kind of influence rather than any effect ascribable solely to a change in potential energy. Moreover, what are involved are not changes in equilibrium but in rate processes. Rates of many chemical reactions are greatly affected by small net energy changes of the proper kind. On the basis of energy it would be preferable to investigate critical or resonance situations as with thermal neutrons.

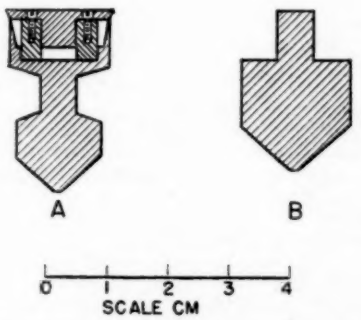

FIG. 1. Rotors.

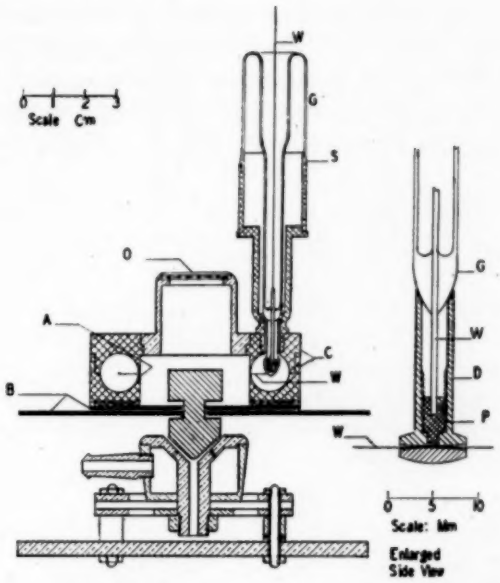

FIG. 2. Toroidal counter with rotor on stator. *W*—tungsten wire; *A*—copper foil window; *B*—baffles; *C*—copper case; *D*—lavite insulator; *G*—glass; *O*—glass window for observing rotation with stroboscope; *P*—copper plug; *S*—glass-copper seal.

The experiments performed divide into two sets. The first in which a Geiger-Mueller tube counter was employed and in the second, an ionization chamber and amplifier. The more sensitive method (set I) had been found necessary because the only means available at the time for inducing radioactivity was a weak neutron source (200 mC radon-beryllium). The two sets differ also in the method for detecting whether the centrifugal field had effected any change in the activity. In set I, the half-lives of the disintegration from the substances in rotation were compared with the published values.[4]

[2] M. A. Tuve, N. P. Heydenberg, and L. R. Hafstad, Phys. Rev. **50**, 806 (1936).

[3] E. Rutherford and A. H. Compton, Nature **104**, 412 (1919); A. H. Compton, Phil. Mag. **39**, 659 (1920).

[4] This comparison was feasible when the decay could be adequately represented by one exponential term. The following procedure was adopted when the counting rate is given as the sum $N=\Sigma_i N0_i e^{-\lambda_i t}$ over i, the separate periods contributing to the decay. The value of the initial intensity $N0_i$ for each period was obtained from the experimental data by use of the method of least squares and by assuming the published values for λ_i to be correct. In order to avoid the use of weighting factors, equal numbers

In set II, instead of comparing the half-lives, the actual radioactive intensities for high speed and low speed were compared by means of the corresponding currents in an ionization chamber. It may be readily shown[5] that to a first approximation any change in the half-lives is proportional to a change in ionization current. This method is not restricted to a single decaying species and requires none of the computational fitting of the first method for groups of atoms disintegrating at the same time, since it is about as simple to determine the displacement of a complex decay curve as of a decay which follows a straight line.

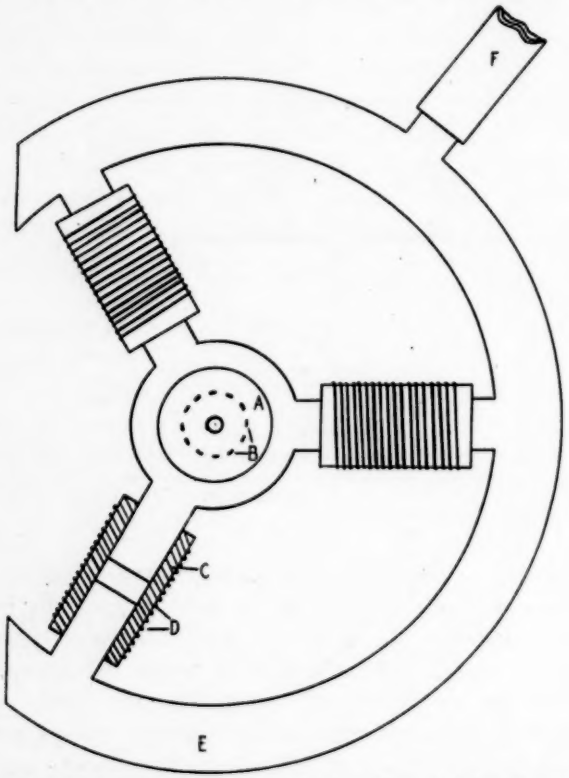

FIG. 3. Symmetrical stator mount. One air inlet shown in cross section. *A*—chromium plated cone; *B*—air jets; *C*—rubber air inlet; *D*—tightly wound and soldered copper wire; *E*—hollow air distributor; *F*—rubber hose from air valve and gauge.

EXPERIMENTAL

The rotors[6] were air driven and supported (Fig. 1A and 1B for rotors, and for stators, Fig. 3 and lower portion of Fig. 2). Where possible the material to be activated constituted a part of the cylindrical surface of the rotor, usually as electroplated metal. The rotors were machined out of beryllium-copper, an alloy of high tensile strength. During activation all but the significant cylindrical surface was heavily shielded. When the substance did not lend itself to this procedure, the activation was performed on the material in powder form and if necessary it was dissolved and co-precipitated with an appropriate substance. The active powder was placed in the thin-walled cavity of the rotor (Fig. 1A).

The rotor represented in Fig. 1A owed its irregular shape to the need of baffles to keep the driving air from impinging on the window of the counter and on objects near it. It had been found[7] that the air deposited the decay products of radon and thoron from the atmosphere on almost all materials exposed to the air stream and depending on the weather, the counts due to this source may reach as many as fifty per minute. Even with the precaution of baffles, the deposited activity often amounted to as much as ten counts.

of counts were taken for each experimental point thus making the relative probable error for that point approximately equal to the errors of any other point. If any systematic deviation between the curve calculated from the N_0, ϵ and λ_i and the experimental points is appreciably larger than the experimental error, it may be concluded that at least one of the decay constants is significantly different from the assumed value.

[5] Assume the exponential decay law, $N = N_0 e^{-\lambda t}$ then $dN/dt = -\lambda N_0 e^{-\lambda t} = -\lambda N$. If Δq is the charge collected in the ionization chamber in the time interval Δt, and if the relative positions of the radioactive material and the ionization chamber remain unchanged, then Δq is proportional to ΔN, the number of particles disintegrating during Δt. If V is the measured voltage and i the current through the grid resistor, $V = iR_{\text{grid}} = (dq/dt)R_{\text{grid}} \propto (dN/dt)$ so $V \propto \lambda N$. If the speed of the rotor can be changed rapidly enough so that N, the number of radioactive atoms present, remains practically constant, then a change in the decay constant with speed will be reflected in a change in the measured voltage. If the decay is too rapid for direct comparison, i.e., if during the interval required to reach the final value in speed the value of N changes appreciably, then a modification of the procedure is necessary. Measurements are taken at two values of the rotational speed, the highest attainable with the air pressure available and the lowest at which the rotors will spin stably. The voltage is measured at short intervals for a number of readings at one of the speeds and the speed is changed to the other after each reading. The resulting voltage (or log voltage) is plotted against time. If an effect of the kind sought is present, the points taken at high speed should lie on a curve displaced somewhat from the curve passing through the points taken at low speed; if the effect is absent all the points should lie on the same smooth curve. It has been assumed that the form of the decay law does not change when the radioactive substance is placed into an accelerational field and that any accelerational effect is expressible simply as a change in λ, an assumption valid in the first approximation for any small effects.

[6] E. Henriot and E. Huguenard, Comptes rendus **180**, 1389 (1925), J. de phys. et rad. [6] **8**, 433 (1927). J. W. Beams and E. G. Pickels, Rev. Sci. Inst. **6**, 299 (1935).

[7] S. Freed and M. L. Schultz, J. Frank. Inst. **231**, 345 (1941).

TABLE I. Decay in centrifugal fields of substances showing single decay periods. Method I of text.

Radioactive isotope	Literature half-life	Observed half-life	Air effect counts/min.	Initial intensity counts/min.	Final intensity counts/min.	R cm	n rev./sec.	Centrifugal field $g \times 10^{-5}$
Mn^{56}	2.59±0.02 hr.	2.65±0.03 hr.	0	172	29	0.79	4025	5.16
Mn^{56}	2.59±0.02 hr.	2.55±0.08 hr.	0	60	17	0.85	4000	5.48
Cl^{38}	37.40 min.	39.1 ±0.2 min.	15	1489	43	0.79	4025	5.16
Cu^{64}	12.8 ±0.1 hr.	13.01±0.02 hr.	5	1420	224	0.85	3700	4.69
ThC′	60.8 min.	62.4 ±0.4 min.	0	614	17	0.79	4000	5.09
ThC′	60.8 min.	58.0 ±0.6 min.	7	353	18	0.79	3950	4.97
ThC′	60.8 min.	59.2 ±1.0 min.	1	143	9	0.79	3950	4.97
ThC′	60.8 min.	61.2 ±1.6 min.	9	316	126	0.79	3900	4.84

TABLE II. Decay in centrifugal fields of substances possessing several radioactive periods. Method II of text.

Metal activated	Radioactive isotopes present	Half-life (literature)	Type of radiation	Precision*	Rev. per sec. Maximum	Rev. per sec. Minimum	Centrifugal field† $g \times 10^{-5}$ Maximum	Centrifugal field† $g \times 10^{-5}$ Minimum
Cu	Cu^{64}	12.8 hr.	β^- β^+ and K	0.25%	4000	3150	5.63	3.49
Cu	Cu^{64}	12.8 hr.	β^- β^+ and K	0.20%	3700	2700	4.82	2.56
Cd	Cd^{117}	3.75 hr.	β^-	0.10%	5250	2850	9.70	2.86
	In^{117}	117 min.	β^-					
	Cd^{115}	2.5 days	β^- and γ					
	In^{115*}	4.1 hr.	I.T., γ and internally converted electrons					
Zn	Zn^{69}	57 min.	β^-	0.20%	5100	2675	9.15	2.52
	Ga^{68}	68 min.	β^+					
	Zn^{69}	13.8 hr.	I.T., γ					
	Ga^{67}	83 hr.	K, γ and internally converted electrons					
Ni	Cu^{61}	3.4 hr.	β^+, K					
	Cu^{66}	5 min.	β^-	0.07%	5125	2025	9.24	1.44
	Ni^{63}	2.6 hr.	β^-, γ					
Cr	Mn^{51}	46 min.	β^+	0.20%	5050	2575	8.97	2.33

* Represents the average absolute deviation of the observed points from the smooth curve drawn through them.
† The radius of each rotor was 0.872 cm.

per minute and had to be determined with unactivated rotors and taken into account (Table I, column 4). The strong radioactivity obtained with deuterons from the cyclotron of this university (set II) made it possible to ignore the air effect and hence a rotor of simple form could be used, which attained about 1,000,000 g (radius = 0.872 cm).

The feeble radioactivity of set I called for a counter so shaped as to surround the rotor. Figure 3 shows its approximate toroidal form. The copper window A, about 0.05 mm thick, was soldered with tin to the copper case B. The latter was made of two rings of copper into each of which was machined a semitoroidal groove so as to form a toroidal cavity within the block M when the two halves were screwed together. The cylindrical copper "window" was co-axial with the rotor. The counter possessed a plateau from 300 volts to 400 volts.[8]

[8] It has been treated by the method of O. S. Duffendack, A. Lifschutz, and M. M. Slawsky [Phys. Rev. **52**, 1231 (1937)]. The circuit of H. V. Neher and W. H. Pickering [Phys. Rev. **53**, 317 (1938)] served to quench the counter discharge and also maintained the counter case at ground potential. A twofold scaling circuit was employed similar to the first stage of the scale of eight of W. G. Shepherd and R. D. Haxby [Rev. Sci. Inst. **1**, 425 (1936)]. The counter was corrected for non-linearity, i.e., the losses due to the finite resolving time of the circuit and of the mechanical recorder according to the procedure of Duffendack, Lifschutz, and Slawsky and of Lifschutz and Duffendack [Phys. Rev. **54**, 714 (1938)]. The basic count varied from 10 to 30 per minute depending mostly on the size of the counter. The method of evaluating the decay rates from the data followed H. Peierls [Proc. Roy. Soc. **A149**, 467 (1935)].

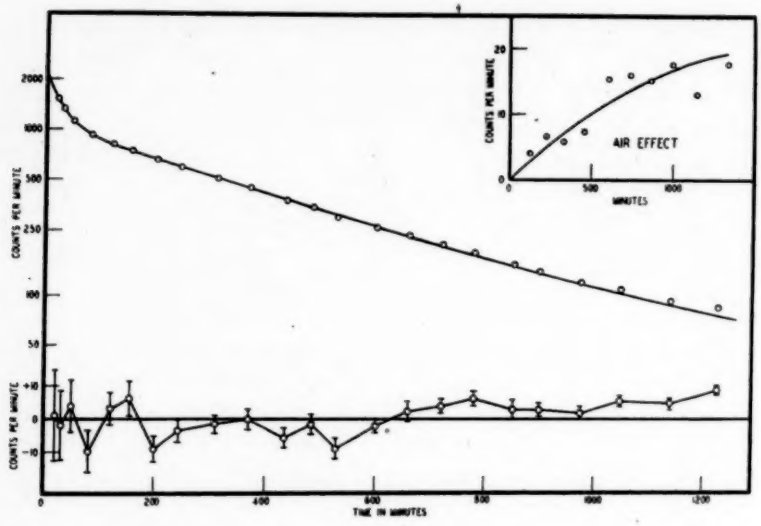

FIG. 4. Decay of activated bromine.

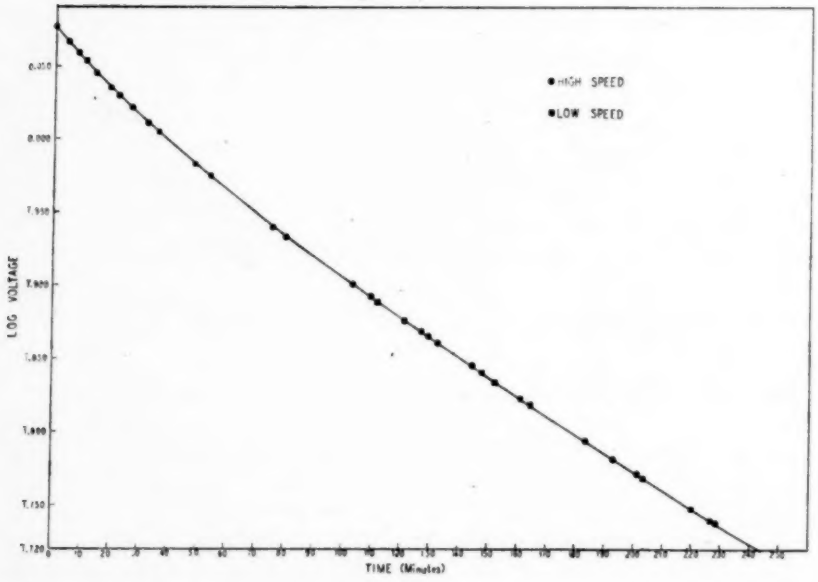

FIG. 5. Decay of activated cadmium.

MEASUREMENTS

The first set of measurements, those listed in Table I and in addition those on aluminum and bromine, both of which decay with several periods, revealed no definite change in the radioactive decay in a centrifugal field within an estimated 3 percent. The actual half-life obtained from copper exceeds by more than this the published values which, moreover, are badly scattered. Separate experiments carried out in connection with set II (see Table II) revealed that the higher value arises from the presence of Zn^{65} with half-life 250 days formed during the activation. The method (as employed in set II) of detecting any change which the centrifugal field might bring about, established that the decay rate remained undisturbed within 0.25 percent when the centrifugal field changed from 2.5×10^5 g to 5.6×10^5 g. The discrepancy in half-life as given in Table I may then be regarded as removed.

The decay of Cu^{64} is of especial interest. It decays by β-ray emission to form Zn^{64} and by positron emission or K-electron capture to form Ni^{64}. Both transformations proceed at the same rate.[9] Under the influence of the centrifugal field some readjustment might occur in the relative intensities of the β-ray and positron activities.

[9] S. N. Van Voorhis, Phys. Rev. **50**, 895 (1936).

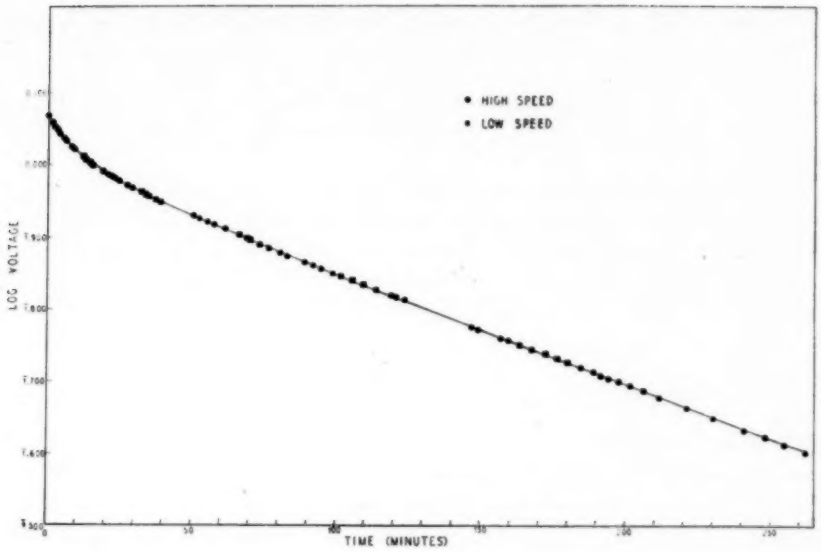

FIG. 6. Decay of activated nickel.

With bromine the possibility existed of influencing a process with no net change in charge in the nucleus, the transition from one isomer of Br^{80} to another. Br^{80} has been shown to have a 4.5-hr. period due to an excited state which decays by gamma-radiation to the ground state, which in turn decays by electron emission with an 18.5-min. period[10] to Kr^{80}.

The decay curve for Br^{80} in which the 33-hr. period is taken into account is given in Fig. 4. The experimental values are shown with vertical lines. An examination of the plot, on an enlarged scale, indicates a small systematic trend (starting at about 200 min.) between the calculated curve and the experimental values. Since the standard deviations represented by the vertical lines do not include the errors in correction for the non-linearity and air-effects, this trend may not be outside the total experimental error since, as is shown in the inset, the air-effect in these experiments was unusually large.

A special procedure was devised for bromine. Lithium bromide as powder was activated in a beam of 8.5-Mev deuterons, then dissolved in water and silver nitrate added. The precipitated silver bromide was fused and the molten salt was transferred to the silver-plated cylindrical surface of a rotor whose temperature was just above the melting point of the salt. The silver surface insured excellent wetting and adhesion; chemical action also had been avoided. Before being set in rotation, the layer was vigorously buffed to remove loosely adhering material. The salt adhered perfectly at 4975 rev./sec. on a rotor 0.834 cm in radius (centrifugal field 6.32×10^5 g).

In Table II are listed data obtained with the ionization chamber.[11] The precision is several tenths of one percent. Figures 5 and 6 illustrate the precision of the data. The centrifugal fields are higher than those of set I since the rotor, because of its simpler form and reduced surface, encountered less air resistance.

It should be added that Table I also includes several measurements on naturally radioactive thorium C′ isolated in different ways.

We wish to express here our gratitude to the group working with the cyclotron of this university and especially to Dr. Louis Slotin.

[10] A. H. Snell, Phys. Rev. **52**, 1007 (1937); E. Segrè R.S. Halford, and G. T. Seaborg, Phys. Rev. **55**, 321 (1939); D. C. DeVault and W. F. Libby, Phys. Rev. **55**, 322 (1939).

[11] The design of the ionization chamber was similar to that of S. W. Barnes [Rev. Sci. Inst. **10**, 1 (1939)] and the current was amplified with an FP-54 electrometer tube. The amplifier circuit was essentially that described by D. B. Penick [Rev. Sci. Inst. **6**, 115 (1935)]. To increase the range and precision it was converted into a null instrument by balancing the ionization current with an accurate potentiometer in the grid circuit. The beam of deuterons was usually directed at the material on the rotor within the vacuum chamber of the cyclotron. The rotor with its shielding of massive copper was placed on a water-cooled spindle entering the vacuum chamber through a Wilson seal [Rev. Sci. Inst. **12**, 91 (1941)]. So disposed, the rotor could be turned in the vacuum at intervals to achieve a rather uniform activation over the surface.

Saturation Characteristics for Alpha-Particles in Purified Gases

E. D. KLEMA* AND H. H. BARSCHALL
Department of Physics, University of Kansas, Lawrence, Kansas

(Received October 29, 1942)

Saturation curves were taken in nitrogen, argon, and an argon-hydrogen mixture. The effect of purification on the saturation properties of argon and the argon-hydrogen mixture was studied. It was found that even unpurified tank argon and nitrogen show saturation at very much smaller field strengths than, for instance, air. Upon purification an appreciable lowering of the field necessary for saturation was observed.

INTRODUCTION

IN many studies of high speed particles it is necessary to fill ionization chambers with gases at high pressure, particularly in investigations of cosmic rays and in determinations of the energy of fast neutrons by use of measurements on the recoiling protons.[1] The use of gases at high pressure introduces several difficulties, the most important of which is caused by lack of saturation. Jaffé's theory[2] of saturation shows that the field strength necessary for saturation increases very rapidly with increasing gas pressure. Another difficulty arises when a linear amplifier is used to amplify ionization pulses. Ortner and Stetter[3] pointed out that for proper operation of the amplifier all the time constants in the coupling circuits between stages should be long compared to the collecting time of the ions in the chamber. In practice it is very inconvenient to make the time constants of an amplifier longer than about 1/50 sec. Thus extremely high voltages have to be used to collect the ions in a chamber filled to high pressures. Both of these difficulties could be overcome if it were possible to increase the mobility of the ions in the chamber.

It was first suggested by Ortner and Stetter[4] that one could take advantage of the high mobilities of the free electrons in very pure gases which do not form negative ions, such as hydrogen, nitrogen, and the inert gases. These authors carried out experiments in nitrogen at atmospheric pressure. The nitrogen was carefully purified before it was admitted to the chamber, and it was shown to give saturation at much lower voltages than air at the same pressure. More recently Jentschke and Prankl[5] used purified argon in experiments on the ionization produced by fission fragments, and obtained saturation for α-particles at field strengths as low as three volts/cm in argon at atmospheric pressure. In spite of these successes very few other workers have used purified gases. Probably the main reason for this was the belief that it would be almost impossible, without unusual precautions, to obtain sufficiently high purities to observe free electrons, since early work on the mobility of negative ions had shown that minute traces of electronegative gases decreased the mobility appreciably. It was the object of the present work to investigate the purity necessary to obtain improved saturation characteristics and to study methods of purification which could be used at high pressures and which would not require outgassing the chamber. The measurements of Helbig[6] on the saturation characteristics of unpurified argon seemed to indicate that it might not be necessary to attain such high purities as had been believed earlier.

EXPERIMENTAL METHOD

As a source of ionization the α-particles from polonium were used. The polonium was deposited in a thin layer on a silver foil. The α-particles were collimated by means of a Lucite sleeve 5 mm long. It had three cylindrical holes 2.2 mm in diameter, the axes of the cylinders being perpendicular to the silver foil. The α-particles leaving this sleeve

* Now at Palmer Physical Laboratory, Princeton University, Princeton, New Jersey.

[1] H. H. Barschall and M. H. Kanner, Phys. Rev. **58**, 590 (1940).

[2] G. Jaffé, Ann. d. Physik **42**, 303 (1913); **1**, 977 (1929).

[3] G. Ortner and G. Stetter, Wien. Ber. **142**, 485 (1933).

[4] G. Ortner and G. Stetter, Wien. Anz. **70**, 341 (1933); Physik. Zeits. **35**, 563 (1934).

[5] W. Jentschke and F. Prankl, Physik. Zeits. **40**, 706 (1939).

[6] E. Helbig, Zeits. f. Physik **116**, 444 (1940).

could have a maximum angle of 24° with respect to the axis of the cylinder; their average angle was about 8°.

To collect the ions an ionization chamber with parallel circular brass plates without guard rings was used. The plates were 5 cm in diameter and 2.9 cm apart. The leads to the plates were brought in through the top and bottom of the chamber and were waxed into Lucite insulators. The chamber proper was made of iron and sealed by means of a rubber gasket. The Lucite insulators were waxed into the chamber.

In all the experiments (unless otherwise stated) α-particles whose paths were nearly parallel to the electric field were investigated, since Jaffé's theory of columnar ionization shows that it is most difficult to obtain saturation in this case. To produce a beam of α-particles approximately parallel to the direction of the electric field, the radioactive source with its collimator was placed behind the top plate of the chamber, so that the α-particles could enter the collecting volume through a hole in the center of the plate. The hole in the plate was covered with an aluminum foil of about one-mm air equivalent stopping power to prevent ionization produced in the collimator from being collected.

The collecting voltages were obtained from "B" batteries up to 300 volts and from a transformer-rectifier power supply with three RC filter stages for potentials up to 4000 volts. The values of the collecting field were obtained by dividing the voltages applied to the chamber by the distance between the plates. The effective field may have been somewhat smaller, since no account was taken of the edge effect.

In all the measurements the ionization currents were measured by means of a vacuum tube electrometer, in which a type FP-54 tube was used in the balanced circuit described by DuBridge and Brown.[7] In order to check the sensitivity of the apparatus, a constant potential could be applied to the grid of the tube. This was done by applying a part of the voltage from a dry cell, obtained through use of a high resistance potential divider, to a fraction of the grid leak resistor.

Since the design of the ionization chamber excluded the possibility of outgassing it, a continuous method for purifying the gas in the chamber had to be used, i.e., a method which would remove impurities given off by the inside surfaces of the chamber. For the purification of argon, which was tried first, a method similar to that described by Jentschke and Prankl[8] was used. Pieces of $\frac{3}{8}''$ copper tubing led from the bottom and the top of the ionization chamber to the two ends of a cylindrical purification chamber made of brass. The axes of the two chambers were vertical. The purification chamber was sealed by means of a water-cooled rubber gasket. In order to remove electronegative gases the purification chamber could be filled with about 50 g of calcium turnings. The calcium was supported in the chamber on copper screens so that the gas could pass through the chamber readily. When the argon was to be purified, the purification chamber was maintained at a temperature of about 250°C. The temperature gradients in the system were then sufficient to make the argon circulate.

This method of purification was satisfactory for argon and would undoubtedly be equally applicable to other inert gases, but could not be used for hydrogen or nitrogen, since these gases react with the hot calcium. To remove any oxygen from hydrogen, or mixtures of hydrogen and argon or nitrogen, the calcium was replaced by platinized asbestos which acts as a catalyst in the combination of oxygen and hydrogen to form water vapor. The platinized asbestos was kept at 300°C both to increase the rate of the catalytic reaction and to provide the necessary temperature gradients. To remove the water vapor so formed, or any other traces of water vapor, a second purification chamber containing potassium hydroxide was placed between the chamber containing the platinized asbestos and the ionization chamber. The desiccating agent, in stick form, was supported by spirals of iron wire and cooled with circulating ice water.

RESULTS

Some preliminary experiments were carried out in *air* at one, two, and three atmos. pressure. The saturation curves under these conditions agree reasonably well with those obtained by Jaffé,[8]

[7] L. A. DuBridge and H. Brown, Rev. Sci. Inst. **4**, 532 (1933).

[8] G. Jaffé, Physik. Zeits. **30**, 849 (1929).

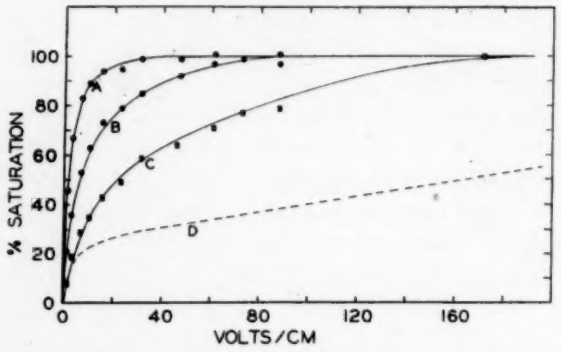

FIG. 1. Saturation curves obtained for α-particles parallel to the electric field in tank nitrogen. Curve *A* represents the results at one atmos., curve *B* at two atmos., curve *C* at three atmos. pressure. Curve *D* is the saturation curve in three atmos. of air.

although he gives slightly higher values for the ratio of ionization current to saturation current. The difference is undoubtedly due to the better collimation of the α-particles used by Jaffé. Our measurements showed about 90 percent saturation for air at two atmos. for a field strength of 1000 volts/cm. In this case the saturation value was obtained by extrapolation according to Jaffé's theory, and by using a graphical method similar to the one described by Zanstra.[9]

Further experiments were carried out in one, two, and three atmos. of *nitrogen*. The nitrogen[10] was oil pumped, and according to the manufacturer had a purity of 99.8 percent. Before the ionization chamber was filled for the measurements, it was flushed several times; but no further purification was attempted. Figure 1 shows the results obtained for nitrogen. The percentage saturation is plotted against the field strength in volts/cm. The saturation current for the curve at three atmos. was obtained from experimental points at high field strengths. For comparison, the saturation curve for air at three atmos. with the same experimental arrangement is also plotted. The figure shows the striking difference between the saturation characteristics of nitrogen and air. No change in the saturation curves for nitrogen was observed when the gas was allowed to enter the chamber through a trap maintained at the temperature of solid carbon dioxide.

[9] H. Zanstra, Physica **2**, 817 (1935).

[10] Purchased from the Ohio Chemical and Manufacturing Company, Cleveland, Ohio.

The next gas investigated was *argon*.[10] According to the manufacturer, the argon had a purity of 99.6 percent. Preliminary measurements showed that the saturation curves for argon depended greatly on how many times the chamber had been flushed with argon and on how long the argon had been in the chamber before the measurements were started; these results indicate a strong dependence on purity. After argon had been purified for about one hour by allowing it to pass over hot calcium, the measurements became quite reproducible. The results in purified argon are shown in Fig. 2. Even at pressures as high as seven atmos., 70 volts/cm were sufficient to obtain saturation, while at one atmos. seven volts/cm gave saturation. In order to study the effect of impurities, air was added to five atmos. of argon. Figure 3 gives the results when two percent and five percent of air, respectively, were mixed with the argon. The effectiveness of the method of purification was tested by purifying for one hour five atmos. of argon to which two percent air had been added. The resulting saturation curve, which is also shown in Fig. 3, agrees with the curve obtained when the tank argon was purified.

Since in some experiments with ionization chambers it might be objectionable to have the gas circulate through the chamber, measurements were taken after the purification chamber was allowed to cool to room temperature. A change in the saturation characteristic was observed after a few hours. The saturation voltage in two atmospheres of argon increased by less than a

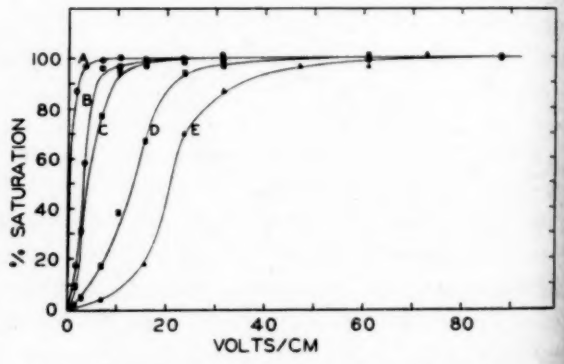

FIG. 2. Saturation curves obtained in argon which was purified by circulating it over hot calcium. The curves were taken at the following pressures: *A*, one atmos.; *B*, three atmos.; *C*, four atmos.; *D*, five atmos.; *E*, seven atmos.

factor of two in a period of twelve hours during which the purification chamber was not operating.

A *mixture of argon and hydrogen* seemed particularly worth investigating, since it might be useful for the measurement of the energies of fast neutrons which produce recoiling protons, the argon serving to stop the protons. According to the manufacturer, the hydrogen had a purity of 99.5 percent. A mixture of three atmos. of argon and one atmos. of hydrogen was used. The saturation curve for this mixture is shown in Fig. 4. In the same figure the curve is given which was obtained after the mixture had been purified for one hour by the use of hot platinized asbestos and potassium hydroxide. Although the effect of the purification is very noticeable, higher field strengths were necessary for saturation in this case than in pure argon. This may be due either to the ineffectiveness of KOH in removing water vapor or to the presence of electronegative gases other than oxygen and water vapor.

Measurements were also carried out for a mixture of nitrogen and hydrogen. The results were very similar to the ones obtained for the argon-hydrogen mixture.

Hydrogen by itself is known[8] to saturate relatively easily. The effect of purification by the use of platinized asbestos and KOH was investigated. It was found that the saturation characteristics were improved by purification, but not as much as in the case of argon.

When the polarity of the collecting voltage was reversed, no change in the voltage necessary for saturation was observed. In the case of purified argon, however, the shape of the lower part of the saturation curve depended on the polarity of the collecting voltage. When the top electrode, near which the ionization took place, was made positive the saturation curves rose more steeply in the initial portion than is shown in Fig. 2. This finding agrees with the observations of Ortner and Stetter[4] in purified nitrogen.

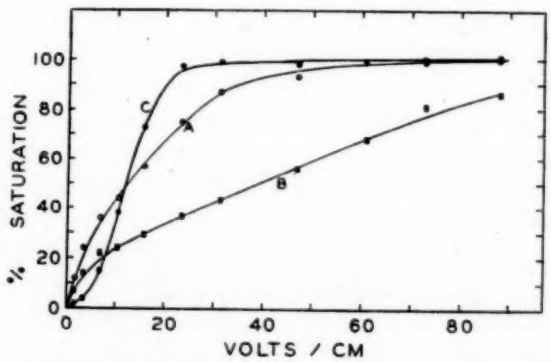

FIG. 3. Curve *A*: Saturation curve in five atmos. of argon plus two percent air. Curve *B*: five atmos. of argon plus five percent air. Curve *C*: Same as *A*, but purified by circulating mixture over hot calcium.

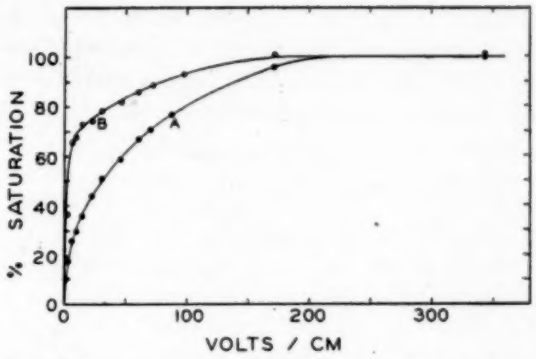

FIG. 4. Saturation curve for mixture of three atmos. of argon plus one atmos. of hydrogen. Curve *A* was taken in the mixture as obtained from the tanks. For Curve *B* the mixture was circulated over hot platinum asbestos and KOH.

An attempt was made to obtain a saturation curve while the radioactive source (without collimator) was placed half way between the two electrodes. For this measurement the surface of the source was parallel to the axis of the chamber and in a plane roughly tangential to the two electrodes. It was electrically at ground potential. Whereas with the source in this position ordinary saturation curves were obtained in air, hydrogen, and argon at one atmos., quite anomalous curves were found in purified argon at higher pressures. The curves showed a maximum at relatively low voltages and then dropped to a considerably smaller saturation value. The height of the maximum increased with both increasing purity of the gas and increasing pressure. Any change in the potential at which the source was kept altered the shape of the curve completely. The only explanation which seemed to cover all these phenomena was to assume that electrons formed by the α-particles in the neighborhood of the source were driven by the electric field against the source and its support. These electrons might then eject secondary electrons. This hypothesis was tested by painting the support of the source with colloidal graphite, which is known[11] to give little

[11] B. H. Porter, Rev. Sci. Inst. 7, 101 (1936).

secondary emission. It was found that the graphite reduced the height of the peak considerably. This bears out the assumption that the peak was due to secondary emission.

DISCUSSION

While Jaffé's theory of columnar ionization is well established, it seems likely that this theory is not applicable when the ionization is produced in the absence of electronegative gases. In this case the diffusion of the ions is probably so rapid that the columnar arrangement of the ions becomes less important than the general diffusion. Furthermore a comparison with theory is rendered difficult by the lack of sufficient experimental data on the recombination and diffusion coefficients in purified gases.

Since Warburg's[12] discovery of the effect of minute traces of electronegative gases on the conduction of electricity through gases, a number of authors[13] have investigated the effect of impurities on the mobility of negative ions. Franck's[14] experiments in argon showed that the mobility of the negative carriers in argon was decreased from 206.3 to 1.7 cm/sec./volt/cm when 1.2 percent oxygen was added. According to Haines[15] the mobility of the negative ions in nitrogen decreased from 158 to 88 cm/sec./volt/cm when 0.05 percent oxygen was added, and to 11 with 0.7 percent of oxygen.

The effect of the addition of two percent of air (0.4 percent of oxygen) to purified argon in the present measurements (see Fig. 3) seems to be relatively small, whereas measurements on ionic mobilities would lead one to expect a decrease of the mobility by a factor of 10 in this case.

A possible explanation for a smaller effect of impurities in measurements of saturation curves might be that a free electron would have to travel only a very short distance to leave the ion column. It then would be sufficiently separated from the positive ions to avoid recombination, even if it were to form a negative ion before it reached the electrode. In order to be observable in measurements of ion mobilities, the electron would have to travel considerably farther without encountering an electronegative molecule.

The occurrence and size of a peak in some of the saturation curves, which we believe was caused by secondary electron emission from the source, seemed to be more sensitive to the presence of impurities. This finding agrees with the above consideration, since to cause secondary emission the electron actually has to travel from its place of formation to the source.

The relatively small effect of impurities on the saturation characteristics may be understood from a different point of view according to Jaffé.[16] In the theory of columnar ionization[8] it is shown that the saturability depends only on the ratio of the diffusion coefficient (or mobility) to the recombination coefficient. If impurities are added to a very pure gas, both the mobility and the coefficient of recombination will decrease, but the ratio of the two will change less rapidly with added impurities than the mobility.

A striking feature of the saturation curves in purified argon at high pressure (see Fig. 2) is their increasing slope at low field strengths. An explanation of this unusual shape according to Jaffé[16] can be found in a calculation by J. J. Thomson[17] concerning the current between two parallel plates when the ionization is confined to a thin layer. This calculation is applicable to the present measurements, because at higher pressures the ionization is increasingly limited to a small region near the top plate. In pure argon the diffusion of the negative carriers is probably sufficiently rapid so that the ion columns spread into a layer. Thomson's calculation yields the result that in this case the ionization current is proportional to the square of the potential difference between the plates and directly proportional to the mobility of the ions moving away from the plate near which the ionization is produced. The curves shown in Fig. 2 may be approximated in their initial portion by a parabola according to Thomson's formula. The fact that the rise of the ionization curves is considerably more rapid when the upper plate is made negative is also in agreement with this idea, since in the absence of electronegative gases the mobility of the negative

[12] E. Warburg, Ann. d. Physik **2**, 295 (1900).
[13] See J. J. Thomson, *Conduction of Electricity through Gases* (Cambridge University Press, London, 1928), Vol. I, p. 133.
[14] J. Franck, Verh. d. Deutsch. Phys. Ges. **12**, 291 (1910).
[15] W. B. Haines, Phil. Mag. **30**, 503 (1915).
[16] Private communication from Professor G. Jaffé.
[17] J. J. Thomson, *Conduction of Electricity through Gases* (Cambridge University Press, London, 1928), Vol. I, p. 206.

carriers is so much greater than that of the positive ions.

Whereas no measurements are available with which the present saturation curves in purified gases could be compared, a saturation curve at one atmos. of tank argon was taken for α-particles at right angles to the electric field. This can be compared with Helbig's[6] curve taken under similar conditions. While the argon used by us was supplied as 99.6 percent pure, Helbig's measurements were carried out in argon supplied as 99.5 percent pure. The two curves agree closely, both giving saturation at a field strength of about 18 volts/cm. It is interesting to note that this value is more than twice as great as the field strength required for saturation in purified argon at the same pressure when the paths of the α-particles are parallel to the field.

We wish to thank Professor J. D. Stranathan for many interesting discussions, and Professor H. P. Cady for his helpful advice on the purification of gases.

JANUARY 1 AND 15, 1943 PHYSICAL REVIEW VOLUME 63

The Angular Correlation of Successive Gamma-Rays*

ROBERT BERINGER
Sloane Physics Laboratory, Yale University, New Haven, Connecticut
(Received October 22, 1942)

The angular dependence of gamma-gamma coincidences has been studied for Na^{24}, Cl^{38}, and Br^{82} in an attempt to evaluate the predicted angular correlations between successive quanta. The coincidence rates were found to be independent of the relative directions of the quanta to within a few percent except as the counters approached each other closely, where an increase was observed. This increase was attributed to scattered quanta and was measured by an independent method.

INTRODUCTION

IT has been pointed out by Pryce and Dunworth[1] that correlations are to be expected between the directions of quanta emitted in cascade from an excited nucleus, due to the coupling between the emitted quantum and the anisotropic radiation field of the preceding quantum. D. R. Hamilton[2] has calculated these spatial correlations for two successive dipole or quadrupole transitions involving three radiation levels. Since this analysis shows that the correlations are determined by the multipole orders of the transitions and the spins of the levels involved, some knowledge of these important quantities should be gained from experimental determinations of the directional correlations.

Several workers,[1,2] using coincidence counting methods, have failed to observe any angular dependence in the rate of gamma-ray coincidences from such sources of successive quanta. Recently, however, Watase,[3] using Cl^{38} gamma-rays, reported a marked difference between the double coincidence rate from quantum pairs having directions differing by π radians and $\pi/2$ radians. No directional dependence in the coincidence rate was observed with Na^{24} gamma-rays.

The present paper describes angular coincidence experiments of somewhat greater completeness than have heretofore been reported. Several extraneous effects inherent in this kind of coincidence experiment are discussed and evaluated.

THE COINCIDENCE METHOD

If $W(\theta)$ represents the probability that two coincidence quanta 1 and 2 be emitted from a point source with a relative angle of θ between their directions, and if two counters of vanishingly

* This paper together with reference 5 is part of a thesis presented to the Graduate School of Yale University for the Degree of Doctor of Philosophy.

[1] J. V. Dunworth, Rev. Sci. Inst. **11**, 167 (1940).

[2] D. R. Hamilton, Phys. Rev. **58**, 122 (1940).

[3] Y. Watase, Proc. Phys. Math. Soc. Japan **23**, 618 (1941).

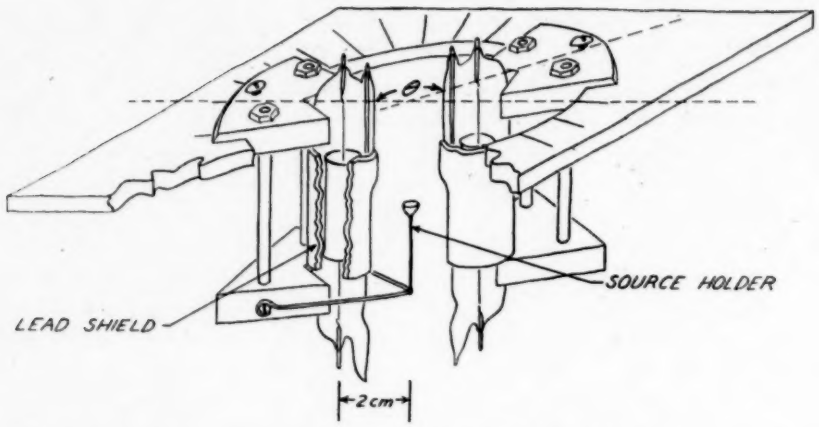

FIG. 1. Counter arrangement showing part of the circular track cut away. The track and counter cradles are brass. The source holder is aluminum foil. The counter to the right is movable from $\theta=60°$ to $\theta=300°$.

small aperture are symmetrically situated so as to intercept such quanta and are connected to an ideal amplifier, the number of true coincidence counts per single count in one counter is

$$C/N=[2\epsilon_1\epsilon_2/(\epsilon_1+\epsilon_2)]W(\theta), \quad (1)$$

where ϵ_1 and ϵ_2 are the net counter efficiencies (including counter aperture) for the respective quanta. In practice, the variation of quantum efficiency over the sensitive counter aperture and the imperfect spatial resolution of the counter set must be considered. The first effect is probably small,[4] while the second is easily calculated for a symmetrical arrangement of source and counters. Both effects may be included in the θ dependent term, and will tend to make the observed variation of C/N with θ somewhat less than the true variation given by $W(\theta)$. When correction has been made for the angular aperture of the counter set, the observed variation of C/N with θ gives $W(\theta)$ to within a multiplicative constant, since for a symmetrical counter arrangement $2\epsilon_1\epsilon_2/(\epsilon_1+\epsilon_2)$ is not a function of the angular settings of the counters. It is this function $W(\theta)$ which is related to the level spins and multipole orders in Hamilton's calculations.

In addition to any intrinsic angular dependence in C/N, the counters will themselves impose a variation of coincidence rate with θ, since they are composed of scattering material. Such coincidences are most probable for the penetration of both counters by a Compton electron originating at one of the counters. Fortunately, these coincidences are easily eliminated by surrounding the counters with absorbing shields. However, the less prevalent coincidences in which the recoil electron traverses one counter and the scattered quantum discharges the second counter cannot be avoided. The coincidence rate from this process may be represented as

$$N\varphi(\theta)\epsilon, \quad (2)$$

where N is the single counting rate, and $\varphi(\theta)$ a probability depending explicitly on θ and implicitly on the quantum energy. This factor $\varphi(\theta)$ could be calculated from the known angular spreads of recoil electrons and scattered quanta. However, it can be measured directly by using sources which emit no coincidence quanta. In such an experiment, the observed coincidence rate is

$$A'=A+N\varphi(\theta)\epsilon, \quad (3)$$

where A is the usual accidental coincidence rate $2\tau N^2$, τ being the resolving time of the coincidence set. It should be noted that in principle N will itself be a function of θ. Actually, this increase in N as the counters approach each other is quite negligible, being of the order of $N\varphi(\theta)\epsilon$.

A further variation of coincidence rate with θ may be due to beta-ray or gamma-ray pair production and subsequent two-quantum annihilation of the positrons in the source region. This is easily identified by the sharp maximum in the rate of coincidences at the in-line position of

[4] D. L. Jorgensen, Rev. Sci. Inst. 10, 34 (1939).

source and counters.[5] The elimination of absorbing material around the source makes this effect quite negligible.

If the angular resolving power of the coincidence apparatus is to be good, high single counting rates must be employed for a reasonable time of experiment. This is particularly true because of the low values of gamma-ray counter efficiencies. The angular aperture of the counter set shown in Fig. 1 was 0.75 steradian. The counters had copper cathodes and were filled with a mixture of 94 percent argon and 6 percent oxygen to a pressure of 9 cm of mercury.[6] One counter was kept fixed and the other moved on a circle about the source position. The cradles holding the counters were designed to keep scattering materials behind the sensitive counting volumes.

The coincidence amplifiers were of the usual three-stage resistance-capacity coupled design. The pre-amplifiers were a modified Neher-Pickering type.[7] Rossi pulse adding was employed with a grid-biased thyratron as coincidence discriminator. The smallest coupling condensers and resistors which permitted full saturation of the Rossi tubes were used throughout. The various grid and plate voltages were taken from glow-tube regulated voltage supplies backed with a constant voltage transformer. The high voltage counter supply used Street and Johnson[8] vacuum-tube regulation.

Single counting rates were measured with a hard-tube scale-of-sixteen[9] and self-quenching thyratron recording circuit. The single counting losses measured with "added sources"[10] and from the decay of sources of known half-life[11] were found to be in good agreement with the relation given by Alaoglu and Smith[12] in their analysis of single counting losses in a system composed of a counter, amplifier, scaling circuit, and recorder. By making use of their criteria, it was concluded that no counts were lost in the scaling circuit or recorder. For this case, the observed single counting rate is given by $N'=N/(1+N\sigma)$. For the amplifiers used, σ had a value of $8.0(10)^{-4}$ sec. This rather large resolving time could be associated only with the counter quenching circuit, and so it was probable that most of the single counting losses occurred at the counters themselves rather than in the amplifiers.

A study was made of the constancy of the coincidence resolving time τ, and it was found to increase with an increasing frequency of counter pulses arriving at the adding stage of the amplifier shown in Fig. 2. The effect was less pronounced as the adding resistance R was diminished, but the variation in τ could not be entirely eliminated.

In addition to the loss of single counts and the variation of coincidence resolving time with counting rate, there was an observed loss of true coincidence counts at high counting rates. This effect, unlike the other two, could not be evaluated quantitatively.

Notwithstanding the difficulties discussed, it was possible to determine the form of the angular correlation function $W(\theta)$ with considerable precision, by standardizing the single counting rates. The method which was used is outlined as follows: The observed coincidence rate over a coincidence counting interval of t_2 seconds is

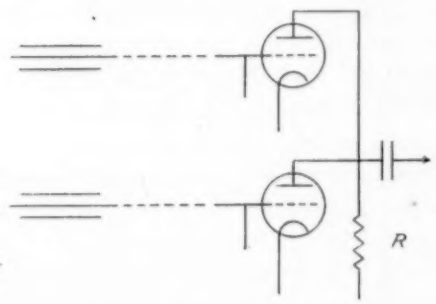

FIG. 2. Schematic circuit of the double coincidence amplifier showing the "adding resistance" R.

$$\bar{C}'+2\bar{\tau}\frac{1}{t_2}\int_0^{t_2}N_0^2e^{-2\lambda t}dt$$

for a source of coincidences with a decay constant λ, where $\bar{\tau}$ is the coincidence resolving time observed with a very slowly decaying source emitting no true coincidences and of such

[5] R. Beringer and C. G. Montgomery, Phys. Rev. **61**, 222 (1942).
[6] C. G. Montgomery and D. D. Montgomery, J. Frank. Inst. **231**, 447–467, 509–545 (1941).
[7] T. H. Johnson, Rev. Sci. Inst. **9**, 218 (1938).
[8] Street and Johnson, J. Frank. Inst. **214**, 155 (1932).
[9] H. Lifschutz and J. L. Lawson, Rev. Sci. Inst. **9**, 83 (1938).
[10] Duffendack, Lifschutz, and Slawsky, Phys. Rev. **52**, 1231 (1937).
[11] A. Flammersfelt, Zeits. f. Physik **122**, 729 (1939).
[12] L. Alaoglu and N. M. Smith, Phys. Rev. **53**, 832 (1938).

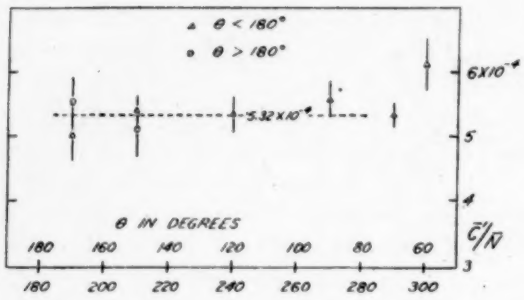

FIG. 3. The number of double coincidences per single count for Na^{24} gamma-rays as a function of the relative angle between the counters at the source.

strength as to produce

$$\bar{N}=\frac{1}{t_2}\int_0^{t_2} N_0 e^{-\lambda t}dt$$

single counts per second. The coincidence rate $\bar{C}'$ is then known, as is the ratio $\bar{C}'/\bar{N}$, which, if no true coincidence counts were lost, would be given by formula (1). When coincidences are lost in the counters and circuits, the factor $[2\epsilon_1\epsilon_2/(\epsilon_1+\epsilon_2)]W(\theta)$ in formula (1) must be multiplied by some complicated function of N containing various circuit constants as parameters. Since this loss term is a function only of the single counting rate for a given amplifier, it may be neglected in comparing observations for which the single counting rates are the same. For such a procedure, the variation of $\bar{C}'/\bar{N}$ with θ gives the form of $W(\theta)$ independently of the several kinds of counting losses.

In the early measurements, various values of $\bar{N}$ were used. These data showed systematic trends which could be attributed to the loss of coincidences at high counting rates. For the later measurements, a constant mean single counting rate was employed in the manner outlined. The coincidence resolving time $\bar{\tau}$ was determined frequently at this mean single counting rate using Ra gamma-rays as a source of accidental coindidences. A small, regular variation of $\bar{\tau}$ around a mean of about two microseconds was observed over periods of several weeks, and was attributed to slow changes in tube characteristics.

Na^{24}

The radiations from the 14.8-hour sodium activity have been widely studied and several level schemes have been advanced. The gamma-ray spectrometer experiments of Curran, Dee, and Strothers[13] and the coincidence experiments of Feather and Dunworth[14] indicate four gamma-ray levels with two modes of quantum dexcitation. Two quanta of 3.0 and 1.5 Mev are emitted in cascade in one mode, and two quanta of 2 Mev in the other mode. This second mode is of much lower intensity. The recent gamma-ray spectrometer experiments of J. Itoh[15] do not show the 2 Mev component, but give a three-level scheme, with two quanta of 2.8 and 1.4 Mev in cascade.

Sodium chloride sources of high specific activity were prepared by deuteron bombardment in the Yale cyclotron. Aged samples, free from Cl^{38} activity, were used for coincidence counting, prepared as pellets about 2 mm in diameter.

The variation of $\bar{C}'/\bar{N}$ with θ was measured twice without controlled singles rates and once with $\bar{N}=70$ sec.$^{-1}$. Each of the three runs showed no angular correlation in the range $90°\leqslant\theta\leqslant 270°$. Outside of this range, the coincidences rose rapidly as the counters approached each other. This rise was attributed to Compton coincidences. Figure 3 shows one set of data, and the results of the three runs are summarized in Table I. The mean $\bar{C}'/\bar{N}$ in Table I was calculated under the assumption of no correlations in the range $90°\leqslant\theta\leqslant 270°$. The agreement of the theoretical standard deviations in the mean $\bar{C}'/\bar{N}$, with the mean experimental deviations calculated from the number of coincidence counts used to determine each point, makes this assumption reasonable. One can say that angular correlations in $\bar{C}'/\bar{N}$ are less than 3 percent statistically. The curves indicate that correlations at any particular angular setting are less than 10 percent. The mean $\bar{C}'/\bar{N}$ is different in the three cases, being

TABLE I. Test for angular correlation.

Run	Mean $\bar{C}'/\bar{N}$ for $90°\leqslant\theta\leqslant 270°$	Standard deviation in mean $\bar{C}'/\bar{N}$	Mean experimental deviation in $\bar{C}'/\bar{N}$	R
1	$5.32(10)^{-4}$	$0.13(10)^{-4}$	$0.18(10)^{-4}$	10^4 ohm
2	4.64	0.06	0.21	10^5
3	5.20	0.12	0.22	$5(10)^4$

[13] Curran, Dee, and Strothers, Proc. Roy. Soc. **A174**, 546 (1940).
[14] N. Feather and J. V. Dunworth, Proc. Camb. Phil. Soc. **34**, 442 (1938).
[15] J. Itoh, Proc. Phys. Math. Soc. Japan **23**, 605 (1941).

higher for runs 1 and 3, where the "adding resistance" of the coincidence amplifier (see Fig. 2) was smallest.

Cl^{38}

The gamma-rays from 37.5-minute Cl^{38} have been observed by many workers, in particular by Curran, Dee, and Strothers[13] and J. Itoh.[15] Their experiments are in essential agreement, indicating two gamma-rays in cascade, with perhaps a third quantum of the same energy as the second of the cascade quanta. Itoh gives the energies as 2.2 and 1.6 Mev.

The Cl^{38} sources were prepared by deuteron bombardment of LiCl in the Yale cyclotron. Decay curves showed inappreciable contamination up to five hours after bombardment; beyond this time a small 15-hour activity, presumably from Na^{24}, was evident. In the coincidence experiments, chemically separated pellets of Cl^{38} in the form of AgCl were used and showed no contamination.

The results of the angular coincidence experiments are shown in Fig. 4. The mean single counting rate for each of these observations was 50 sec.$^{-1}$. As in the case of Na^{24}, no angular

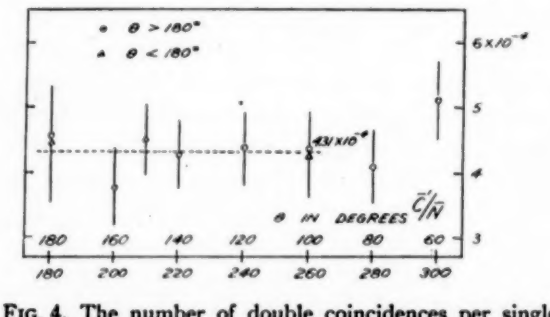

FIG. 4. The number of double coincidences per single count for Cl^{38} gamma-rays as a function of the relative angle between the counters at the source.

correlation was observed. The mean experimental deviation from the mean $\bar{C}'/\bar{N}$ was $0.17(10)^{-4}$ as compared with the theoretical standard deviation in the mean of $0.22(10)^{-4}$. Thus correlations are less than four percent statistically and less than about ten percent at any particular value of θ. This is in disagreement with the previous report which gave $(C/N)_{\theta=180°}/(C/N)_{\theta=90°}=0.85$ from coincidence counting at these two positions.

Br^{82}

Several recent studies of the gamma-rays from 36-hour Br^{82} have been reported.[16,17] Roberts, Downing, and Deutsch[16] give a level scheme with three gamma-rays of 0.547, 0.787, and 1.35 Mev in cascade. It was thought to be of some interest to see whether any angular correlations were detectable for this three-quantum process.

Br^{82} was produced by the bombardment of ethylene-dibromide with slow neutrons from the

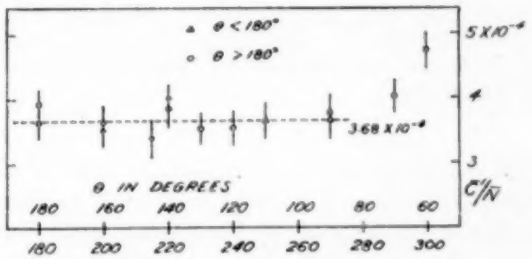

FIG. 5. The number of double coincidences per single count for Br^{82} gamma-rays as a function of the relative angle between the counters at the source.

Yale cyclotron. The active sample was concentrated by gravity separation in aqueous solution and the radio-bromine precipitated as AgBr, which was then aged for twenty-four hours before counting. The results of the angular coincidence experiments are shown in Fig. 5. The mean single counting rate for each of these observations was 70 sec.$^{-1}$. As before, no angular correlation is indicated in the range $90°\leqslant\theta\leqslant270°$. In this range, the theoretical standard deviation from the arithmetic mean $\bar{C}'/\bar{N}$ of $3.68(10)^{-4}$ was $0.08(10)^{-4}$ and the mean observed deviation was $0.14(10)^{-4}$. Angular correlations are less than four percent statistically.

THE COMPTON COINCIDENCES

In each of the angular coincidence experiments, an increase in the coincidence rate was observed as the counters approached each other, as is to be expected for the Compton coincidences given by formula (2). This quantity $N\varphi(\theta)\epsilon$ was evaluated by means of formula (3), using Cu^{64} positron annihilation radiation as a source of uncorrelated quanta, which is valid in the region outside of the

[16] Roberts, Downing, and Deutsch, Phys. Rev. **60**, 544 (1941).
[17] J. Rotblat, Nature **148**, 371 (1941).

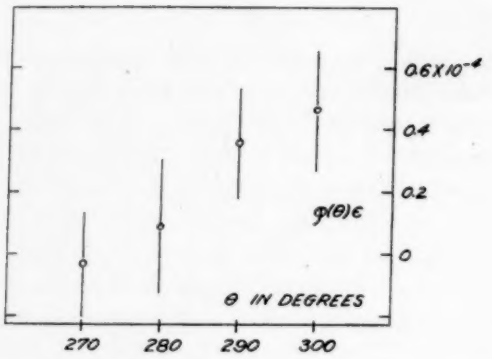

FIG. 6. The number of double coincidences per single count for Cu^{64} positron annihilation radiation as a function of the relative angle between the counters at the source. The coincidences are attributed to Compton scattering of the quanta.

allowed cone for two-quantum annihilation coincidences.[5]

The sources were prepared by bombarding copper foils with deuterons in the Yale cyclotron. The activated samples were then pressed into small pellets and wrapped in enough lead to stop all of the positrons. The results are shown in Fig. 6. The rise in the number of coincidences per single count from $\theta=270°$ to $\theta=300°$ is about $0.5(10)^{-4}$; slightly smaller than the contributions observed in Figs. 3, 4, and 5, but in accord with the low counter efficiency for the 0.5-Mev annihilation quanta.

THE COUNTER EFFICIENCY

Direct measurements of the gamma-ray counter efficiencies were not carried out. However, a comparison of the coincidence rates from the various sources was made, in which we used the generally accepted form of the change of efficiency with quantum energy for counters with copper cathodes as given by Dunworth and von Droste[1] and recently checked by Roberts, Downing, and Deutsch.[16] The coincidence rates under comparison were all taken at about the same mean single counting rate and with the same amplifiers. The scale of the efficiency curve was fixed with the measured $\bar{C}'/\bar{N}$ for Na^{24} of $5.2(10)^{-4}$, and by the four level scheme and the energies given by Curran, Dee, and Strothers.[13] The value of $\bar{C}'/\bar{N}$ calculated from this curve for Cl^{38} was $4.7(10)^{-4}$ for Itoh's level scheme,[15] which is in good agreement with the observed value of $4.3(10)^{-4}$. For Br^{82} the calculated value of $4.2(10)^{-4}$, obtained from the level scheme of Roberts, Downing, and Deutsch,[16] is in fair agreement with the observed value of $3.7(10)^{-4}$.

DISCUSSION

The lack of observed spatial correlations in the gamma-gamma coincidences from Cl^{38} and Na^{24} indicates that for these elements, this method of assigning level spins is not sufficiently sensitive under the limitations of present counting techniques. These negative results obtained do not constitute a check of the theory, since some of the calculated correlations are within the experimental errors. Further, nothing can be said as to which of these calculated correlations is most probable, since nothing is known of the level spins of these elements. The results of the experiments are therefore without satisfactory explanation, and a check of the theory must be made in a case in which the multipole orders and level spins can be independently assigned. Even if the theoretical predictions are verified, it is believed that considerable improvements must be made in counting methods, particularly as regards permissible resolving times, before the method of angular correlations can be used as a reliable means of investigating nuclear angular momenta.

Electron Polarization

C. G. SHULL,* C. T. CHASE, AND F. E. MYERS†
Department of Physics, New York University, University Heights, New York, New York
(Received October 13, 1942)

The double scattering experiment has been repeated with a 400-kev beam of electrons obtained from a Van de Graaff electrostatic generator. The electrons are scattered by thin gold foils and are counted by Geiger-Müller counters. After eliminating spurious asymmetries, a polarization asymmetry of 8 percent for gold foils is found, which becomes 1 percent in the opposite direction when an aluminum foil is inserted in place of one of the gold foils. Reducing the atomic number of the scattering centers in this way should reduce the theoretical polarization asymmetry to a much smaller value. The reflection-transmission effect found by Chase and Cox has been confirmed and is shown to play an important part in polarization experiments. A reflection polarization experiment (in which only electrons which have been "reflected" from the inclined foils are studied) is shown to produce a much smaller asymmetry than does a transmission polarization experiment (in which only electrons which have been transmitted through the inclined foils are studied). A final polarization ratio of 1.12 ± 0.02 is obtained for comparison with the theory.

I. INTRODUCTION

IN a number of experiments, starting with that of Cox, McIlwraith, and Kurrelmeyer[1] in 1928, the attempt has been made to find evidence of polarization in a beam of free electrons. The early experiments were made without the guidance of any clear theory, their methods being suggested by analogy with phenomena of light or x-rays or with the Stern-Gerlach experiment. The results were either negative or were rendered questionable by the results of later experiments or by theoretical developments.

The most recent experiments have been guided by Mott's theory. Using the Dirac equations in treating the scattering of electrons by atomic nuclei, Mott[2] has shown that under suitable conditions a beam of initially unpolarized electrons (no preferential spin direction) will become partially polarized (more spin axes pointing in one direction than in any other) upon scattering by atomic nuclei. By projecting a beam of electrons onto a thin foil (polarizer), and passing some of the scattered electrons onto a second thin foil (analyzer), one should observe a difference in the number of electrons scattered in the two directions F_2S and F_2N, cf. Fig. 1. The two positions S and N will be referred to in the later discussion as the anti-parallel (180°) and parallel (0°) positions, respectively.

In order that the polarization ratio η (the ratio of the number of electrons scattered in the direction F_2S to the number scattered in the direction F_2N) be not too close to unity, the following experimental conditions should be fulfilled:

(1) Energy of the incident electrons should not be too small,
$$E>30 \text{ kev}.$$

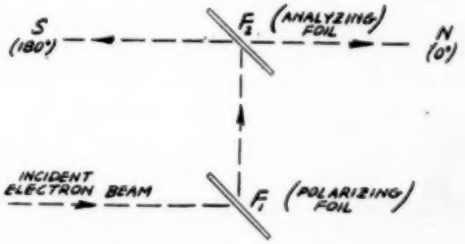

FIG. 1. Schematic diagram of experiment.

(2) Atomic number (Z) of the scattering nuclei should be such that
$$(Z/137)^2 \sim 1.$$
(3) Scattering angles should be large, comparable with 90°.
(4) Scattering foils should be thin enough to insure single scattering.

The variation of η with electron energy as calculated by Mott for gold with scattering angles

* Now with The Texas Company, Beacon, New York.
† Now at Frankford Arsenal, Philadelphia, Pennsylvania.
[1] R. T. Cox, C. G. McIlwraith, and B. Kurrelmeyer, Proc. Nat. Acad. Sci. **14**, 544 (1928). Some of the first experiments are described by G. P. Thomson, *Wave Mechanics of Free Electrons* (McGraw-Hill Book Company, New York, 1930). Most of the others are listed by F. E. Myers, J. F. Byrne, and R. T. Cox, Phys. Rev. **46**, 777 (1934).
[2] N. F. Mott, Proc. Roy. Soc. **124**, 425 (1929); **135**, 429 (1932).

of 90° can be seen in Fig. 2. Bartlett and Watson[3] have published recalculations of the equations used in Mott's treatment and their values are also shown in this graph. Recently, Massey and Mohr[4] have considered the effect of nuclear screening by the extra-nuclear electrons upon the expected polarization asymmetry values. Their results are also shown in Fig. 2. Unfortunately, the Massey-Mohr calculations did not consider electronic energies as high as those actually used in the present experiment. It might be mentioned, however, that the Massey-Mohr curve should merge into the Bartlett-Watson curve at the higher energies, where nuclear screening becomes less effective.

Of the several experiments on electron polarization which have been performed during the last decade, those of Dymond[5] and Richter[6] are perhaps the most noteworthy, in that they met the above experimental requirements most faithfully. Dymond scattered electrons of energy 160 kev from thin gold foils and obtained *no* polarization asymmetry within his experimental error of 1 percent. Using electrons of 120-kev energy and photographic technique in the determination of scattered intensity, Richter also has reported no observable effect. Kikuchi[7] has recently reported a positive effect but his use of thick scattering targets makes his results open to question. All of these experiments will be discussed in greater detail in a later section of this paper.

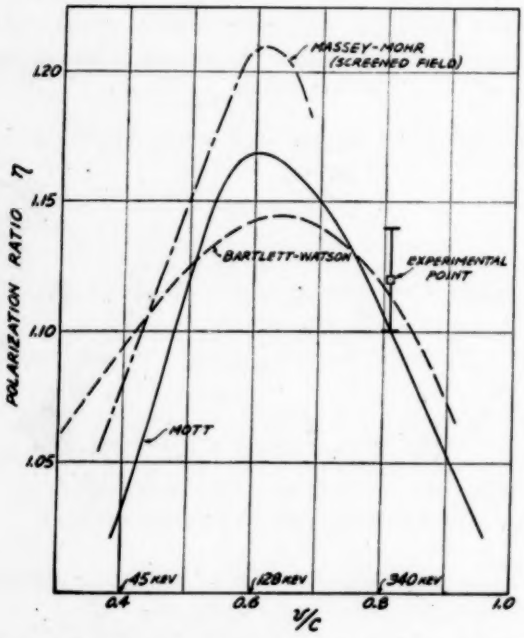

FIG. 2. Theoretical values for the polarization ratio as a function of the velocity v of the scattered electrons. ($c=3\times10^{10}$ cm/sec.).

II. EXPERIMENTAL APPARATUS

A. Electron Beam

The incident electron beam was obtained from a Van de Graaff electrostatic generator. The beam (normally 0.5–2μa) enters the scattering chamber through an insulated quadrant assembly (similar to that used on the electrostatic generator at M. I. T.). Four insulated steel quadrants surround the entrance diaphragm and each quadrant is connected electrically to ground through a small condenser shunted by a ½ watt neon "blinker" tube. Frequency of blinking is thus a measure of beam position. Convenient control over the beam spot position is afforded by two large field coils used for neutralizing the earth's magnetic field along the beam trajectory.

A string of calibrated resistances was used in measuring the voltage of the generator. No great accuracy is claimed in the absolute voltage determination, but the voltage was maintained constant by a stabilizing circuit which controlled the spray current on the charging belts. Variations in voltage were thus kept less than ½ of one percent. In a polarization experiment of this type, it is much more important to keep the energy of the electrons constant than to know that energy absolutely. For all of the data presented in this paper, the energy of the scattered electrons was 400 kev.

B. Scattering Chamber

Detail of the scattering chamber is shown in Fig. 3. The scattering chamber was designed so as to permit study of and correction for any spurious asymmetries which might mask the true

[3] J. H. Bartlett and R. E. Watson, Phys. Rev. **56**, 612 (1939).
[4] H. S. W. Massey and C. B. O. Mohr, Proc. Roy. Soc. **A177**, 341 (1941).
[5] E. G. Dymond, Proc. Roy. Soc. **A145**, 657 (1934).
[6] H. Richter, Ann. d. Physik **28**, 533 (1937).
[7] K. Kikuchi, Proc. Phys. Math. Soc. Japan **22**, 805 (1940).

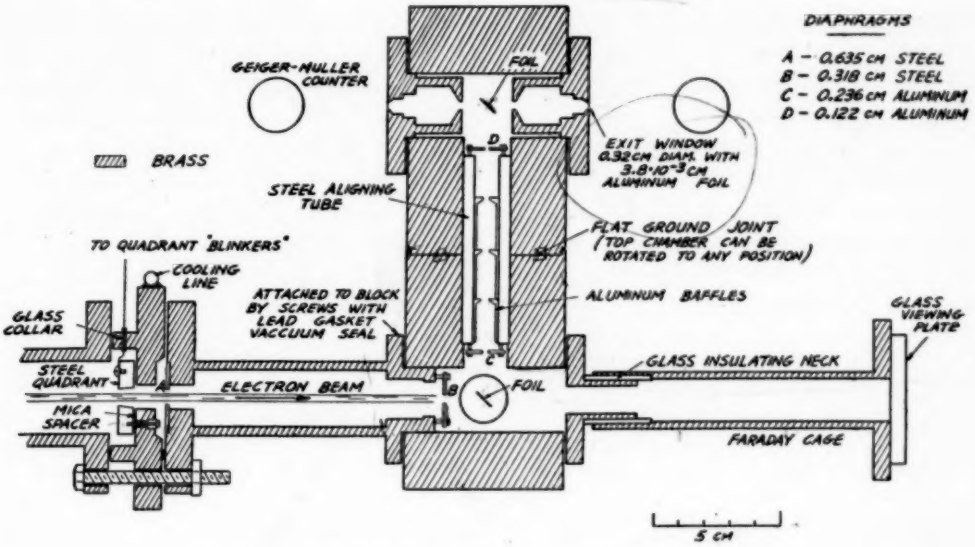

FIG. 3. Scattering chamber assembly.

polarization effect. These asymmetries will be considered at greater length in a later section.

Electrons which have been scattered at the first foil through angles of 90° pass up through two limiting diaphragms and three baffle diaphragms (all of aluminum) to the second foil. Those which are again scattered through angles of 90° pass through thin exit windows of aluminum ($t=3.8\times10^{-3}$ cm) and thence into Geiger-Müller counters. Simultaneous counting is done at the two positions, thereby eliminating the need for monitoring the incident beam.

The scattering chamber was constructed from two brass blocks which were joined together by a vacuum-tight flat ground joint. The analyzing chamber (containing the second scattering foil) could rotate about the vertical axis connecting the two foils without disturbing the vacuum system.

C. Scattering Foils

The foils were prepared by evaporating gold upon a thin collodion sheet and the collodion was dissolved away later in several rinses of acetone. The foil thickness was calculated according to the inverse-square law of deposition as 4.1×10^{-5} cm. Since the foils are inclined at an angle of 45° with the incident electron direction, the effective foil thickness was 5.8×10^{-5} cm—a value nearly four times thinner than the maximum thickness allowed by Wentzel's criterion for single scattering. It would appear that on the basis of Wentzel's criterion, single scattering is clearly insured.

The foils are mounted over quarter-inch holes cut in small tantalum strips. An uncovered, identical quarter-inch hole, adjacent to the one covered by the foil, can be inserted into the beam path by means of a sylphon bellows so as to permit investigation for electrons scattered from the chamber walls, foil holders, etc. Furthermore the whole foil assembly can be rotated 90° about an axis perpendicular to the plane of scattering.

D. Counters and Electrical Circuits

The Geiger-Müller counters were placed immediately outside the exit windows on the two sides of the second scattering foil. Because the counter area exposed toward the foil is considerably larger than the solid angle permitted the electrons by the exit window, counting rates should be independent of counter position. The counters, of thin-walled glass construction, were filled with argon (9-cm pressure) and alcohol vapor (1-cm pressure), and were operated at voltages of 1100 volts (about 100 volts above threshold) obtained from a stabilized power pack. Unfortunately in counting electrons of 400-kev energy, a rather large counter asymmetry developed. This asymmetry, due to a difference in wall thickness, was

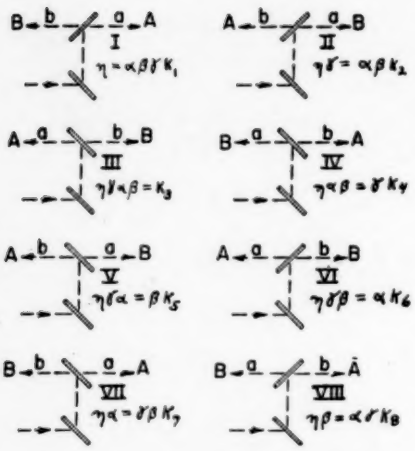

FIG. 4. Diagram which shows the eight different orientations that are possible with the analyzing foil set in the transmission orientation. *A* and *B* represent the two Geiger-Müller counters while *a* and *b* refer to the two exit faces of the analyzing chamber.

eliminated, however, in the calculation of the polarization asymmetry.

Each counter had its own electrical recording circuit consisting of a three-stage amplifier, a pulse skimmer (for elimination of small extraneous pulses), a scale-of-eight scaling circuit, and a mechanical recorder. The circuit pulses were continuously observed and checked with a cathode-ray oscilloscope. Inverse square tests were performed on the counters and their associated circuits and they seemed perfectly reliable with counting rates as high as 1500 per minute. In taking the actual data, counting rates were nearly always below 1000 per minute.

III. COLLECTION AND ANALYSIS OF DATA

Great care must be taken either to eliminate or correct for spurious asymmetries in an experiment of this kind. If no experimental asymmetries were present, then a direct comparison of the rates at the two positions, parallel and anti-parallel, would give the desired polarization result immediately. Three effects are recognized, however, which might contribute to the experimental result and these will be given detailed discussion in the following:

A. Geometrical Asymmetry

A geometrical asymmetry could be caused by factors originating in either the analyzing chamber or the polarizing chamber. Included in the former are differences in the solid angles or effective scattering angles of the two exit windows as seen from the analyzing foil. These can be eliminated by rotating the analyzing chamber 180° on its supporting flat ground joint (mentioned earlier), thereby interchanging the chamber sides with respect to the two counting positions and reversing the asymmetry. An asymmetry caused by a displacement of the incident electron beam from the axis of the polarizing chamber or by a wrinkle (unsymmetrically located with respect to the axis of the beam) in the polarizing foil, would not be eliminated by this chamber rotation procedure. It would be reversed by a 90° rotation of the polarizing foil about an axis perpendicular to the plane of scattering.

B. Reflection-Transmission Asymmetry

Chase and Cox[8] have observed a difference in the number of electrons scattered through angles of 90° on the two sides of an inclined foil. We shall refer to these electrons as "reflected" and "transmitted" electrons, implying those scattered to the side of incidence and to the side of transmission, respectively. Since in the present experiment, electron counting is done simultaneously on both sides of the foil, this reflection-transmission effect should be important. This asymmetry can be eliminated by rotating the analyzing foil through 90° about an axis per-

TABLE I. Sample set of data for scattering foils of gold ($t=4.1\times10^{-5}$ cm) set in orientation VII of Fig. 4.

Counter *A*		Counter *B*		Electron counts		*B/A*
Total count (5 min.)	Background (2 min.)	Total count (5 min.)	Background (2 min.)	*A*	*B*	
3648	104	3656	120	3376	3416	1.012
3896	104	3840	80	3624	3600	0.993
4112	112	4112	80	3840	3872	1.008
3936	120	3744	104	3664	3504	0.956
3936	104	3808	88	3664	3568	0.974
Average background (corrected to 5 min.)	272		240		Mean *B/A*	0.988

$\kappa_7=0.988\pm0.7\%$

[8] C. T. Chase and R. T. Cox, Phys. Rev. **58**, 243 (1940).

pendicular to the plane of scattering, thus reversing the "reflecting" and "transmitting" sides with respect to the two counting directions.

C. Counter Asymmetry

It might be expected that the two counters would respond differently to a beam of 400-kev electrons. This dissimilarity, caused by a difference in thickness of the glass walls, could be studied by simply interchanging the counters while keeping everything else unchanged. The two counters will be referred to as A and B.

For purposes of data analysis, let the following be defined:

η = true polarization ratio (i.e., number of electrons scattered to the 180° position divided by the number scattered to the 0° position, after correction for the other asymmetries which follow).

β = geometrical asymmetry ratio (i.e., ratio of the effect of face a upon the number of electrons scattered through it divided by that of face b).

α = reflection-transmission ratio (i.e., number of electrons scattered to the side of incidence of the foil divided by the number scattered at the same angle through the transmission side of the foil).

γ = counter asymmetry ratio (i.e., number of electrons counted by counter A and its associated circuit divided by the number counted by counter B with the same number incident on both).

κ_i = experimental counting ratio in the ith orientation (i.e., electron counts recorded at the 180° position divided by the number recorded at the 0° position).

TABLE II. Experimental counting ratios for gold scattering foils with the polarizing foil set in transmission orientation. Total electron count: 308,000.

$\kappa_1 = 0.399$	$\kappa_5 = 2.870$
$\kappa_2 = 1.249$	$\kappa_6 = 1.136$
$\kappa_3 = 2.923$	$\kappa_7 = 0.988$
$\kappa_4 = 0.972$	$\kappa_8 = 0.390$

With the polarizing foil in the orientation shown in Fig. 1, there exist eight possible orientations of the analyzing chamber and its assembly. These are shown diagrammatically in Fig. 4. The markings a and b refer to the two exit faces of the analyzing chamber block. As an illustration of the significance of the various orientations (I to VIII), consider orientations I and IV. In the transition from I to IV, the analyzing chamber (foil and exit windows) has been rotated 180° about an axis connecting the foils while the two counters, A and B, remain unchanged.

With the above definitions for the asymmetries, a series of symbolic equations can be written, one for each orientation, and these are included in Fig. 4. For example in orientation I, all of the ratios (except the polarization ratio) favor counting in the 0° position over that in the 180° position. By combining various equations suitably, the different asymmetries can be evaluated in terms of the experimentally-observed κ's. Thus for example:

$$\eta^2 = \kappa_1\kappa_3, \quad \text{and} \quad \alpha^2 = \kappa_3/\kappa_6.$$

TABLE III. Experimental counting ratios for the aluminum-gold combination experiment. Polarizing foil; gold ($t = 4.1\times10^{-5}$ cm) set in transmission orientation. Analyzing foil; aluminum ($t = 1.1\times10^{-3}$ cm). Total electron count: 309,000.

$\kappa_1 = 0.266$	$\kappa_5 = 4.110$
$\kappa_2 = 0.854$	$\kappa_6 = 0.932$
$\kappa_3 = 3.756$	$\kappa_7 = 1.113$
$\kappa_4 = 1.103$	$\kappa_8 = 0.2296$

IV. EXPERIMENTAL DATA

In taking data, five-minute electron counting periods were alternated with two-minute background periods. Two methods of taking the background rates were used: (*a*) the foils could be removed from the beam path and the uncovered holes inserted into position, and (*b*) an aluminum sheet of thickness 1.5 mm (sufficiently thick to stop all 400-kev electrons) could be placed between exit window and counter. Both methods were tried with no significant difference between the results. It appears from this then, that the electrons counted were necessarily those scattered by the foils and not by the foil holder or chamber walls. It might be mentioned that the background correction removes the possibility of the antiparallel counter giving consistently high results because of its location closer to the main beam-limiting diaphragms.

Table I shows a typical set of data obtained with gold foils in orientation VII. The percentage error as applied to the mean value of the ratio has been obtained from the internal consistency of the data. The results of a complete set of data for all of the various orientations listed in Fig. 4 are given in Table II. In obtaining the results in Table II, over 300,000 electron counts were recorded and tabulated.

From the eight different ratios given in Table II, η may be evaluated in four completely independent ways:

$$\eta^2=\kappa_1\kappa_3=\kappa_5\kappa_8=\kappa_2\kappa_4=\kappa_6\kappa_7$$

from which

$$\eta_{Au}=1.08,\ 1.06,\ 1.10,\ \text{and}\ 1.06,$$

with a geometric mean

$$\eta_{Au}=1.08\pm0.01.$$

A residual asymmetry of 8 percent is thus obtained for gold foils. As a test on the reality of this asymmetry, the gold analyzing foil was replaced by one of aluminum (thickness 1.1×10^{-3} cm). Since the expected polarization asymmetry varies approximately as Z^2 for like foils, the combination of aluminum and gold foils should give a theoretical asymmetry of 1.7 percent.

The results obtained with the aluminum-gold combination are shown in Table III. If we calculate the residual asymmetry in the same manner as for the gold foils above, we find

$$\eta_{Al-Au}=1.00,\ 0.97,\ 0.97,\ \text{and}\ 1.02,$$

with a geometric mean

$$\eta_{Al-Au}=0.99\pm0.01.$$

This indicates a residual asymmetry of one percent in the direction opposite to the polarization effect. The 2.7 percent difference between the theoretical and experimental values for η_{Al-Au} is ascribed to some constant geometrical error which is not eliminated by the rotation of the analyzing chamber as outlined in Section III A. Such an error does not invalidate the main conclusion since it is present in all of the data preceding the evaluation of both η_{Au} and η_{Al-Au}. Thus a positive effect has been found for gold foils which is considerably reduced upon the insertion of an aluminum foil, in qualitative agreement with the theory.

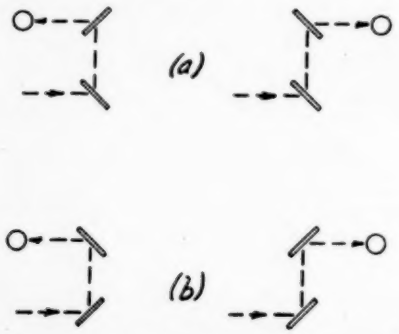

FIG. 5. Diagram showing (a) an ideal transmission experiment and (b) an ideal reflection experiment. Comparison of the two counting rates in either experiment would give directly the corresponding polarization asymmetry.

V. THE REFLECTION-TRANSMISSION EFFECT

It has been mentioned earlier that the reflection-transmission asymmetry plays a prominent role in double scattering experiments. The numerical value of this asymmetry can be easily obtained from the equations in Fig. 4 and the data given in Table II. Thus,

$$\alpha^2=\kappa_7/\kappa_1=\kappa_5/\kappa_2=\kappa_4/\kappa_8=\kappa_3/\kappa_6,$$

and substituting in values of the κ's for gold, we find $\alpha_{Au}=1.59$, 1.54, 1.59, and 1.50 with a geometric mean, $\alpha_{Au}=1.55\pm0.015$. In a similar manner, the reflection-transmission ratio for the aluminum foil ($t=1.1\times10^{-3}$ cm) can be obtained from the data in Table III. This results in $\alpha_{Al}=2.12\pm0.035$.

This large asymmetry is interesting in that past theories of particle scattering by thin foils have overlooked the possibility of such an effect. Goertzel and Cox[9] show that an effect of this kind may be caused by a type of plural scattering which consists in the combination of two deflections of the same order of magnitude. Such plural scattering is unimportant at normal incidence on foils thin enough to satisfy Wentzel's criterion, but it may be serious at oblique incidence for the "reflected" electrons of our experiment. Their method allows the calculation of only a minimum value of the reflection-transmission asymmetry, which might be several times exceeded by the

[9] G. Goertzel and R. T. Cox, Phys. Rev. 63, 36 (1943).

actual value. The minimum value of the asymmetry calculated from their equation is 9 percent for the gold foil and 7 percent for the aluminum foil of our experiment. According to a calculation made for us by Goertzel, the minimum asymmetry for the gold foil is about doubled if Mott's theory of scattering is used.

If plural scattering is responsible for this effect, it is possible that a polarization experiment similar to the present one might be seriously affected by it because of the depolarization which accompanies plural scattering.[10,11] There is the possibility then that a reflection polarization experiment (in which only "reflected" electrons are studied) will yield an asymmetry different from a transmission experiment (in which only "transmitted" electrons are studied). These two types of ideal experiments are shown in Fig. 5. Since both "transmitted" and "reflected" electrons were utilized in calculating the polarization value given in IV, the result obtained is intermediate between that of a pure transmission experiment and that of a pure reflection experiment.

Values for the reflection polarization ratio η_r and the transmission polarization ratio η_t can be obtained by suitably combining the experimental data. All of the data presented in Tables II and III were taken with the first scattering foil set in the transmission position. In order to resolve the data into calculations of η_t and η_r, data must be available with the first foil set in the reflection position. Such data have been acquired and the values for κ are shown in Table IV. By combining all of the data taken with both foils gold, this distinction between the two polarization ratios can be quantitatively determined. The analysis and numerical calculations are included in the Appendix.

The results of these calculations can be written:

$$\eta_t = 1.11 \quad \text{and} \quad \eta_r = 1.02.$$

This indicates a transmission asymmetry of some five times that of a reflection asymmetry. The data preceding these calculations are subject to the same geometrical uncertainties as were present in the evaluation of η_{Al-Au} mentioned earlier. Thus these values are all uncertain to the same degree, about two percent.

[10] M. E. Rose and H. A. Bethe, Phys. Rev. **55**, 277 (1939).
[11] M. E. Rose, Phys. Rev. **57**, 280 (1940).

VI. DISCUSSION OF RESULTS

The data presented above indicate a positive polarization effect which can be resolved into a transmission polarization asymmetry and a relatively small reflection polarization asymmetry. It is interesting to compare these results with those found in other experiments of this type.

As mentioned earlier, the work of Dymond showed no polarization effect greater than the experimental error of one percent. It would appear from the figure given in his publication, that his experiment was of the reflection type—all of the electrons studied were scattered through the "reflecting" sides of the foils. In view of the present findings in a reflection experiment, the results of Dymond are not in marked disagreement with those reported here. The calculations of Goertzel and Cox indicate that the plural scattering effect varies approximately as t/E^2 where t is the foil thickness and E is the electronic energy. This ratio is roughly the same for the two experiments and thus plural scattering, with its accompanying depolarization, would be as prominent in Dymond's work as in the present. Thus the difference between his result and ours is a matter of a very few, perhaps two, percent. It seems to us likely that, if he had happened to design his apparatus so that the electrons passed through the foils, the experiment would have shown an asymmetry in the twice scattered beam.

TABLE IV. Experimental counting ratios for gold scattering foils with the polarizing foil set in "reflection" orientation. Total electron count; 701,000.

$\kappa_1 = 0.392$	$\kappa_5 = 2.664$
$\kappa_2 = 1.130$	$\kappa_6 = 1.077$
$\kappa_3 = 2.551$	$\kappa_7 = 1.050$
$\kappa_4 = 0.921$	$\kappa_8 = 0.404$

These same arguments will apply to Richter's work, where the conditions of scattering (*viz.*, foil thickness, electron energy, "reflecting" orientation of foils, etc.) were much the same as in Dymond's experiment. It would be expected then that these two experiments should yield an

asymmetry considerably smaller than the original value predicted by Mott.

Kikuchi's experiment made use of thick scattering targets ($\sim 10^{-3}$ cm) also arranged as in a reflection experiment. His experiment has already been criticized by Rose[11] in that thick targets depolarize the scattered electrons. Kikuchi avoids counting inelastically scattered electrons by use of an energy analyzer, but even then the elastically scattered electrons could have suffered depolarizing collisions in the thick targets. In addition to the criticism against the use of thick scattering targets, the "reflecting" orientation of Kikuchi's targets makes his results all the more unexplainable.

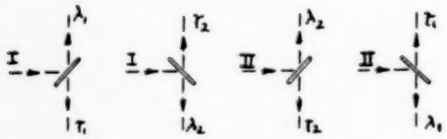

FIG. 6. Definitions of scattered currents when unit intensities of electrons with polarizations I and II strike inclined foils.

The polarization asymmetry for gold foils given in Section IV represents a value intermediate between η_t and η_r, the transmission and reflection asymmetry values. In comparing experimental results with the theoretical predictions those obtained in an ideal transmission experiment should be used, since here the theoretical requirement of single scattering is met most faithfully. The experimental evidence indicates a transmission asymmetry somewhat larger than the 10.4 percent polarization asymmetry calculated by Bartlett and Watson. The uncertainty in the evaluation of the geometrical asymmetry found by means of the aluminum data, prevents accurate determination of η_t. It is believed, however, that a value of $\eta_t = 1.12 \pm 0.02$ is representative of the experimental data. This has been included on the graph of Fig. 2, along with the theoretical curves.

ACKNOWLEDGMENTS

The authors wish to express their sincere appreciation to those who have assisted in this investigation. To Professor Richard T. Cox who has given so generously and helpfully of his time, effort, and encouragement, the authors are greatly indebted. Much of the electrical recording equipment was graciously loaned by Dr. M. D. Whitaker and Dr. H. P. Manning, Jr., with invaluable assistance in the correct adjustment and operation of the circuits by the former. Lastly, Dr. Morton Hamermesh assisted greatly in the task of generator construction and Mr. L. J. Strohmeyer in the collection of data.

APPENDIX

We can consider our initially unpolarized beam of electrons to consist of two components, those with polarization I and those with polarization II. We assume unit intensity of one polarization component as incident upon a scattering foil, then the four quantities λ_1, λ_2, τ_1, and τ_2 are defined as the scattered intensities shown in Fig. 6.

In a double scattering experiment, there are four orientations to be considered, and these are shown in Fig. 7. Here the electron intensities are written as sums, the first term in any sum referring to those electrons with polarization I and the second term to those with polarization II. The values of the anti-parallel, parallel ratio, numbered as

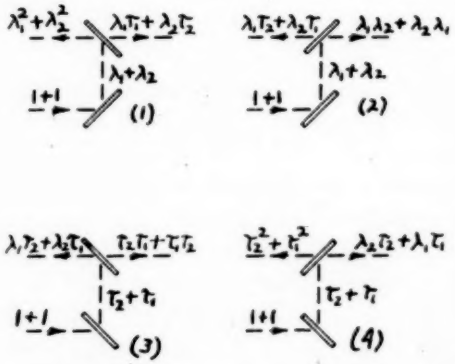

FIG. 7. Diagram showing the four orientations which furnish data for the evaluation of reflection and transmission polarization asymmetries. The first term in any sum represents those electrons with polarization I, cf. Fig. 6.

in Fig. 7 are given by

$$c_1 = (\lambda_1^2 + \lambda_2^2)/(\lambda_1\tau_1 + \lambda_2\tau_2), \quad (1)$$

$$c_2 = (\lambda_1\tau_2 + \lambda_2\tau_1)/(2\lambda_1\lambda_2), \quad (2)$$

$$c_3 = (\lambda_1\tau_2 + \lambda_2\tau_1)/(2\tau_1\tau_2), \quad (3)$$

and

$$c_4 = (\tau_1^2 + \tau_2^2)/(\lambda_1\tau_1 + \lambda_2\tau_2). \quad (4)$$

A true reflection experiment would determine a reflection polarization ratio η_r as

$$\eta_r = (\lambda_1^2 + \lambda_2^2)/(2\lambda_1\lambda_2), \quad (5)$$

while a true transmission experiment would determine a transmission polarization ratio η_t as

$$\eta_t = (\tau_1^2 + \tau_2^2)/(2\tau_1\tau_2). \quad (6)$$

The experimental data do not permit evaluation of the individual λ's and the τ's, but nevertheless, η_r and η_t can be calculated from the c's, which are obtainable directly from the experimental data. We have from (1), (2), (3), and (4) above,

$$c_3/c_2=(\lambda_1\lambda_2)/(\tau_1\tau_2), \tag{7}$$

$$c_1/c_4=(\lambda_1^2+\lambda_2^2)/(\tau_1^2+\tau_2^2), \tag{8}$$

$$2c_3=(\lambda_1/\tau_1)+(\lambda_2/\tau_2), \tag{9}$$

and

$$2c_2=(\tau_2/\lambda_2)+(\tau_1/\lambda_1). \tag{10}$$

Combining (9) and (10), one obtains

$$(\lambda_2/\tau_2)=c_3[1-(1-[1/c_2c_3])^{\frac{1}{2}}] \tag{11}$$

and

$$(\lambda_1/\tau_1)=c_3[1+(1-[1/c_2c_3])^{\frac{1}{2}}]. \tag{12}$$

Substituting (11) and (12) into (8), we can obtain the ratios τ_1/τ_2 and λ_1/λ_2 and these ratios suffice in determining η_r and η_t.

Using data given for gold foils in Tables II and IV, we can evaluate the c's and from these, then,

$$\eta_t=1.11 \quad \text{and} \quad \eta_r=1.02.$$

JANUARY 1 AND 15, 1943 PHYSICAL REVIEW VOLUME 63

The Effect of Oblique Incidence on the Conditions for Single Scattering of Electrons by Thin Foils

GERALD GOERTZEL AND R. T. COX
New York University, University Heights, New York

(Received October 13, 1942)

In setting up and applying criteria for the single scattering of electrons by thin foils, it has been usual to assume that the principal deviations from single scattering are caused by the combination of small deflections with one large one. It is here shown that with electrons obliquely incident on the foil much more serious deviations may be caused by the combination of two deflections of the same order of magnitude. It is concluded that the difference observed by Chase and Cox between the scattering at 90° to the two sides of a foil on which electrons are incident at 45° may be ascribed to this cause. The bearing of this factor on the negative result of Dymond's experiment on the polarization of electrons is also considered.

IN the theory of scattering of charged particles by thin foils it has been usual to assume normal incidence. In this case most of the deviations from single scattering are caused by the combination with one large deflection of one or several much smaller ones. Scattering through a large angle by two deflections of the same order of magnitude is an occurrence of lower probability.

The theory so derived has often been used in the discussion of experiments at oblique incidence. Thus when theoretical criteria of single scattering, such as Wentzel's, have been applied to experiments, it has been usual to assume that no more allowance for obliquity had to be made than to use the oblique thickness as the effective thickness of the foil. Bartlett[1] has called attention to the need for a more careful consideration of the effects of obliquity, but he published no calculations on the subject. Lately Chase and Cox,[2] studying the scattering of electrons incident at 45° on thin aluminum foils, observed that the scattering at 90° was greater toward the side from which the electrons were incident than toward the other side. This was in spite of the fact that their foil was much thinner than was necessary at this angle to satisfy Wentzel's criterion. Another, more empirical criterion, which they developed for the purpose, was also much more than satisfied. However, in developing this criterion they assumed that the probability of scattering at a large angle by the combination of two deflections of the same order of magnitude could be ignored.

This assumption is investigated in the present calculation. The calculation is made for incidence at 45° with the normal and scattering in the plane of incidence, also at 45° with the normal and thus at right angles to the direction of incidence. In Fig. 1, Oz is the normal. The electrons come from the direction of A, and hence the direction of their velocity at incidence is that of OA', the

[1] J. H. Bartlett, Jr., Phys. Rev. **57**, 843 (1940).
[2] C. T. Chase and R. T. Cox, Phys. Rev. **58**, 243 (1940).

extension of AO. The collecting chamber for the scattered electrons is in the direction of B, OB being perpendicular to OA' and in the plane of incidence.

The electrons most likely to undergo plural scattering will be those first deflected in a direction giving them the possibility of a rather long path in the foil, so that their chance of a second large deflection is relatively great. Consider an electron deflected in a direction OC parallel to

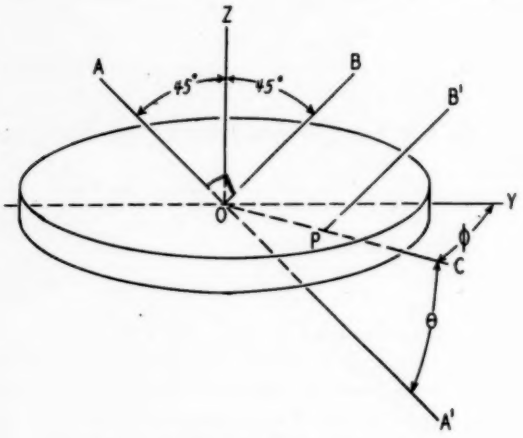

FIG. 1. Directions of incident and scattered electrons.

the plane of the foil. Let θ denote the angle of this deflection, which is the angle between OA' and OC. Let Oy be the trace of the plane of incidence in the plane of the foil, and let φ be the angle between OC and Oy. Then φ is the projection of θ on the plane of the foil. Since the angle between OA' and Oy is 45°, it follows that

$$\cos\varphi=\sqrt{2}\cos\theta. \tag{1}$$

At a point P along OC let the electron undergo a second deflection to the direction PB', parallel to OB. The angle of this deflection is that between PC and PB', equal to the angle between OC and OB. But, since OB and OA' are symmetrical with respect to the plane of the foil, they must make equal angles with OC, which is in that plane. Hence the angle of the second deflection is also θ.

The problem now is to find the probability that two deflections through approximately the same angle θ will result in a combined deflection to the direction of the collecting chamber. This probability is to be compared with that of a single deflection through 90° to the collector. The estimate of the effect of plural scattering obtained by the comparison will be a minimum estimate, since only that plural scattering is included in which the first deflection gives the electron a path roughly parallel to the plane of the foil. It turns out that it is unnecessary to define a "roughly parallel" path except to say that its length in the foil, if the electron undergoes no second deflection, is taken as several times greater than the thickness of the foil. The minimum length of the path to be considered will be denoted by kh, where h is the thickness of the foil and k is then a number several times unity.

For convenience, the first deflection will be assumed to occur midway between the surfaces of the foil, at O in Fig. 2. The electrons considered are those deflected at any azimuth φ to directions between the lines OD and OD', the length of each of these lines being kh. The angle between these lines is approximately h/kh or $1/k$. If also the direction of the deflected ray is in the element of azimuth $d\varphi$, it must lie within the solid angle $d\varphi/k$.

Let the probability P of a single deflection to a small solid angle Ω in a direction making an angle α with the incident ray be given by

$$P=ntf(\alpha)\Omega,$$

where n is the number of scattering centers per unit volume of the foil, t is the length of path in the foil of the undeflected ray, and $f(\alpha)$ is the function given by the theory of single scattering. For the electron incident at 45°, $t=\sqrt{2}h$. The solid angle Ω has just been shown to be $d\varphi/k$, and α is approximately the angle θ, related to φ by Eq. (1). The probability of this deflection is thus $n\sqrt{2}hf(\theta)d\varphi/k$.

The probability to be found next is that of a second deflection which will bring the electron to the collecting chamber. For this deflection α is again approximately equal to θ, as shown earlier, and Ω is now the solid angle subtended by the collector at the foil. The length of the undeflected path may be taken as kh, since this is the minimum length for the electrons considered, and since the problem is that of finding the minimum effect of plural scattering. The use of the equation of single scattering for a path as long as kh might

be questioned, but it may be justified by the fact that the results are to be compared with observations in which the criteria of single scattering were more than satisfied except for the effects of obliquity. The obliquity is being allowed for here by considering the probability of two deflections. The minimum probability of the second deflection is, by the foregoing discussion, $nkhf(\theta)\Omega$. The minimum probability that both deflections shall occur is the product of the two probabilities found, or $n^2\sqrt{2}h^2f^2(\theta)d\varphi\Omega$. It is to be noted that k has disappeared. This product must be integrated over all values of φ to find the minimum probability that two roughly equal deflections shall bring the electron to the collecting chamber. If this probability be denoted by $P(2)$, then

$$P(2)=2\sqrt{2}n^2h^2\Omega\int_0^\pi f^2(\theta)d\varphi.$$

The factor 2 on the right takes account of the integration clockwise and counter-clockwise from 0 to π.

The probability $P(1)$ that the electron shall reach the collector by a single deflection is given by

$$P(1)=\sqrt{2}nh\Omega f(\pi/2).$$

Hence the ratio of plural to single scattering at 90° on the side of incidence will not be less than

$$[P(2)]/[P(1)]=2nh\frac{\int_0^\pi f^2(\theta)d\varphi}{f(\pi/2)}. \qquad (2)$$

It is not difficult now to obtain the corresponding ratio for the electrons emerging at 90° with the direction of incidence from the surface of the foil opposite to that on which they are incident. In Fig. 1, the direction of motion of the twice deflected electron in this case is opposite to PB. Consequently the angle of the second deflection, instead of being equal to the angle of the first deflection, is supplementary to it. The equation in this case, corresponding to Eq. (2) in the other, is therefore,

$$\frac{P(2)}{P(1)}=2nh\frac{\int_0^\pi f(\theta)\cdot f(\pi-\theta)d\varphi}{f(\pi/2)}. \qquad (3)$$

While the limits of φ in the integrals of Eqs. (2) and (3) are 0° and 180°, those of θ are 45° and 135°. Within these limits, and for the energies of the electrons here considered, Rutherford's equation, with the relative mass, will give a tolerable approximation for the present requirements, which are only qualitative. Hence we take

$$f(\alpha)=b^2\csc^4(\alpha/2), \qquad (4)$$

where

$$b=[Ze^2(1-v^2/c^2)^{\frac{1}{2}}]/[2mv^2],$$

Z is the atomic number of the scattering element, and e, m, and v are, respectively, the charge, rest mass, and speed of the electron. Equations (2) and (4) give for the scattering on the side of incidence

$$[P(2)]/[P(1)]=\tfrac{1}{2}nhb^2\int_0^\pi \csc^6(\theta/2)d\varphi. \qquad (5)$$

Equations (3) and (4), with a little transformation, give similarly for the scattering to the side opposite that of incidence,

$$[P(2)]/[P(1)]=8nhb^2\int_0^\pi \csc^4\theta d\varphi. \qquad (6)$$

Approximate numerical values can be found without much trouble for the integrals of Eqs. (5) and (6). The equations then become

$$[P(2)]/[P(1)]=500nhb^2 \qquad (7)$$

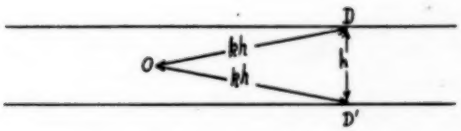

FIG. 2. Scattering within foil.

for scattering to the side of incidence and

$$[P(2)]/[P(1)]=53nhb^2 \qquad (8)$$

for scattering to the other side.

As already mentioned, these equations give the minimum effect of the plural scattering which involves the combination of two deflections of the same order of magnitude. They are sufficient to show that this effect may be much greater than that of the plural scattering which results from

the combination of small-angle scattering with one large deflection.

In the experiment of Chase and Cox already referred to, composite foils were used, made by evaporating aluminum on thin collodion films. The thickest foil used was equivalent in scattering power to an aluminum foil probably a little more than 10^{-5} cm thick. The electrons were accelerated by 50 kv. Incidence was at 45°. The plural scattering given by Eq. (8) for the electrons passing through the foil and scattered at 90° is in this case 0.3 percent of the single scattering. This is about the same as their estimate of the increase in scattered intensity caused by the combination of small- and large-angle scattering. Since Eq. (8) gives a minimum estimate, it is likely that even on this side of the foil the scattered intensity is increased more by the combination of large deflections than by the process usually considered responsible.

For the plural scattering on the side of the foil from which the electrons were incident, Eq. (7) gives a value of about three percent of the single scattering. Actually it was observed that the scattered intensity at 90° was, with this foil, 20 percent higher than on the other side. Thus Eq. (7) does not account for the whole of this excess. On the other hand, this excess scattering was observed to increase with the thickness of the foil, as would be expected if it were due to plural scattering, and the difficulties of any other explanation are considerable, in view of the precautions taken in the experiment. For these reasons it seems likely that the excess was principally or wholly due to plural scattering of the kind considered here.

The agreement found by Chase and Cox between their observations and Mott's theory of the nuclear scattering of electrons is not appreciably affected by this conclusion. For the electrons passing through the foil, the effect of plural scattering should be within their estimate of the experimental uncertainty, which was five percent in relative intensity and 20 percent in absolute intensity. Most of their observations were made on this side of the foil. For the others, their method of correction, while arbitrary, would scarcely have introduced a serious error.

An experiment in which the type of plural scattering here considered would seem to have been more serious is that in which Dymond[3] looked for the asymmetry predicted by Mott in the scattering by a second foil of electrons previously scattered at 90°. From Dymond's diagram of his apparatus, it appears that all the electrons used were scattered to the side of the foils from which they were incident. The voltages used in this experiment were 90, 125, and 160 kv. The foils were of gold and varied from 2.5×10^{-5} cm to ~4 or 5×10^{-6} cm, the thicker foils being used at the higher voltages to yield a measurable scattered intensity. Equation (7) gives a value for the plural scattering equal to about 15 percent of the single scattering for the highest voltage and the thickest foil used, and to about 30 percent for the lowest voltage and the thinnest foil. The equation is not so applicable here as with a lighter element than gold, since Rutherford's equation is a poor approximation at higher atomic numbers. But if it be assumed (and observations of Shull, Chase, and Myers[4] indicate that the assumption is reasonable) that the actual plural scattering, as in the experiment of Chase and Cox, is some six times greater than indicated by the equation, then it must be concluded that half or more of the scattering in Dymond's experiment was plural in spite of the precautions taken against it. The polarization in this event would have been much reduced, and it seems possible that it may have been so much diminished as to escape detection.

We are indebted to Dr. Theodore Holstein for the suggestion, made in a discussion of the experiment of Shull, Chase, and Myers,[4] that with oblique incidence enough electrons might be deflected to directions giving them long paths in the foil that the probability of plural scattering would be materially increased.

Note added in proof.—The problem of this paper seems to have been considered by Petukhov and Vyshinsky.[5] We have been unable to see the original article, and the abstract does not describe the method of their calculation.

[3] E. G. Dymond, Proc. Roy. Soc. **A145**, 657 (1934).
[4] Shull, Chase, and Myers, Phys. Rev. **63**, 29 (1943).
[5] V. A. Petukhov and I. A. Vyshinsky, J. Phys. U.S.S.R. **5**, 137–139 (1941); Phys. Abs. 2369 (Sept. 1942).

Isotope Shifts in Some Lines of Nitrogen

JOHN R. HOLMES
Department of Physics, University of California, Berkeley, California
(Received October 5, 1942)

The line spectrum of a mixture of approximately 70 atomic percent N^{15} to 30 atomic percent N^{14} was photographed with a Fabry-Perot interferometer. The source used was a liquid-air cooled quartz tube with external electrodes excited by a 12-meter oscillator. The tube was charged with helium at a few mm pressure containing about 0.03 mm of the before-mentioned nitrogen isotope mixture. The lines from this discharge were so sharp that it was possible to resolve the two components due to N^{14} and N^{15} in nine infra-red lines. No nitrogen lines were found in this type of discharge in the visible or ultraviolet. The oscillator excitation produced a remarkably high intensity in the lines observed. The lines arising from $^4P \rightarrow {}^4P$ and $^4S \rightarrow {}^4P$ transitions showed a negative isotope shift of the order of 0.06 cm^{-1}. Those from $^2P \rightarrow {}^2P$ transitions showed a positive shift of the order of 0.07 cm^{-1}. The variations in the isotope shifts within the $^2P \rightarrow {}^2P$ multiplets indicate some deviation from Russell-Saunders coupling. No hyperfine structure in either component was observed in any of the lines. The directions of the shifts were checked by obtaining the abundance ratio of the isotopes in the discharge from the intensities of the isotopic heads in the second positive N_2 bands.

INTRODUCTION

HUGHES and Eckart have formulated a theory to account for the isotope shifts in the spectra of light elements and have applied it successfully to the cases of Li I and Li II.[1] The same theory has been applied by Opechowski and De Vries[2] and by Vinti[3] to the isotope shift in boron with close agreement with the measured shift.[4] This theory also accounts fairly well for the isotope shift in Ne I but breaks down in the case of Ne II.[5] Thus it was felt worth while to measure the isotope shift in some lines of nitrogen.

EXPERIMENTAL

The present measurement was made possible through the generosity of Professor H. C. Urey, who kindly furnished a sample of NH_4Cl in which the nitrogen had been enriched to 70 atomic percent N^{15} by the exchange reaction technique developed in his laboratory.[6] The nitrogen was extracted from the NH_4Cl by means of a reaction with a eutectic mixture of NaOH and KOH.[7]

The experimental difficulties in exciting the atomic lines of nitrogen without a background of the molecular bands are quite great, but fairly good results have been obtained in the past by mixing a trace of nitrogen with one of the rare gases and exciting the mixture with a high current-density discharge.[8] The theory of this excitation is that the atomic nitrogen spectrum is produced by collisions of the second kind; first the nitrogen molecule is dissociated by collision with a metastable atom of the rare gas, after which the nitrogen atoms thus formed collide with other metastable atoms of the rare gas and are excited by them.[9]

The foregoing process is carried on most efficiently with a high current density; in fact, in previous attempts to excite these lines it has been found that without an extremely high current density the atomic lines fail completely to appear and only the bands of nitrogen are emitted. In any attempt to measure isotope structure, however, it is impossible to use a high current density since this increases the width of the lines to such an extent that the isotope structure is likely to be obscured.

It is impractical in a problem of this sort to use a conventional discharge tube such as a Schuler tube since there is too rapid an electrical clean-up on the metal electrodes for the small amount of N^{15} available. The tube which was finally used

[1] D. S. Hughes and C. Eckart, Phys. Rev. **36**, 694 (1930).
[2] W. Opechowski and D. A. De Vries, Physica **9**, 913 (1939).
[3] J. P. Vinti, Phys. Rev. **56**, 1120 (1939).
[4] S. Mrozowski, Zeits. f. Physik **112**, 223 (1939).
[5] J. H. Bartlett and J. J. Gibbons, Phys. Rev. **44**, 538 (1933).
[6] H. C. Urey, J. Chem. Phys. **5**, 856 (1937).
[7] R. W. Wood, J. Chem. Phys. **6**, 734 (1938).
[8] M. Kamiyama and T. Sugiura, Sci. Pap. Inst. Phys. Chem. Res. Tokyo **37**, 479 (1940).
[9] K. T. More and O. E. Anderson, Phys. Rev. **38**, 1995 (1931).

was remarkably successful in all respects. It consisted simply of a quartz tube in which the gas mixture was excited by means of external electrodes connected to a twelve-meter oscillator. The electrical clean-up was inconsiderable and only very small amounts of nitrogen were necessary. Quite sharp lines could be obtained and the intensity was very great.

The discharge tube was about 22 cm in length and consisted of a narrower portion 15 cm long and 11 mm in diameter and a thicker portion which was about 3 cm in diameter, and terminated in a plane window. The tube was mounted vertically so that the narrow part could be immersed in liquid air and the discharge was photographed end-on through the top window. With a pressure of a few mm of helium and a trace of nitrogen in the tube the discharge is concentrated in the narrow portion and can thereby be kept below the level of the liquid air.

Very strong nitrogen lines appear when a mixture of about 10 mm of helium and 0.06 mm of nitrogen are excited at high current density in this discharge. As soon as the current density is lowered for the purpose of investigating the isotope structure of the lines not only do the nitrogen lines decrease in intensity, but several nitrogen bands of the first positive system appear, and these increase in intensity as one goes toward the visible. The lowered intensity makes it difficult to obtain exposures in a reasonable length of time in the infra-red, and the presence of band heads in the background naturally makes the analysis of the lines very difficult.

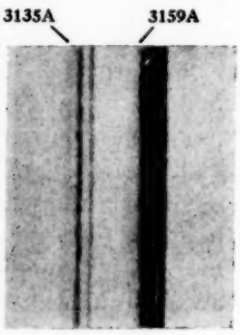

FIG. 1. Triple heads on second positive bands of isotope mixture.

It was found that the nitrogen bands could be attenuated, without seriously diminishing the intensity of the line spectrum, by decreasing the amount of nitrogen in the discharge. Consequently, for each group of lines and each current density, there is an optimum gas mixture, which just produces those lines without any appreciable band intensity. The final plates were taken with a total pressure of about three mm to reduce pressure broadening of the lines, and at nitrogen pressures ranging from 0.01 mm for the lines closest to the visible to 0.03 for those of longer wave-length. During a long exposure there is some clean-up of the nitrogen so that the concentration decreases during the exposure. This can be minimized by running a discharge of the nitrogen isotopes alone in the tube before the exposure is started so that the walls of the tube become impregnated with the isotope mixture.

The ratio of N^{15}/N^{14} in the discharge was checked by photographing the spectrum of the second positive bands of nitrogen in the ultraviolet, which are triple-headed in the case of this mixture of two isotopes.[10] The intensity ratios of these heads will be in the ratio $r^2 : 2r : 1$, where r is the ratio N^{15}/N^{14} in the discharge. Figure 1 is an enlargement of the bands given by an approximately 40 : 60 mixture of N^{14} and N^{15}. If the discharge tube has not been thoroughly outgassed before the N^{14-15} mixture is admitted, sufficient N^{14} may be given off from the walls during the discharge to reverse the abundance ratio and lead to a false conclusion as to the direction of the isotope shift unless this ratio is checked.

The spectrograph used was a Fabry-Perot interferometer in series with a three-prism glass spectrograph, the interferometer being mounted between the collimator lens and the prisms. The spectra were taken on plates especially developed for this experiment by the Eastman Company and designated by them "Experimental Infra-Red Plates" Emulsion No. 193684. These plates are very fast and have a remarkably good contrast and clear background. Before exposure the plates were hypersensitized by a two-minute immersion in a four percent ammonia solution in forty percent alcohol.[11]

[10] G. Herzberg, Zeits. f. physik. Chemie **B9**, 43 (1930).
[11] F. A. Jenkins and S. Mrozowski, Phys. Rev. **60**, 225 (1941).

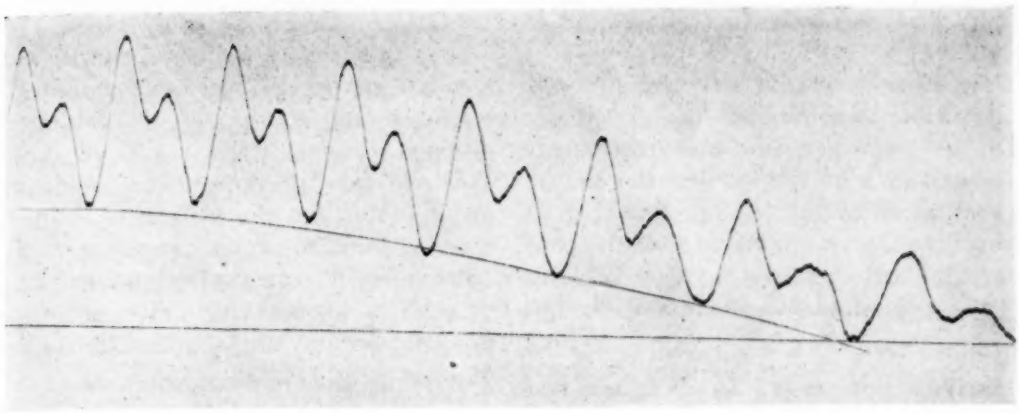

FIG. 2. Microphotometer trace of λ8629.2.

To measure the isotope shifts, each line was microphotometered on a Zeiss microphotometer. A microphotometer trace of one of the lines is shown in Fig. 2. By means of a second degree equation the isotope shifts were calculated from measurements on the traces.

RESULTS

The final measurements were made on plates taken with the etalon separation 2.8001 cm. In most cases the lines were microphotometered several times and a mean value taken from measurements on the various traces. As can be seen from the figures, the components of none of the lines were so completely resolved as to be entirely free from overlapping. If one is to measure the isotope shifts by measuring the peak separation it is first necessary to check the amount of overlapping. If a tail of one component overlaps the maximum of another to any appreciable extent, the two peaks may be shifted toward each other because of this superposition, and thus give a spuriously small value to the isotope shift.

In order to estimate the amount of overlapping, the contour of one of the lines was plotted on coordinate paper in such a way that the abscissa scale is linear in wave numbers, and the ordinate values give true relative intensities. It appeared from the resultant contour (Fig. 3) that overlapping would have a negligible effect on the peak separation in this case. Since the effect of the overlapping seemed so small, no attempt was made to correct for it in any of the lines measured. It is of some interest to note that the half-width of the lines, if it is assumed to be due entirely to Doppler broadening, corresponds to a temperature of about 164°C, a value not far different from that found in liquid-air cooled Schuler tubes.[4]

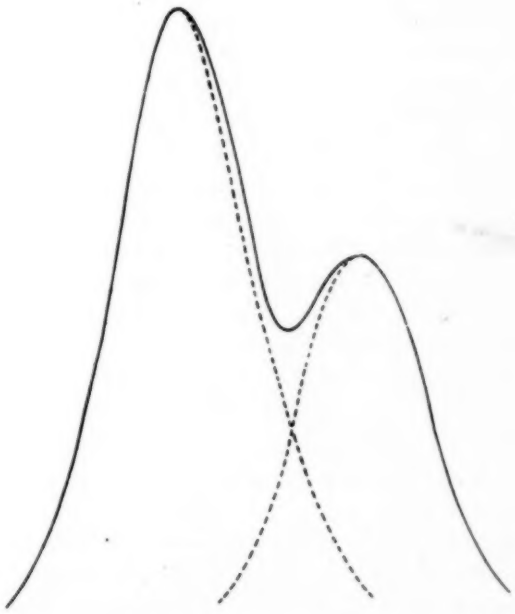

FIG. 3. Contour of λ8595.1.

The nitrogen lines for which the isotope shifts were finally measured are listed in Table I, which contains the average shifts measured and their probable errors. The signs assigned to the isotope shift follow the usual convention that a shift to

higher frequencies in going from N^{14} to N^{15} is called positive.

There are other strong lines on the infra-red side of the 8656.3 line, but they are too closely grouped to be investigated on this instrument. What appeared to be an extremely strong line at 8683A revealed itself in the etalon pattern (Fig. 4) to be two strong lines completely overlapping each other. Similarly there are three weaker lines at 8703A which might be investigated by the use

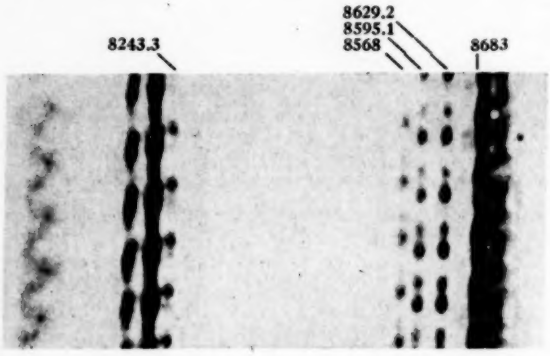

FIG. 4. Interferometer pattern of two groups of nitrogen lines, showing the strong component due to N^{15} and the weaker component due to N^{14}.

of a higher dispersion spectrograph, but which overlapped each other on all of my plates.

Kamiyama and Sugiura[8] observed many nitrogen lines in this region which did not appear on my plates. Also in many cases the relative intensities and wave-lengths of the lines observed here did not agree with the values assigned by them. Usually the wave-lengths obtained agreed more closely with the results of Duffendack and Wolfe[12] than with those of Kamiyama and Sugiura. Perhaps these differences may be ascribed to the different methods of excitation used.

It is seen in Table I that the strong nitrogen lines tend to appear in rather closely spaced groups which actually constitute multiplets. In the $^4P \rightarrow {}^4P$ group at about 8200A the spacing was so small that it was impossible to microphotometer the line λ8223.9 because of the presence of a very close neighboring line, the pattern of which overlapped that of λ8223.9 between orders. It was possible, however, to estimate the shift in this line by visual comparison with the line λ8243.3. As closely as could be seen with an eyepiece the shift was the same in the two lines. Hence it was decided to assign a value for λ8223.9 roughly equal to that of λ8243.3 but with a probable error ten times as great.

Three lines appeared in the $^4S \rightarrow {}^4P$ group at about 7400A, but the weakest of them, λ7423.9, was too faint to produce a measureable etalon pattern in a reasonable exposure time. The presence of band heads in this region made the investigation of such a weak line even more difficult.

It will be noticed that the magnitude of the shift is greatest in the four lines in which the shift is positive. This result might be expected because of the fact that the normal mass effect is always positive and would therefore increase the magnitude of a positive shift and decrease that of a negative one, the normal mass effect for these lines being about 0.03 cm^{-1}. If one calls the difference between the observed isotope shift and the normal mass effect the specific shift, one finds the magnitude of the specific shift to be much greater for the lines which stem from $^4P \rightarrow {}^4P$ and $^4S \rightarrow {}^4P$ transitions than for those from $^2P \rightarrow {}^2P$ transitions.

In all of the microphotometer traces it can be clearly seen that both components of the lines are completely symmetrical. Thus no trace of hyperfine structure is detected in either the N^{14} or N^{15} lines. As can be seen in Table I the isotope shifts are of the order of magnitude of 0.05 cm^{-1}; inasmuch as these shifts were so cleanly resolved it seems likely that any hyperfine structure as great as 0.03 cm^{-1} would at least reveal itself as an asymmetry in the components. It seems safe to say that there is no hyperfine structure in these lines with an over-all spread as great as 0.03 cm^{-1}.

TABLE I. Isotope shifts in N.

Wave-length	Transition	Intensity	Isotope shift cm^{-1}
8656.3 IA	$3p\ ^2P_{1/2} \rightarrow 3s\ ^2P_{3/2}$	4	0.0785 ± 0.0014
8629.2	$3p\ ^2P_{3/2} \rightarrow 3s\ ^2P_{3/2}$	10	0.0694 ± 0.0008
8595.1	$3p\ ^2P_{1/2} \rightarrow 3s\ ^2P_{1/2}$	6	0.0751 ± 0.0006
8568.0	$3p\ ^2P_{3/2} \rightarrow 3s\ ^2P_{1/2}$	4	0.0678 ± 0.0009
8243.3	$3p\ ^4P_{3/2} \rightarrow 3s\ ^4P_{3/2}$	4	-0.0596 ± 0.0006
8223.9	$3p\ ^4P_{1/2} \rightarrow 3s\ ^4P_{3/2}$	4	-0.06 ± 0.006
8216.6	$3p\ ^4P_{5/2} \rightarrow 3s\ ^4P_{5/2}$	6	-0.0579 ± 0.0005
7468.7	$3p\ ^4S_{3/2} \rightarrow 3s\ ^4P_{5/2}$	10	-0.0565 ± 0.0011
7442.6	$3p\ ^4S_{3/2} \rightarrow 3s\ ^4P_{3/2}$	6	-0.0485 ± 0.00117

[12] D. S. Duffendack and R. A. Wolfe, Phys. Rev. **34**, 409 (1929).

DISCUSSION OF RESULTS

The measured isotope shift of a line in the spectrum of an element does not give the isotope shift in the energy levels of the atom, but simply the difference in the isotope shifts of the two levels involved in the transition. The primary theoretical interest, however, is in the absolute shift in the levels themselves.

In general it is possible to obtain the shifts in the energy levels if one has made experimental measurements on enough lines. The usual procedure is to assume that the isotope shift in a level of high principal quantum number is zero.[13] This assumption can be verified by studying transitions between this level and other levels of higher principal quantum number; the observed shifts in such lines should be zero if the above assumption is true. Then if a shift is observed in a transition from the level of high principal quantum number it will be equal to the shift in the lower level. Knowing the shift in this level we can find transitions to other levels and thereby obtain the isotope shift in a great many levels of the atom. Also if there are many transitions that show the same isotope shift and have one energy level in common, the shifts of all the other levels must be the same or zero. If they are unrelated levels it is reasonable to assume that the shifts are probably all zero and that the total shift is due to the common level.

TABLE II. Differences in the isotope shifts of levels of a multiplet.

$\Delta\nu(\lambda 8629.2)-\Delta\nu(\lambda 8656.3)=\Delta(3p\ ^2P_{3/2})-\Delta(3p\ ^2P_{1/2})=$	-0.0091
$\Delta\nu(\lambda 8568.0)-\Delta\nu(\lambda 8595.1)=\Delta(3p\ ^2P_{3/2})-\Delta(3p\ ^2P_{1/2})=$	-0.0073
Mean $\Delta(3p\ ^2P_{3/2})-\Delta(3p\ ^2P_{1/2})=$	-0.0082
$\Delta\nu(\lambda 8568.0)-\Delta\nu(\lambda 8629.2)=\Delta(3s\ ^2P_{3/2})-\Delta(3s\ ^2P_{1/2})=$	-0.0016
$\Delta\nu(\lambda 8595.1)-\Delta\nu(\lambda 8656.3)=\Delta(3s\ ^2P_{3/2})-\Delta(3s\ ^2P_{1/2})=$	-0.0034
Mean $\Delta(3s\ ^2P_{3/2})-\Delta(3s\ ^2P_{1/2})=$	-0.0025
$\Delta\nu(\lambda 8216.6)-\Delta\nu(\lambda 8243.3)=\Delta(3p\ ^4P_{5/2})-\Delta(3p\ ^4P_{3/2})=$	0.0017
$\Delta\nu(\lambda 7442.6)-\Delta\nu(\lambda 7468.7)=\Delta(3s\ ^4P_{5/2})-\Delta(3s\ ^4P_{3/2})=$	0.008

As can be seen from Fig. 5, which shows the levels and transitions for the lines here studied, either of the above procedures is impossible with the limited data at hand. From the measurements it can be seen, however, that within a multiplet the difference in the level shift is very small, never much more than 10 percent of the measured shift in the lines. For instance the difference between the observed shifts in the lines $3s\ ^2P_{3/2}-3p\ ^2P_{1/2}$ and $3s\ ^2P_{3/2}-3p\ ^2P_{3/2}$ gives the difference in the shifts of the levels $3p\ ^2P_{1/2}$ and $3p\ ^2P_{3/2}$.

Let us call the shift in the $3p\ ^2P_{3/2}$ level $\Delta(3p\ ^2P_{3/2})$, and designate the other shifts similarly. It is then possible to apply the combination principle to the observed differences from Table I to obtain Table II which shows the differences of isotope shift of the levels of a multiplet.

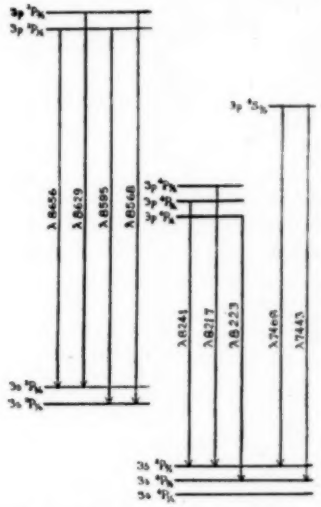

FIG. 5. Energy levels of the lines in which isotope shift has been measured.

If the nitrogen atom were a case of pure Russell-Saunders coupling one would expect the shift in the energy levels to be independent of the J value and therefore the lines of a multiplet should exhibit the same isotope shift. As is shown in Table II this is not true, indicating that there is some deviation from pure Russell-Saunders coupling in the case of nitrogen.

It appears from these figures that in the ^2P states the shift within a multiplet is greater in the state with the smallest J value. On the other hand, in the ^4P states, in any particular multiplet, the shift seems to be greater for the levels of higher J value. The differences, however, are not much greater than the probable error, and accordingly no great weight should be given to these conclusions.

It appears to be impossible to assign an upper limit to the magnetic moment of the N^{15} nucleus on the basis of the absence of hyperfine structure in the lines observed, as was done for N^{14} by

[13] H. Kallman and H. Schuler, Ergeb. d. exakt. Naturwiss. 11, 162 (1932).

Bacher.[14] It seems that the lines observed by Bacher did not appear in this discharge and none of those that did appear were favorable for such a calculation. Any estimate based upon these lines would be too large to be significant.

[14] R. F. Bacher, Phys. Rev. **43**, 1001 (1933).

In conclusion I wish to acknowledge the kindness of Professor H. C. Urey in supplying me with the sample of enriched nitrogen; furthermore, I wish to acknowledge my indebtedness to Professor F. A. Jenkins for his stimulating direction of my work.

JANUARY 1 AND 15, 1943 PHYSICAL REVIEW VOLUME 63

Dispersion of Elastic Waves in Solid Circular Cylinders*

G. E. HUDSON†
Department of Physics, Brown University, Providence, Rhode Island
(Received November 4, 1942)

The theory of elastic vibrations in solid circular cylindrical rods of homogeneous isotropic materials is redeveloped from the general equations of elasticity with the following general results: 1. For any mode of vibration the ratio of the velocity of any elastic wave traveling along the rod to the velocity c_0 of shear waves is the same for any two rods whose Poisson ratios are equal and whose ratios of circumference to shear wave-length are equal; 2. If the velocity of propagation for any particular mode remains less than c_0 as the frequency or radius is increased indefinitely, this velocity approaches that of Rayleigh surface-waves; 3. If the velocity of propagation for any particular mode remains greater than c_0 as the frequency or radius is increased indefinitely, this velocity approaches c_0 in the limit; and 4. A considerable simplification is introduced into the method of computing dispersion curves for any mode. This investigation not only generalizes and extends the work of D. Bancroft on elongational waves but further includes the computation of an exact table of dispersion curves for the flexural mode of vibration. The dispersion curves for magnesium are compared with the experimental results of Shear and Focke. Excellent agreement between theory and experiment is obtained for the first elongational and flexural branches.

INTRODUCTION

THE last few years have seen much progress, from both experimental[1] and theoretical[2–4] viewpoints, in the study of the phenomena associated with the vibrations of rods, particularly dispersion at high frequencies. Without exception, the exact theoretical treatments take as their starting points the solutions of the general dynamical equations of elasticity obtained originally by L. Pochhammer[5] for infinitely long rods. The most complete of these discussions is that of D. Bancroft,[2] who has calculated a table of velocities of elongational waves as a function of the ratio of the diameter of the rod to the wave-length for a wide range of values of Poisson's ratio.

An examination of experimental data reveals the existence of several types of rod vibrations often occurring either in conjunction with or to the exclusion of the elongational mode. This suggests the extension of the theoretical treatment to higher modes of vibration, to obtain dispersion curves for the associated elastic waves. Such calculations will be extremely useful in the future study of the stability and interaction of various modes of vibration and the study of the vibrations of a bar of finite length. The present article gives a general treatment of the problem of the propagation of longitudinally-traveling waves along a solid circular cylinder of infinite length, and presents a simplified method for the exact calculation of dispersion curves.

With a few important exceptions the quantities used in the analysis are similar to those

* Submitted in partial fulfillment of the requirements for the degree of Doctor of Philosophy at Brown University, Providence, Rhode Island.

† Now at the David Taylor Model Basin, Navy Department, Washington, D. C.

[1] S. K. Shear and A. B. Focke, Phys. Rev. **57**, 532 (1940).

[2] D. Bancroft, Phys. Rev. **59**, 588–593 (1941).

[3] E. Giebe and E. Blechschmidt, Ann. d. Physik **11**, 905 (1931); **18**, 417–485 (1933).

[4] G. S. Field, Can. J. Research **5**, 619–624 (1931); **8**, 563–574 (1933); **11**, 254–263 (1934).

[5] L. Pochhammer, J. f. d. reine u. angew. Math. (Crelle) **81**, 33–80 (1875).

introduced by Bancroft. The symbols denoting them are compared with Bancroft's in Table I.

TABLE I. Comparison of notations.

Symbol	Description	Bancroft's notation
$d=2a$	diameter of rod	d
α	$(1-2\sigma)/(1-\sigma)$; σ = Poisson's ratio	β
c	velocity of the wave	v
c_0	velocity of shear-waves $=(\mu/\rho)^{\frac{1}{2}}$	$v_0[2(1+\sigma)]^{\frac{1}{2}}$
z	$\frac{1}{2}(c/c_0)^2$	x
ν	frequency	v/L
τ_0	number of shear wave-lengths in a circumference $=\pi d\nu/c_0$	$\gamma av[2(1+\sigma)]^{\frac{1}{2}}/v_0$
x	$\tau_0[(2z-1)/2z]^{\frac{1}{2}}$	ka
y	$\tau_0[(\alpha z-1)/2z]^{\frac{1}{2}}$	ha
$\theta_\beta(\xi)$	$\xi J_\beta'(\xi)/J_\beta(\xi)$	
$\theta_1(\xi)+1$	$\xi J_0(\xi)/J_1(\xi)=-\xi^2/\theta_0(\xi)$	$\phi(\xi)$

THEORY AND CALCULATIONS

We choose solutions of the differential equations of motion in the form of expressions for the components of the displacement vector $\mathbf{u}$ which represent a wave traveling along the axis of the rod (the ζ axis), and which are single-valued functions of the cylindrical coordinates r, θ, ζ. By imposing the boundary condition on these solutions, that the stress vector vanish at the lateral surface, we find the infinite set of secular equations, defining c/c_0 as a function of τ_0,

$$0=\begin{vmatrix} \left\{\beta^2-y^2-\frac{1}{2}\tau_0^2\frac{\sigma}{1-\sigma}\right\}J_\beta(y)-yJ_\beta'(y), & 2\beta\{xJ_\beta'(x)-J_\beta(x)\}, & \{\beta^2-x^2\}J_\beta(x)-xJ_\beta'(x) \\ \beta\{yJ_\beta'(y)-J_\beta(y)\}, & \{2\beta^2-x^2\}J_\beta(x)-2xJ_\beta'(x), & \beta\{xJ_\beta'(x)-J_\beta(x)\} \\ yJ_\beta'(y), & \beta J_\beta(x), & (1-z)xJ_\beta'(x) \end{vmatrix}, \tag{1}$$

where β takes on any integral value, and in this way determines the mode of vibration. This form naturally suggests the introduction of the θ_β functions (cf. Table I), by dividing (1) by $J_\beta^2(x)\cdot J_\beta(y)$. After some manipulation, (1) becomes

$$0=\begin{vmatrix} \beta^2-1-x^2(z-1)/(2z-1), & 2(\beta^2-1)\theta_\beta(x)-x^2, & \beta^2-1-x^2 \\ -1, & \beta^2-2\theta_\beta(x)-x^2, & z\theta_\beta(x)-1 \\ \theta_\beta(y), & \beta^2, & (1-z)\theta_\beta(x) \end{vmatrix}. \tag{2}$$

As has been recognized by Field and Bancroft, the function c/c_0 of τ_0 defined by the secular Eqs. (1) or (2) is not always single-valued, but in certain cases may have many branches. This is true in particular of the elongational and torsional modes, obtained when $\beta=0$. However, it is not the case for the flexural mode, whose dispersion curve consists of just one branch. It should be pointed out here that there is some experimental evidence for the existence of the higher branches of the elongational or torsional modes (cf. Figs. 2 and 3).

In order to discuss the calculation of the dispersion curves obtainable from this set of equations, it is necessary first to investigate some properties of the θ_β functions.

As a consequence of the recursion relations satisfied by the Bessel functions $J_\beta(\xi)$ the θ_β functions satisfy the non-linear recursion relations

$$[\theta_\beta(\xi)-\beta]=\frac{-\xi^2}{2(\beta+1)+[\theta_{\beta+1}(\xi)-(\beta+1)]}. \tag{3}$$

From this, it follows immediately that we can develop the functions into the infinite continued fraction

$$\theta_\beta(\xi)-\beta=\frac{-\xi^2}{2(\beta+1)+}\,\frac{-\xi^2}{2(\beta+2)+}\cdots\frac{-\xi^2}{2(\beta+n)+}\cdots, \tag{4}$$

which can be shown to converge to

$$[\xi\{J_\beta'(\xi)/J_\beta(\xi)\}-\beta]$$

for all real and imaginary values of ξ. It is seen that the value of the function $\theta_\beta(\xi)$ for a particular ξ can be approximated as closely as we wish by taking a large enough number of components of the continued fraction expansion (4). This computation proceeds very quickly on a

modern high speed calculator; to calculate $\theta_1(\xi)$ correct to nine places, it is only necessary to perform twelve successive divisions for values of $|\xi|$ as large as 5.0.

For both real and imaginary arguments we have, when $|\xi|$ is small,

$$\theta_\beta(\xi) \doteq \beta - \xi^2/[2(\beta+1)]$$

and, for any ξ, as β becomes large,

$$\theta_\beta(\xi) \doteq \beta.$$

When ξ is imaginary,

$$\theta_\beta(\xi) \doteq -i\xi - \tfrac{1}{2},$$

when $|\xi|$ takes on large values, while for ξ real,

$$\theta_\beta(\xi) \doteq \xi \cot [\xi - \tfrac{1}{4}(2\beta-1)\pi],$$

as $|\xi|$ becomes great.

From the approximate expressions for the θ_β functions, it is easy to show by substitution into (2) that, when the frequency or the rod-diameter is small enough so that τ_0 is very small, we have the approximate secular equation

$$0 \doteq a_0(z, \alpha, \beta) + a_1(z, \alpha, \beta)\tau_0^2 + a_2(z, \alpha, \beta)\tau_0^4, \quad (5)$$

in which

$$a_0 = 8z\beta(\beta+1)(\beta^2-1)\{z(\alpha-2)+1\},$$
$$a_1 = -4z(\beta+1)\{z(\alpha-2)(2\beta-1)-(2\alpha-3)(\beta-1)\},$$
$$a_2 = (2z-1)\{z(\alpha-2)-(2\alpha-3)\},$$

for the velocity ratio c/c_0 as a function of τ_0. For higher modes of vibration, β is very large, and the velocity becomes accordingly

$$c = c_0[2(1-\sigma)]^{\frac{1}{2}},$$

when τ_0 is small. As far as the author is aware, waves of this velocity have never been observed.

TABLE II. Minimum velocity ratios and asymptotic behavior of elongational wave dispersion curves.

σ	$(c/c_0)_{\min}$	$(\tau_0)_{\min}$	$(c/c_0)_{\tau_0=\infty}$	$\left(\frac{c}{c_0}\Big/\frac{1}{\tau_0}\right)_{\tau_0=\infty}$
0.00	0.855557	7.33337	0.8740320	−0.2173949
0.10	0.881559	9.05149	0.89310	−0.172540
0.15	0.893279	10.1115	0.90223	−0.151562
0.20	0.904174	11.3470	0.91099	−0.131860
0.25	0.914277	12.8025	0.91940	−0.113543
0.30	0.923626	14.5362	0.92742	−0.0967458
0.35	0.932264	16.6270	0.93501	−0.0815527
0.40	0.940233	19.1850	0.94220	−0.0679408
0.50	0.954375	26.4389	0.9553125	−0.04535197

On the other hand, if, as τ_0 is increased indefinitely, the wave velocity of some mode of vibration remains less than c_0, then this velocity c is obtainable from

$$(1-z)^2 = (1-\alpha z)^{\frac{1}{2}}(1-2z)^{\frac{1}{2}}. \quad (6)$$

This equation is identical, except for a change in notation, with the equation for the velocities of Rayleigh's surface waves in an infinite medium.[6] Similarly, if c remains greater than c_0 for some mode, it is seen that this velocity must approach c_0 in the limit as the product of frequency and rod-diameter approaches infinity. To apply these deductions, then, it is necessary to determine which modes have velocities greater or less than c_0 as τ_0 becomes large. Hence, we find the largest root, τ_0, of the equation obtained from (2) by letting $z \to \frac{1}{2}$, i.e., $c \to c_0$, *viz.*,

$$0 = \frac{\tau_0^4}{4}\left(\frac{\beta-1}{\beta+1}\right) + \frac{\tau_0^2}{2}(2\beta-3)[\beta-\theta_\beta(y)] + \beta(\beta^2-1)[\beta-\theta_\beta(y)], \quad (7)$$

where $y^2 = \tau_0^2(\alpha-2)/2$. Then if the slope of the dispersion curve in the $(\tau_0, c/c_0)$-plane is negative at this root, the velocity becomes less than c_0, and conversely.

When β is set equal to zero in (2), the secular determinant factors into the product of two expressions, which, when set equal to zero in turn, give the equations of the dispersion curves of torsional and elongational waves, respectively. These become identical with the equations given by Bancroft for these modes if we introduce the change of notation indicated in Table I. However, Bancroft's results and calculations for elongational waves may be extended as follows. By taking the asymptotic expansion for $\phi(\xi)$, ξ imaginary, valid for large $|\xi|$, we find near $\tau_0 = \infty$ that the elongational curve has the slope

$$\left[\frac{d(c/c_0)}{d(1/\tau_0)}\right]_{\tau_0=\infty} = \frac{(1-z)^2-(1-z)^4}{(1-2z)^{\frac{1}{2}}\{\alpha/2+(1-z)^4-2(1-z)\}}, \quad (8)$$

where z is determined by (6).

[6] Lord Rayleigh, Proc. London Math. Soc. **17**, 4–11 (1885).

TABLE III. Flexural wave dispersion curves for various values of Poisson's ratio.

τ_0 =	σ =0.00	0.10	0.15	0.20	0.25	0.30	0.35	0.40	0.50
0.0	0.0000000	0.0000000	0.0000000	0.0000000	0.0000000	0.0000000	0.0000000	0.0000000	0.0000000
0.2	.3555010	.3640608	.3681160	.3720349	.3758288	.3795038	.3830692	.3865318	.3931709
0.4	.4775240	.4889918	.4944082	.4996310	.5046750	.5095520	.5142708	.5188420	.5275762
0.6	.5576783	.5710290	.5773082	.5833474	.5891622	.5947667	.6001742	.6053962	.6153268
0.8	.6160680	.6307710	.6376520	.6442482	.6505770	.6566550	.6624978	.6681200	.6787528
1.0	.6608194	.6765492	.6838712	.6908618	.6975420	.7039325	.7100500	.7159128	.7269328
1.2	.6961910	.7127362	.7203908	.7276680	.7345922	.7411860	.7474712	.7534670	.7646630
1.4	.7247312	.7419508	.7498658	.7573562	.7644502	.7711738	.7775522	.7836090	.7948402
1.6	.7480972	.7658980	.7740240	.7816770	.7888910	.7956950	.8021174	.8081858	.8193600
1.8	.7674272	.7857478	.7940542	.8018392	.8091400	.8159908	.8224248	.8284742	.8395332
2.0	.7835359	.8023430	.8108092	.8187060	.8260740	.8329519	.8393790	.8453910	.8563025
2.2	.7970260	.8163020	.8249200	.8329180	.8403432	.8472390	.8536492	.8596158	.8703660
2.4	.8083570	.8280960	.8368642	.8449620	.8524408	.8593510	.8657432	.8716620	.8822500
2.6	.8178838	.8380912	.8470120	.8552120	.8627478	.8696760	.8760512	.8819258	.8923618
2.8	.8258888	.8465730	.8556530	.8639628	.8715628	.8785152	.8848820	.8907188	.9010172
3.0	.8326003	.8537732	.8630212	.8714494	.8791232	.8861100	.8924768	.8982860	.9084667
3.2	.8382070	.8598770	.8693030	.8778620	.8856208	.8926532	.8990318	.9048250	.9149098
3.4	.8428650	.8650388	.8746530	.8833530	.8912110	.8983020	.9047048	.9104942	.9205070
3.6	.8467108	.8693870	.8791982	.8880520	.8960212	.9031842	.9096252	.9154230	.9253888
3.8	.8498592	.8730310	.8830460	.8920648	.9001572	.9074062	.9138980	.9197190	.9296608
4.0	.8524131	.8760632	.8862868	.8954793	.9037082	.9110556	.9176120	.9234680	.9334112
4.2	.8544618	.8785662	.8889990	.8983722	.9067470	.9142062	.9208400	.9267438	.9367120
4.4	.8560860	.8806110	.8912502	.9008090	.9093398	.9169202	.9236438	.9296070	.9396230
4.6	.8573530	.8822620	.8931022	.9028468	.9115390	.9192510	.9260752	.9321100	.9421950
4.8	.8583318	.8835750	.8946062	.9045352	.9133930	.9212442	.9281788	.9342960	.9444688
5.0	.8590708	.8846020	.8958110	.9059189	.9149430	.9229395	.9299930	.9362010	.9464833

Further, an extended analysis shows that the elongational curve for a certain α has a minimum lying on the locus defined by

$$\phi\left[i\frac{\tau_0}{(2z)^{\frac{1}{2}}}\left(\frac{1-z}{\phi(x)-z}\right)b\right]=\frac{b^2}{\phi(x)-z}, \tag{9}$$

where

$$b^2=\phi^2(x)-2z+\tfrac{1}{2}\tau_0^2 z.$$

Corresponding to each point (τ_0, z) on this locus, there is a dispersion curve defined by a particular α which has this point as a minimum. α is obtained from

$$\alpha=\frac{1}{z}\left[1-\left(\frac{1-z}{\phi(x)-z}\right)^2 b^2\right]. \tag{10}$$

Table II gives the values at $\tau_0=\infty$ of the velocity ratio c/c_0, and the slope, $[d(c/c_0)/d(1/\tau_0)]$, calculated from (6) and (8) for various values of σ, Poisson's ratio. Also included in this table is a list of coordinates, calculated from (9) and (10), of the minima of those elongational curves characterized by these same values of σ.

Let us now turn to a consideration of the flexural modes of motion. If we give β the value unity in (2), define

$$\psi(\xi)=\theta_1(\xi)-1, \tag{11}$$

and reduce the resulting secular determinant of order three to one of order two by the pivotal method, there results the equation,

$$0=\begin{vmatrix} \psi(y)(1-2z)+(1-z)\{2\psi(x)+x^2\}, & \\ & -3\psi(x)-x^2 \\ \psi(y)(1-2z)-z, & -(1-z)\psi(x)+z \end{vmatrix}, \tag{12}$$

of the dispersion curve of the flexural waves. It is possible to show that, for a given value of Poisson's ratio, this curve has contact of the first order, but not higher, at $\tau_0=\infty$ with the lower branch of the dispersion curves of the elongational waves, characterized by the same value of σ. Equation (7), with $\beta=1$, gives a good approximation to the flexural wave dispersion curves provided τ_0 is not too large.

Table III, accurate to six places, is the result of calculating, by (12), c/c_0 as a function of τ_0 and σ for flexural waves. It should be emphasized again that the units used in the construction of this table are not the same as those in Bancroft's table for elongational waves. Conversion formulae between the two forms of tables are easily obtained from the list of symbols given in Table I. Bancroft's units are convenient if Young's modulus E is known accurately; the units τ_0 and

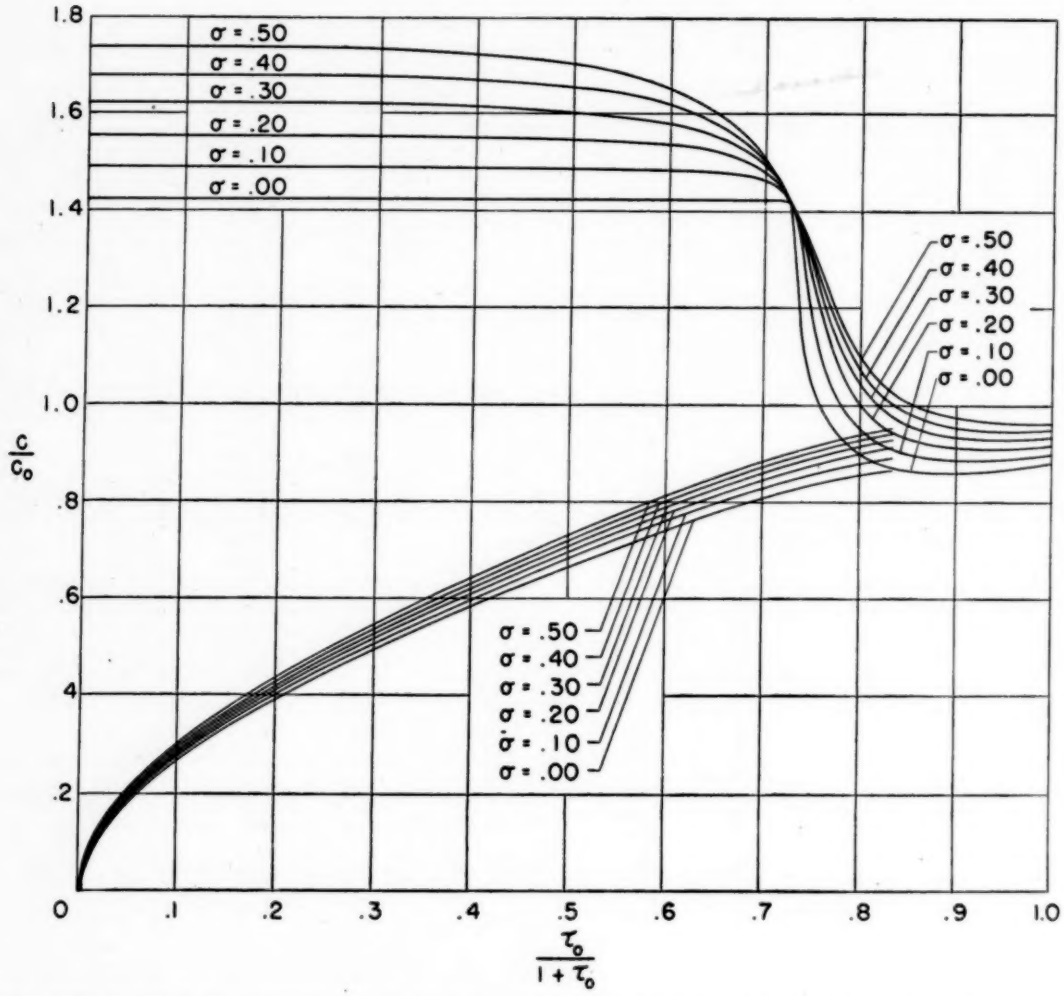

FIG. 1. Theoretical elongational wave dispersion curves (upper family) and flexural wave dispersion curves (lower family) for various values of Poisson's ratio.

c/c_0 are more convenient to the experimenter if the shear modulus is known accurately, or if the constant velocity c_0 of torsional waves is obtained from an experiment. c_0 constitutes a natural reference velocity at *any* frequency at which an experiment on the propagation of waves in rods is being conducted.

Figure 1 shows the comparison in the units of $(\tau_0, c/c_0)$ between the family of elongational wave dispersion curves computed by Bancroft, and the flexural wave dispersion curves presented in Table III. For convenience, the variable $\tau_0/(1+\tau_0)$ is plotted as abscissa, rather than τ_0 itself. This serves to emphasize the minima of the elongational curves as well as the slopes at $\tau_0=\infty$. Note the universal point, $c/c_0=1.4142\cdots$, $\tau_0=2.6038\cdots$, at which all the elongational curves are tangent. This point is quite helpful in obtaining rough estimates of the shape of curves in the elongational family. It appears from this figure that the flexural curves have very slight maxima for certain large values of τ_0. A calculation of these maxima would be interesting to carry out.

COMPARISON WITH EXPERIMENT

For the purpose of comparing theory and experiment, Shear's data[1] for two magnesium rods (machined sticks) with diameters equal to 5.895 mm and 4.615 mm, and two silver rods (hard-drawn) with diameters 5.009 mm and 4.061 mm, were recomputed in the units of τ_0

and c/c_0. For magnesium, c_0 was chosen as 30.97×10^4 cm/sec., while for silver, c_0 was taken as 15.78×10^4 cm/sec.

Figure 2 shows the data for the magnesium rods compared with the theoretical curves for $\sigma=0.25$. It is seen that both the flexural and elongational curves agree well with the data for both rods except for a few isolated points, which probably lie on curves corresponding to higher order modes of vibration.

Figure 3 illustrates the effect of non-isotropy resulting from the hard-drawing treatment of the silver rods. The data for both rods are compared with the theoretical curves for $\sigma=0.39$ and $\sigma=0.49$. The flexural mode agrees best with the choice $\sigma=0.49$ for the theoretical curve whereas the choice $\sigma=0.39$ for the theoretical curve is closer to the empirical curve for elongational waves, denoted by the dashed line A. However, this latter agreement is not at all as good as it is for the flexural branch; it appears that no choice of σ can bring about agreement in the shapes of the curves. This difference in shape, then, is one of the effects of non-isotropy which would have to be derived from a theory of non-isotropic rod vibrations. The dashed empirical curves B, C, and D are likely due to the presence of higher modes of vibration.

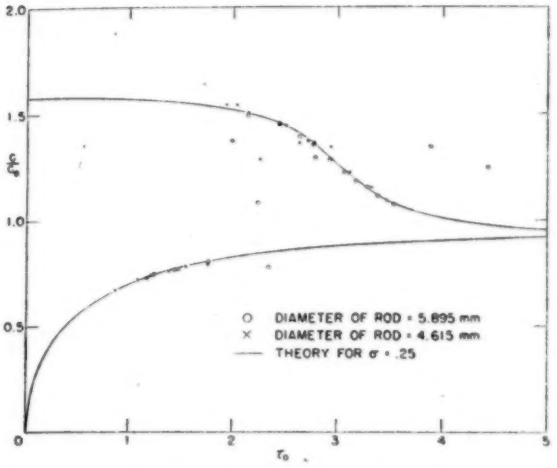

FIG. 2. Experimental data for magnesium rods compared with the theoretical curves for $\sigma=0.25$.

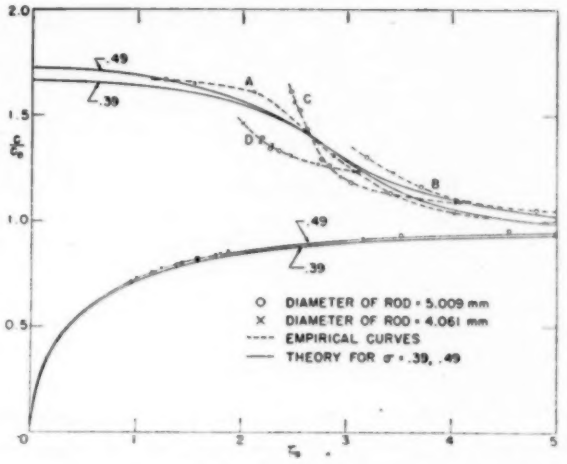

FIG. 3. Experimental data for hard-drawn silver rods compared with the theoretical curves for $\sigma=0.39$ and 0.49.

The author wishes to express his thanks to Professor R. B. Lindsay for his many useful suggestions throughout the research, and to Professor W. Feller for his helpful suggestions concerning the practical computational procedure.

The Preparation and Efficiency of the Fast Geiger-Müller Counter

G. D. ROCHESTER AND L. JÁNOSSY
Physical Laboratories, The University, Manchester, England
(Received November 10, 1942)

The dependence of the efficiency of the fast Geiger-Müller counter upon the partial pressures of argon and alcohol is investigated. No change in the efficiency of an argon-alcohol counter is found when the pressure of the argon is changed from 11 cm to 74.5 cm; furthermore a change exceeding 0.5 percent is incompatible with the results.

I. INTRODUCTION

IN the course of a recent investigation[1] we had occasion to use a large number of Geiger-Müller counters in anticoincidence. The use of many counters required that a simple method of preparation should be employed, and their use in anticoincidence required that they should have efficiencies as nearly as possible one hundred percent. The present paper describes briefly the preparation of the counters and the measurement of their efficiencies. The result of the work is to show that the argon-alcohol counter filled without careful chemical treatment of the counter sheath is as efficient as any other type of counter.

II. THE PREPARATION AND PROPERTIES OF THE COUNTERS

Nearly 100 counters were used and they were all of the copper-in-glass type[2] with the cathode a bright copper sheath or 0.1-mm thickness and the anode a tungsten wire of 0.1-mm diameter. The sheath was cleaned by rubbing over with a rag soaked in benzene. The counters varied in diameter from 3.0 to 3.5 cm and in length from 20 to 80 cm. They were filled immediately they came from the glass blower with a mixture of argon (11 cm) and alcohol (1.5 cm) and then sealed off, the whole operation for each counter taking only one quarter of an hour. Counters so prepared had the following properties:

1. Efficiency: 99.5 percent (see Section III).
2. Starting potential: 1000 volts.
3. Length of plateau: 300 volts.
4. Anode-cathode resistance could be as low as 20,000Ω.

Counters of this type were in continuous use for two years without appreciable changes in their properties. Trost,[3] the discoverer of the argon-alcohol counter, was the first to use the simple method of preparation we have adopted but his method seems subsequently not to have been followed except by Curran and Petrzilka.[4] Other workers in this field, notably Neher,[2] Shonka,[5,6] Locher,[7] Loeb,[8] and Collie[9] recommend methods involving the careful cleaning of the counters with acid, frequent rinsings with water and baking on the pump or in the presence of gases rich in oxygen. Many of these more elaborate procedures result in reliable counters but it would appear from our experience that most of the chemical treatment is unnecessary.

III. THE MEASUREMENT OF THE EFFICIENCY OF A COUNTER

There are two reasons why an ionizing particle may pass through a counter without being recorded.

1. The particle may not produce an ion because of fluctuation. An ionizing particle produces about 40 ion pairs per cm path in air at N.T.P. or approximately 5 ion pairs per cm in the gas of a counter filled at 10-cm pressure. Thus the path of a particle through the sensitive volume of a counter must exceed several millimeters in length or there is an appreciable chance of no ion being produced. This effect was

[1] L. Jánossy and G. D. Rochester, Nature **148**, 531 (1941); Proc. Roy. Soc., in press.
[2] J. Strong, *Modern Physical Laboratory Practice* (Blackie & Son Ltd., London, 1940), chapter VII, p. 268, fig. 9.
[3] A. Trost, Zeits. f. Physik **105**, 399 (1937).
[4] S. C. Curran and V. Petrzilka, Proc. Camb. Phil. Soc. **35**, 309 (1939).
[5] Quoted by J. Barton Hoag, *Electrons and Nuclear Physics* (Chapman & Hall Ltd., 1938), p. 432.
[6] F. R. Shonka, Phys. Rev. **55**, 24 (1939).
[7] G. L. Locher, Phys. Rev. **55**, 675 (1939).
[8] L. Loeb, *Fundamental Processes of Electrical Discharges in Gases* (John Wiley & Sons, New York, 1939), p. 500.
[9] C. H. Collie and D. Roaf, Proc. Phys. Soc. **52**, 186 (1941).

first observed by Danforth and Ramsey.[10] The decrease in the efficiency of a counter with decrease in pressure reported in Section V (see Table II) is due to this cause.

2. The counter is insensitive to ionizing particles for a definite time after each discharge. This insensitive time is of the order of 10^{-3} sec. for an argon-alcohol counter.

The most important cause of lack of efficiency is (2). The efficiency of a counter is defined as the probability of the counter responding to an ionizing particle crossing the sensitive volume and it has been measured by many observers.[6,11–13] In the present instance the efficiency was measured by the apparatus illustrated diagrammatically in Fig. 1. The counter under test, A', was placed between C and D of a threefold coincidence set BCD. Counters B, C, and D were 20 cm long and A' and A 40 cm long. The coincidence set BCD was shielded from side-showers by a bank of 14 counters, A, connected with A' to an anticoincidence set. The anode-cathode resistance for A' and A was 20,000Ω and the coupling condenser 100μf. The pulses from the anticoincidence counters were amplified by a three-stage, resistance-capacity amplifier, mixed with the pulses from BCD and then passed on to a Rossi anticoincidence set[14] which had an efficiency of 100 percent. Since every ionizing

TABLE I. Counter data.

Observer and reference	Type	Dimensions d (cm)	Dimensions l (cm)	Filling	Total pressure (cm Hg)	ϵ %
Street and Woodward[11]	Copper in glass	3.8	13.0	Air	8	95*
Ehmert and Trost[12]	Brass in glass	4.5	14.2	Argon-Alcohol (90%–10%)	10	100 ±0.3*
Shonka[6]	Copper in glass	4.1	38.0	Air or H_2	7–10	98*
Neher[3]	Copper in glass	7.0	?	Argon-Xylene (95%–5%)	6–10	100 ±1†
Rose and Ramsey[13]	Copper in glass	1.0	15.0	Argon-Oxygen (94%–6%)	9	97
Rochester and Janossy	Copper in glass	3.0	40.0	Argon-Alcohol (90%–10%)	12.5	99.3 ±0.1*

* Corrected for accidentals and side showers.
† Not stated if corrected for accidentals and side showers.

[10] W. E. Danforth and W. E. Ramsey, Phys. Rev. **49**, 854 (1936).
[11] J. C. Street and M. H. Woodward, Phys. Rev. **46**, 1029 (1934).
[12] A. Ehmert and A. Trost, Zeits. f. Physik **100**, 553 (1936).
[13] M. E. Rose and W. E. Ramsey, Phys. Rev. **59**, 616 (1941).
[14] B. Rossi, L. Jánossy, G. D. Rochester, and M. Bound, Phys. Rev. **58**, 761 (1940).

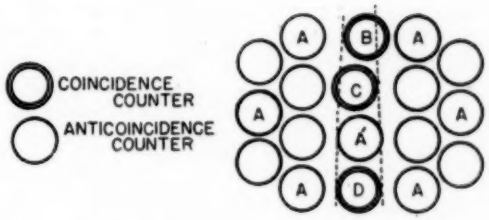

FIG. 1. Arrangement of counters.

particle crossing BCD had also to cross A', every coincidence BCD should have been accompanied by a discharge in A' if A' was 100 percent efficient and no anticoincidence $BCDA'$ should have been recorded. Thus the efficiency of the counter was given by

$$\epsilon=[1-(BCDA'/BCD)]\ 100 \text{ percent},$$

where $BCDA'$ was the rate of anticoincidences and BCD the rate of the coincidences.

In a detailed experiment the efficiency of one counter was found to be 99.3±0.1 percent after correcting for casual coincidences B, C, D which simulate anticoincidences. All other counters used in the investigation were tested and nearly all had efficiencies exceeding 99 percent.

IV. COMPARISON OF THE EFFICIENCIES OF DIFFERENT TYPES OF COUNTERS

The efficiencies of different types of counters are given in Table I from which it is seen that the argon-alcohol counter has the highest efficiency; it is therefore the most suitable counter for use in anticoincidence experiments. The slight differences in the results for different argon-alcohol counters are probably due to the differences in the dimensions of the counters and the different conditions under which the efficiencies have been measured.

V. THE DEPENDENCE OF THE EFFICIENCY OF THE ARGON-ALCOHOL COUNTER ON THE PARTIAL PRESSURES OF ARGON AND ALCOHOL

Five counters ($l=40$ cm, $d=3$ cm) were placed one above the other in a vertical plane. The counters had a common exhausting tube by which the pressure could be changed easily. If the efficiency of a counter filled at a pressure p was $\epsilon(p)$ and the rate of fivefold coincidences at p was $R(p)$ the ratios of the efficiencies at two

pressures p and P were

$$\epsilon(p)/\epsilon(P)=[R(p)/R(P)]^{1/5}.$$

Putting

$$\epsilon(P)=100, \quad \epsilon(p)=[R(p)/R(P)]^{1/5}\,100.$$

A rough survey was first made of the change in efficiency of a counter with the pressure of argon or alcohol. The results are given in Table II, the efficiencies recorded in the last column being relative to the maximum efficiency.

A comparison of the efficiencies of counters filled with (*a*) argon at 11 cm and alcohol vapor at 1.5 cm and (*b*) argon at 74.5 cm and alcohol vapor at 1.5 cm was then made. Alternate readings were taken for several days with the fivefold set first filled with the mixture (*a*) and then with the mixture (*b*).

Fluctuations in the intensity of the cosmic beam due to changes in barometric pressure, etc., during the course of the experiment were compensated for by setting up near the fivefold set a threefold set of sealed counters, and comparing the ratio of the fivefold to the threefold ratio at the two argon pressures. The results are given in Table III from which it is seen that the efficiency does not change when the pressure of argon is

TABLE II. Dependence of efficiency on pressure.

Pressure of alcohol vapor (cm)	Pressure of argon (cm)	Pressure of air (cm)	Count	Fivefold rate (c. per min.)	Relative efficiencies % ($\epsilon(p)$)
0.25			very short plateau, unstable		
1.00			1044	7.8±0.2	91
2.00			1157	11.7±0.3	98
3.00			very short plateau,		
4.00			counter unstable		
1.0	1.8		215	10.3±0.7	96
1.0	11.0		434	12.7±0.6	100
2.0	11.0		483	12.7±0.6	100
2.5	10.5		3920	12.8±0.2	100
2.5	50.0		7270	12.6±0.2	100
4.0	10.0		very short plateau, counter unstable		
2.5		1.0	1694	12.2±0.3	99

TABLE III. Efficiency dependence on argon pressure.

Pressure of alcohol (cm)	Pressure of argon (cm)	Counts: Fivefold	Counts: Threefold	Ratio: Fivefold: Threefold
1.5	11.0	71426	62645	1.140±0.0054
1.5	74.5	50480	44243	1.141±0.0065
			Difference	0.001±0.008

increased from 11.0 cm to 74.5 cm. Excluding fluctuations which exceed four times the standard deviation it is concluded that a change in the efficiency of the fivefold set by more than $4\times0.008=3$ percent, or a change of 0.6 percent in the efficiency of an individual counter, is incompatible with the observations. This result is not in agreement with the results of Stever,[15] who in a recent paper predicts theoretically the direct proportionality of the insensitive time of a counter and the pressure. Since the insensitive time σ is related to the efficiency by the formula

$$\epsilon=(1-n\sigma)100,$$

where n is the rate of discharges in the counter, it follows that the change in the efficiency $\delta\epsilon$ resulting from a change in the insensitive time of $\delta\sigma$ is

$$\delta\epsilon=-n\delta\sigma\ 100.$$

Stever finds that a change in the pressure of 6.4 cm (13.4–7.0) results in a change in σ of 2×10^{-4} sec. for a counter filled with an argon-xylol mixture. Since $n\sim6$ c. per sec.

$$\delta\epsilon=-6\times2\times10^{-4}\times100=-0.12 \text{ percent.}$$

Assuming that the insensitive time is directly proportional to pressure the change in efficiency of a counter when the pressure is changed from 11.0 to 74.5 cm should be 1.2 percent. The change in the fivefold rate should therefore be 6 percent. As no change in efficiency of this magnitude has been found one must conclude that the insensitive time is not directly proportional to pressure in the range 11.0 to 74.5 cm.

[15] H. G. Stever, Phys. Rev. **61**, 38 (1942).

Letters to the Editor

PROMPT publication of brief reports of important discoveries in physics may be secured by addressing them to this department. The closing date for this department is the third of the month. Because of the late closing date for the section no proof can be shown to authors. The Board of Editors does not hold itself responsible for the opinions expressed by the correspondents. Communications should not in general exceed 600 words in length.

The Polarization of Electrons

EDMUND TROUNSON AND JOHN A. SIMPSON, JR.
Department of Physics, New York University, University Heights, New York
October 13, 1942

RECENTLY experiments have been performed to determine electron polarization as predicted by the Mott theory on scattering.[1] The present experiment was carried out to test the previous results with apparatus redesigned to reduce to a minimum any spurious asymmetries in the experimental method. This was accomplished, principally, by using Geiger counters in a coincidence arrangement.

Electrons accelerated to an energy of 400 kev by a Van de Graaff electrostatic generator were used throughout the experiment so that a comparison with previous results would be possible.[1] The accelerating potential was stabilized to within ±0.5 percent. The same assembly for double scattering as constructed for the previous experiment was used, with the exception that ground conical joints with centered apertures replaced the aluminum exit windows. Into these joints were accurately fitted metal cylindrical units, each with a thin, vacuum-tight, aluminum window. Each cylinder contained two Geiger counters mounted parallel to each other and to the entrance window. Both units were evacuated and filled with a gas mixture of argon and alcohol. The counter cathodes were of oxidized aluminum with thin entrance and exit windows large enough to include the solid angle defining the electron beam. Two advantages of the above arrangement are evident. First, the coincidence counter units may be interchanged precisely with respect to the exit windows; secondly, the whole top foil assembly may be rotated as one unit without disturbing the existing geometry.

Two separate twofold coincidence circuits operated two scaling and recording circuits. The counter-circuit resolving time was much better than required for successful operation. Background counts from twofold coincidences were almost negligible with the beam on. Backgrounds were taken by interchanging the top foil and holder with an identical blank holder. The lower foil holder contained a gold foil interchangeable with an aluminum foil. Adequate shielding was obtained by enclosing the whole rotating top assembly in a circular lead box; additional shields were placed along the accelerating tube, around the Faraday cage, and over defining apertures.

Gold foils were prepared by evaporation, and the thickness was calculated by utilizing the inverse square law, those used in this experiment being 3.8×10^{-5} cm thick. This would give a calculated ω of 5° on Wentzel's criterion. The aluminum foil was 7.6×10^{-5} cm in thickness and was commercially prepared.

The ratios of the number of electrons scattered into the two resulting beams were obtained with all the orientations necessary to determine the reflection-transmission ratios of gold and aluminum, the counter-geometrical asymmetry, and the percent polarization of the electrons in transmission. Table I lists a few of the more important corrected ratios. The letters *A* and *B* refer to the two coincidence counter assemblies, and the orientations are as listed in reference 1, Fig. 4.

The counter-geometry asymmetry was 1 percent. Note that no separation of the asymmetry into that due to the counter or geometry alone was made.

The apparent asymmetry due to polarization for gold is 6.8 percent, a result in agreement with that of Shull, Chase, and Myers,[1] while the apparent asymmetry for aluminum is −2.1 percent.

The reflection-transmission ratio[2] for gold foils, as well as that obtained by using an aluminum bottom foil in transmission, was 1.49. The complete results of this experiment will be published at an early date.

TABLE I. Ratio of electrons scattered into the two beams.

Orientation of foils, and counter units	Ratio
II Gold upper and lower foil	1.41
IV Gold upper and lower foil	1.58
V Gold upper and lower foil	1.56
V Aluminum lower foil	1.46
VIII Aluminum lower foil	1.51

[1] Shull, Chase, and Myers. Phys. Rev. 63, 29 (1943), and references therein.
[2] For a discussion of the importance of these ratios, see paper by Goertzel and Cox, Phys. Rev. 63, 37 (1943).

The Cepheid Theory of the Origin of the Solar System

A. C. BANERJI
University of Allahabad, India
December 22, 1942

THE regular features of the solar system are well known and various theories have been proposed to explain them. However, these have been found to be inadequate on the general grounds of angular momentum and of energy, e.g., Jeans and Jeffreys' tidal theory has been criticized by Russell, and Lyttleton's "enticement" theory criticized by Luyten and Hill. The author, while considering the large adiabatic pulsations of the Cepheid variable, was led to an entirely different theory of the origin of the solar system, based on the instability of radial oscillations of a variable star. The square of the amplitude has been neglected in most investigations on oscillating stars, which are restricted to the consideration of small oscillations. The author has found that the oscillations are no longer stable when terms of the order of the square of the amplitude are retained. He has considered in detail the star

models: (1) A star of uniform density; and (2) a star in which the density varies as a power of the distance from the center, except in a small central homogeneous core.

In the author's Cepheid theory of the origin of the solar system,[1] a star of about nine times the sun's mass is supposed to pass so near a Cepheid variable of about the same mass as to make, by its tidal influence, the oscillations of the Cepheid unstable. Matter of the sun's mass is ejected from the Cepheid together with a ribbon initially connecting the two. The planets of the solar system would be formed out of the portion of the ribbon attached to the sun's mass. The solar system would have to take about two-fifths of the energy of the parent Cepheid in order to escape from the latter. It has also been shown that the visiting star will have sufficient angular momentum to impart the necessary amount to the planets. The parent Cepheid too, on this theory, will have a planetary system of its own. A less number of assumptions is made in the theory than in any other existing theory, and the probability of existence of other planetary systems is definitely increased.

On the lines of the author, instability of radial oscillations of even small amplitude has been found for stellar models in which the laws of density are (1) $\rho=a-br$, (2) $\rho=a-br^2$, and (3) $\rho=k/r^n$, except in a small, homogeneous core. The analysis suggests that for the stability of radial oscillations the distribution of density in the star must be more or less uniform. The investigations of Chandrasekhar and Kopal on the central condensation in Cepheids lend support to this view.

[1] A. C. Banerji, Proc. Nat. Inst. Sci. India **8**, 173–197 (1942).

Scattering of Protons by Magnesium Nuclei

GERALD A. WRENSHALL,
McMaster University, Hamilton, Canada
December 15, 1942

IN earlier reports[1,2] angular distribution and energy measurements on 6.9-Mev protons scattered by magnesium nuclei were presented along with a description of the emulsion track camera with which exposures were made. Further analyses of runs, referred to in the above papers as numbers III and IV,[3] have yielded the following additional results:

(*a*) The intensity distribution of scattered protons as a function of scattering angle ϕ has been measured for a series of 26 emulsion plates exposed during run No. IV at angles extending from $\phi=20\pm0.5°$ to $\phi=170\pm0.5°$, inclusive. Exposure factors for each plate were determined by passing the unscattered portion of the primary proton beam into a Faraday chamber with attached condenser arranged to discharge on attaining a critical potential difference. Exposure was then measured in terms of the number of condenser discharges occurring during a run, and was adjusted for different angles so that the number of emulsion tracks per plate was approximately constant.

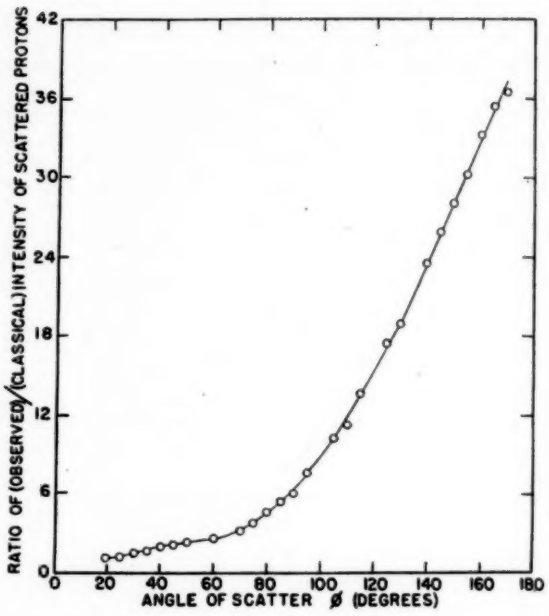

FIG. 1. Ratio of (observed/classical) intensities of 6.9-Mev protons scattered by magnesium. Scattered protons of all ranges were counted.

From knowledge of the exposure factor and the number of tracks scattered for each angle, relative intensities of scatter as a function of ϕ were obtained. The ratio of observed intensities to values calculated from Rutherford's classical formula for inverse square law scattering is plotted against ϕ in Fig. 1. Plates measured contained an average of 1700 tracks each while check number counts agreed to within 0.8 percent. Pronounced deviations from inverse square scattering are evident at angles greater than 20°.

(*b*) Relative intensities of the four proton groups reported earlier[2] have been estimated for a few plates (Table I). The symbols E, I_1, I_2, I_3, are again used to identify the elastic and inelastic scatter proton groups of energies 5.94, 4.62, 3.25, and 2.04 Mev, respectively. Probable accuracy of the results of Table I was limited by the necessity of estimating the intensities of peaks E and I_1 relative to I_2 and I_3 from two separate runs normalized to the same exposure. Omission of values of I_2 and I_3 at certain angles merely indicates that their intensities were not measurable to the order of accuracy indicated, not that they were absent.

(*c*) Evidence of the existence of a fifth group I_1' of

TABLE I. Relative intensities N_E, N_{I_1}, N_{I_2}, N_{I_3} of proton groups E, I_1, I_2, I_3, respectively, as functions of scattering angle ϕ.

$\phi=$	25°	45°	70°	95°	130°	160°	Est. error
N_E	6,100	1,100	327	144	198	308	5%
N_{I_1}	0	140	268	292	159	211	5%
N_{I_2}	0	480	25	46	—	126	15%
N_{I_3}	—	180	42	54	—	74	15%

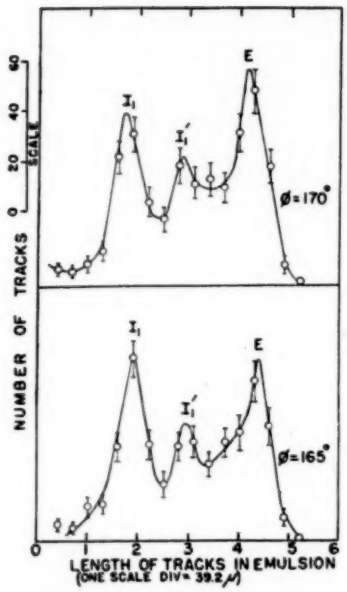

FIG. 2. Range distribution curves for 6.9-Mev protons scattered by magnesium, indicating presence of additional proton group I_1'.

scattered protons with estimated energy equal to 5.3 Mev has been obtained, especially at large scattering angles (Fig. 2). Further indications of what appears to be the same group have also been observed at the scattering angles 45°, 60°, 105°, and 125°. It is calculated that were this measured value slightly lower (i.e., 5.1 Mev) it would, when associated with the proton groups described above, predict gamma-ray energies in fair agreement with those listed by Livingston and Bethe[5] at 0.94, 1.93, and 3.08 Mev for the abundant isotope Mg^{24}.

The results presented in the present communication are based on measurements from runs made by the late Professor T. R. Wilkins at the University of Rochester, Rochester, New York.

[1] T. R. Wilkins and G. Wrenshall, Phys. Rev. **58**, 758 (1940).
[2] T. R. Wilkins, Phys. Rev. **60**, 365–373 (1941).
[3] In run No. III a suitable thickness of aluminum stopping foils was inserted between scattering foil and photographic plates in order to prevent the scattered protons from penetrating through the emulsion layer to the glass backing of the photographic plates. This run was supplemented by No. IV in which no stopping foils were inserted. Proton groups shown in Fig. 2 were measured from plates of run No. III, while total number counts and measurements of shorter range proton groups were made from plates of run No. IV. One plate ($\phi=95°$ of run No. IV) was found to show all groups.
[4] No inelastically scattered proton groups were observed at $\phi=20°$ in either of runs III or IV, while evidence of the shortest inelastic scatter group was found at $\phi=25°$.
[5] M. S. Livingston and H. A. Bethe, Rev. Mod. Phys. **9**, 245 (1937).

Proceedings of the American Physical Society

MEETING AT CHICAGO, ILLINOIS, November 27–28, 1942

THE "Thanksgiving meeting" of 1942, being the 251st of the American Physical Society, was held on November 27 and 28 at our traditional meeting place of the season, the University of Chicago. The Local Committee, headed by A. J. Dempster, earned the gratitude of the Society by making satisfactory arrangements in spite of handicaps without precedent, which deprived us of our habitual meeting rooms both for the scientific sessions and for the dinner. Though many once familiar figures were absent for reasons which can be divined, the attendance was fairly good, and over eighty people came to the dinner and subsequent speeches. The Physics Club of Chicago joined in our meetings and dinner.

The scientific programme was headed by three invited papers, the following:

Applications of Nuclear Physics to the Biological Sciences. I. PERLMAN, *University of Chicago.*

Problems in the Theory of Atmospheric Cosmic-Ray Showers. P. AUGER, *University of Chicago.*

The Theory of Random Processes. G. E. UHLENBECK, *University of Michigan.*

There were thirty contributed ten-minute papers, of which the abstracts (including those of two, Numbers 10 and 20, which were read by title) are appended.

The dinner was held on Friday evening at the Quadrangle Club. Henry Crew and Arthur Compton spoke briefly in honor of the late Henry Gordon Gale, and Pierre Auger then described to the gathering the *Centre National de la Recherche* instituted in France a few years before the present war.

The Council met on November 27 and 28. One hundred and thirty-three candidates were elected to Membership and four to Fellowship; their names are appended. Word was received by the Council of the loss to the Society through death of eight Fellows and Members:

HENRY GORDON GALE, *University of Chicago,* President of the Society 1929–30, noted for his work in spectroscopy and in the testing of the theory of relativity.

E. C. BRYANT, *Middlebury College,* a member since 1902 or earlier.

O. HOVDA, *Evansville College.*

E. G. LUNN, *Washington.*

O. LUHR, formerly of *Union College.*

H. J. MCNICHOLAS, *National Bureau of Standards.*

E. A. NAHUM, *Cambridge University,* known for research on transmutation; killed in an air-raid on Cambridge.

H. C. SNOOK, retired, formerly active in the development of x-ray tubes.

Owing to the circumstances which brought about the cancellation of the New York meeting of the A.A.A.S. and the postponement (to January 22–23, 1943) of the Annual Meeting of the Physical Society, the Council recommended an amendment to the By-Laws which would give it new powers for dealing with similar situations in the future. This amendment was offered at the Saturday morning session and adopted by unanimous vote of the Fellows there present. The By-Laws of the American Physical Society therefore stand amended by the addition of the following paragraph to Article II thereof:

"During an emergency caused by war, the Council is empowered to authorize fewer than four regular meetings each year and to set for the Annual Meetings a date not between the 26th and 31st of December."

The Council further ratified the decision of the officers of the Society not to publish a membership list in 1943.

Elected to Fellowship: Julian M. Blair.

Advanced from Membership to Fellowship: G. Antonoff, L. C. Marshall, R. Smoluchowski.

Elected to Membership: Agnew, Harold; Allen, Arthur Beverly; Anderson, William; Atchison, Fred Stanley; Barsy, Imre J.; Beattie, John Orne; Beck, Clifford K.; Berry, Herbert W.; Bertelink, Everhard H. B.; Betz, Howard; Bouricina, Willard G.; Bridge, Herbert S.; Brown, Robert Arnold; Brumbaugh, D. Q.; Burgess, John S.; Burkhard, Donald G.; Carpenter, Robert O'B.; Carstensen, Edwin L.; Cashwell, Edmond D.; Cook, Donald B.; Cooter, Irvin L.; Davis, Leo; de Carvajal-Forero, Jose; Degani, Meir H.; Dennison, Capt. Richard W.; Downey, Joseph V.; Eilers, Walter; Epstein, Benjamin; Feld, Bernard T.; Fitzgerald, James W.; Foldy, Leslie L.; Fry, Cleota Gage; Gas-

teiger, Edgar Lionel, Jr.; George, Thomas Waller; Goertzel, Gerald; Goldberg, Harold D.; Goodman, Isaac S.; Grace, Frank; Graham, R. Beardsley; Hadley, Lawrence N., Jr.; Hanau, Richard; Hanley, Thure E.; Hanson, Victor F.; Hershkowitz, Joseph; Hiatt, Ralph E.; Hibbon, Carl; Hinton, Joan; Honig, Richard E.; Howell, Alvin H.; Hughes, Vernon; Humiston, Homer A.; Jacobs, Harold; Josephson, Vernal; Kashdan, William H.; Kohman, Truman P.; Kotelchuck, Abraham; Kretsch, Hans W.; Kupferberg, Kenneth; Kupferberg, Max; Lafferty, James M.; Langmuir, Robert V.; Larsen, Jack; Laufer, Arthur Russell; Lawson, James R.; Lewis, Harold W.; Lewis, Lloyd George; Liebson, Sidney H.; Little, John L.; Loewenthal, Morton; Lorentz, Lilly; Mairson, Theodore; Mayer, Harris L.; McFarland, Robert H.; McGowan, Francis K.; Meister, Arnold George; Merle, John, Jr.; Miehle, William; Mills, Carroll B.; Miner, W. B.; Mitchell, John J.; Montgomery, Edward B.; Mulvihill, Patrick E., Bro.; Nelson, Roy A.; Nelson, R. W.; Newberry, Sterling P.; Newton, Robert R.; Nielsen, Carl E.; Osborn, John Alford; Pearce, Willard John; Picard, Robert G.; Powell, Roger S.; Purbrick, Robert L.; Ramo, Simon; Reitz, John R.; Retherford, Robert Custis; Rhoten, Rex R.; Ringo, George Roy; Roberts, Louis D.; Rogozinski, Anatole; Russell, B. Roswell; Rustad, Brice Miles; Sakmann, Bernhard Walter; Schatz, Frederick U.; Sharkey, Andrew Gans, Jr.; Shore, Ferdinand; Simard, Roger G.; Skolil, Lester L.; Smith, Howard Lambert; Smith, Sidney T.; Smith, Warren Harding; Spence, Robert D.; Stifler, William W., Jr.; Stoner, Thomas Arthur; Such, John J.; Tabin, Julius; Tralli, Nunzio; Suydam, B. R.; Turner, C. M.; Vandivere, Edgar; Van See, Arthur F.; Vigliante, John R.; Vineyard, George H.; Walkup, Lewis E.; Wehle, Louis B., Jr.; Welch, Homer W., Jr.; White, R. S.; Wiedenbeck, Marcellus L.; Wilkening, Marvin H.; Wilson, Paul Bernes; Wineland, W. C.; Woernley, Donald L.; Wollan, Abner J.; Wooten, Benjamin A., Jr.

Correction: F. R. Hirsh, Jr., whose initials were wrongly given in the Proceedings on an earlier occasion, was advanced to Fellowship on June 26, 1942.

Abstracts of Contributed Papers

1. Disintegration of the Long-Life Radioactive Isotope of Tantalum. R. V. Zumstein, J. D. Kurbatov, and M. L. Pool, *Ohio State University.*—Two radioactive isotopes of tantalum have been reported, Ta^{180}—8.2 hr. obtained by activation of tantalum with fast neutrons and Ta^{182}—97 days by activation with slow and fast neutrons. The second period has now been produced by a prolonged deuteron bombardment of tantalum. It emits intense gamma-radiation with energy of 1.6 Mev. Beta-rays have been resolved into the following groups: 0.98±.1 Mev; 0.32±.04 Mev and approximately 50 kev. The half-life obtained independently from gamma- and beta-radiation measurements is 117±3 days. In addition to the disintegration of Ta^{182} to W^{182}, the third group may be interpreted as evidence for the disintegration of Ta^{182} to Hf^{182} by means of *K*-electron capture. A stable isotope of Hf^{182} is therefore indicated.

2. Transmutation of Barium. Katherine E. Weimer, M. L. Pool, and J. D. Kurbatov, *Ohio State University.*—New evidence has been obtained for the existence of a radioactive barium isotope with half-life 29±0.5 hours after barium was bombarded with 10-Mev deuterons and fast neutrons. The energy of the beta-rays emitted is estimated to be 260 kev. Low intensity gamma-rays with energy of approximately 340 kev are found to be present. X-rays corresponding to the *K* series of barium have been observed. Deuteron bombardment of barium has also yielded an isotope with 14.2 day half-life, which is identified with a previously reported barium isotope with same half-life obtained by bombardment of cesium with deuterons. This confirms the assignment as Ba^{133}. The ratios of radiation intensities of barium isotopes produced by deuteron bombardment have been computed. Bombardment of barium with protons revealed a lanthanum isotope with 17.5-hr. period. Activation of cerium with fast neutrons produced Ba^{139} with half-life of 85 minutes, but radiation intensity was not sufficient to identify a longer period. Bombardment of cesium with α, d, and p did not reveal 29-hr. barium. Nuclear reactions observed and type of radiations emitted by 29-hr. barium suggest isomeric position of it with one of a stable isotope of barium, probably Ba^{135}.

3. Thresholds for the Nuclear Photo-Effect. G. C. Baldwin and H. W. Koch, *University of Illinois.*—By integrating the voltage on the main coils of the 20-Mev betatron with an RC circuit, the orbit expander can be actuated when a predetermined amount of flux has been linked with the electrons' orbit. This permits continuous energy control and defines the peak x-ray energy more precisely than the phase-shifting method previously described.[1] This tech-

nique has been applied to measurement of threshold energies for the (γ, n) reaction. Activities are measured with thin-walled G-M counters as a function of maximum x-ray energy, the resulting curves permitting the threshold to be estimated closely. Preliminary measurements indicate the following thresholds in Mev: Cu (10 m), 10.8–10.9; Mo (17 m), 13.3–13.7; Fe (9 m), 14.1–14.3; O (2 m), 16.3–16.7; C (21 m), 18.7–19.5. The limits given are set by accuracy of detection. Absolute calibration may lead to systematic revision of these figures, but they are considered reliable to within 400 kev. The threshold for carbon agrees, within the limits of error, with that expected from known data. Other reactions are being investigated.

[1] D. W. Kerst, Rev. Sci. Inst. 13, 387 (1942).

4. The Nuclear Excitation of Indium by X-Rays and Electrons. BERNARD WALDMAN AND MARCELLUS L. WIEDENBECK, *University of Notre Dame.*—Using x-rays produced by a pressure electrostatic generator, nuclear excitation experiments[1] on indium were extended to 2.85 Mev. The threshold for the process is $1.12 \pm .03$ Mev and activation levels are found at 1.55 Mev, 2.13 Mev, and 2.64 Mev. The direct excitation of indium by electrons[2] showed the same threshold and activation levels as the x-ray excitation. Since the electron beam is homogeneous the electron excitation curve was a series of peaks indicating resonance absorption of the electrons by the indium nucleus.

[1] Waldman, Collins, Stubblefield, and Goldhaber, Phys. Rev. 55, 1129 (1939); Collins and Waldman, Phys. Rev. 59, 109 (1941).
[2] Collins and Waldman, Phys. Rev. 57, 1088 (1940).

5. A High Energy Gamma-Ray from Radio-Yttrium (100 Days). G. R. GAMERTSFELDER,* *University of Illinois.*—It has been known for some time that Rd Y (100 days) emits γ-rays of about 1.9 Mev[1,2,3] and 0.9 Mev[2,3] in cascade. The transition of about 2.8 Mev, corresponding to the sum of these energies, appears to be "forbidden" and has not been observed so far. It seemed worth while to search for this transition with a more sensitive method than those previously employed. If this 2.8-Mev γ-ray were emitted, one should be able to observe with it the photo-disintegration of deuterium (threshold 2.17 Mev). A Rd Y source of a few millicuries intensity which had been produced in the 60″ cyclotron in Berkeley by bombarding strontium with deuterons was available for this investigation. A search for photo-neutrons from Rd Y$+D_2O$ was made and was successful. The intensity of the 2.8-Mev γ-ray was compared with that of the 1.9-Mev γ-ray by a series of experiments and found to be about 1 percent.

* Now at the Radiation Laboratory, Massachusetts Institute of Technology, Cambridge, Massachusetts.
[1] G. Scharff-Goldhaber, Phys. Rev. 59, 937A (1941).
[2] J. R. Richardson, Phys. Rev. 60, 188 (1941).
[3] J. R. Downing, M. Deutsch, and A. Roberts, Phys. Rev. 60, 470 (1941).

6. A Method for Measuring Total Cross Sections for Low Energy Neutrons. C. O. MUEHLHAUSE, *University of Illinois.*—The possibilities and limitations of existing methods for measuring total cross sections for low energy neutrons (usually photo-neutrons of a few hundred-kev energy) are discussed. It is shown that a new procedure for such measurements is desirable. A method based on the particular phenomena arising in the slowing down of low energy neutrons[1] has been developed and applied in a few cases. Photo-neutrons from RdTh$+D_2O$ (220 kev) were used in this work. The possibilities and limitations of the new method will be discussed.

[1] M. Goldhaber and R. D. O'Neal, Phys. Rev. 60, 834 (1941).

7. Absorption of High Energy Quanta. G. D. ADAMS AND R. K. CLARK, *University of Illinois.*—Absorption measurements have been made for quanta of the high energy tip of the Bremsstrahlung spectrum from the 20-Mev betatron.[1] The tip is isolated by using Cu monitor and detector sheets, assuming the maximum energy of the spectrum is above the threshold ($\sim$10.5 Mev) for the Cu^{63} (γ, n) Cu^{62} reaction. The positron activity of Cu^{62} is observed with Lauritzen electroscopes.

Be, C, Al, Fe, and Pb have been used as absorbers. The resulting absorption checks within 1 percent the theoretical values calculated from standard formulae[2] for an equivalent quantum energy.

Running the betatron at 13 Mev max., the equivalent quantum energy is about 11.75 Mev, for which the absorption coefficients follow:

Z	$_4$Be	$_6$C	$_{13}$Al	$_{26}$Fe	$_{82}$Pb
τ (cm^{-1})	0.0278	0.0292	0.0601	0.234	0.635

Experiments with other monitor and detector sheets are now in progress.

[1] D. W. Kerst, Rev. Sci. Inst. 13, 387 (1942).
[2] W. Heitler, *Quantum Theory of Radiation* (Oxford, 1936).

8. The Nature of the Primary Cosmic Radiation. MARCEL SCHEIN AND MARIO IONA, JR., *University of Chicago.*—Using a cosmic-ray balloon apparatus, the number of cosmic-ray showers below a lead thickness of 2 cm was measured in coincidence with the vertical rays passing through 4 cm of lead. To register a maximum number of showers, two Geiger-Mueller counters were placed directly below the 2-cm lead block. This arrangement made it possible to measure all the showers of 2 or more particles with an angular divergence of more than 20 degrees. Since a primary electron, entering the earth's atmosphere at Chicago (latitude 52° N), carries a minimum energy of 3×10^9 ev, it is expected that in the first radiation unit each of these electrons passing through a lead thickness of 4 cm generates below 2 cm of lead a shower of more than 15 particles. At altitudes corresponding to an average pressure of 2.5 cm Hg, it was found that from all the particles passing through the 4 cm only 9.8 percent emerge below 2 cm of Pb with a shower of 2 or more particles. This is in accordance with the results of previous experiments* and demonstrates that the main body of the primary cosmic radiation does not consist of electrons.

* Marcel Schein, William P. Jesse, and E. O. Wollan, Phys. Rev. 59, 615 (1941); W. F. G. Swann, Phys. Rev. 59, 770 (1941); 59, 836 (1941).

9. Slow Mesotrons in the Stratosphere. MARIO IONA, JR. AND MARCEL SCHEIN, *University of Chicago.*—With a set of Geiger-Mueller counters in fourfold coinci-

dence, the vertical intensity of cosmic rays through 4 cm of Pb was measured in the high atmosphere. A second fourfold coincidence set was used for measuring the intensity of the penetrating component through 8 cm of Pb. Plotting the difference between the two intensities as a function of altitude, we obtained a curve with a maximum at an altitude of 20 kms (atmospheric pressure 4.5 cm Hg). The majority of the cosmic rays with a penetrating power between 4 and 8 cm of Pb must consist either of mesotrons or of protons. This follows from the fact that only very few of these particles generate showers below a lead thickness of 2 cm (previous abstract). Mesotrons, having their momentum in the above given range, have a specific ionization in air which is nearly equal to the average specific ionization of cosmic rays on the surface of the ground. On the other hand protons with these momenta show a much heavier ionization than that mentioned above. Since the average specific ionization of cosmic rays in the stratosphere is nearly equal to that on the ground, it can be concluded that the majority of the particles which penetrate 4 cm but are stopped by 8 cm of Pb consist of low energy mesotrons (average kinetic energy 1.2×10^8 ev).

10. Experimental Determination of the Disintegration Curve of Mesotrons. BRUNO ROSSI AND NORRIS NERESON, *Cornell University.*—The disintegration curve of mesotrons at rest has been experimentally determined by investigating the delayed emission of electrons which takes place after the absorption of mesotrons by matter. For the purpose of this measurement, a circuit has been developed which records the time intervals between the discharges of two sets of Geiger-Müller counters. As a preliminary experiment the natural time lags of the counters to be used in the main experiment were investigated. Most of the time lags were found to be smaller than 0.2 microsecond with very few larger than 0.5 microsecond. In the main experiment two sets of counters were used to detect the arrival of the mesotron on a brass plate and the emission from the plate of the corresponding decay electron, respectively. About 500 disintegration processes were recorded in which the delays between the discharges of the two sets of counters were greater than 0.55 microsecond. Within the experimental errors the distribution of the observed delays follows an exponential law corresponding to a mean lifetime of 2.3 ± 0.2 microseconds.

11. Acceleration of Decay in the Anode Effect by Partial Excitation. PAUL L. COPELAND, *Illinois Institute of Technology.*—After the apparent contact potential of an unheated electrode in a vacuum tube relative to the cathode has been shifted by passing an abnormally large current to it for a short time (a process called excitation), there is a drift toward the normal condition (decay). The contact potential shift is nearly linear when plotted against the logarithm of the time measured from the change in the exciting current.[1] In the present work a large shift in the contact potential of the grid in a triode was produced by excitation for one minute. Then the decay was followed for several minutes. After this an excitation current was allowed to flow for 0.004 sec. This pulse resulted in: (1) a temporary increase in the contact potential relative to the normal state, and (2) an increased rate of drift. The net result was a more rapid approach to normal. If the decay curve is broken into sections divided by the exciting pulses and in each section the contact potential is plotted as a function of the logarithm of the time after the beginning of the section, it is found that each section is nearly linear.

[1] P. L. Copeland, Phys. Rev. **57**, 625 (1940); P. L. Copeland and G. G. Carne, Phys. Rev. **61**, 635 (1942).

12. The Temperature Coefficient of Secondary Emission and the Work Function of Molybdenum Targets Coated with Beryllium and Treated with HCl. WILLIAM R. KENNEDY AND PAUL L. COPELAND, *Illinois Institute of Technology.*—Molybdenum strips about three mm wide were outgassed in a vacuum, and thick films of beryllium were evaporated on them. These strips were washed in air with HCl and then used as targets in an experimental secondary emission tube. Temperature control of the target was provided by means of an external battery connected across the target. Secondary electron emission measurements as a function of primary electron energy were made for temperatures from room temperature up to temperatures at which thermionic emission became appreciable. It was found that the secondary electron emission remained substantially constant over this range of temperatures. A maximum of about 2.5 secondaries per primary appeared at primary electron energies of around 500 electron volts. Thermionic emission data were taken, and the Richardson plot gives a work function of about 5.5 volts.

13. Diffusion Rate of Carbon in Iron Alloys. R. SMOLUCHOWSKI, *General Electric Company, Schenectady, New York.*—Studies of rates of various transformations and reactions in iron alloys seem to indicate that certain elements have a definite influence on the rate of diffusion of carbon in gamma iron. In particular, cobalt shows a pronounced accelerating influence. By direct measurement of the rate of carbon diffusion in iron-cobalt alloys, this conclusion is confirmed and an increase of the diffusion coefficient established. An addition of 4 percent cobalt decreases the activation energy by about 2500 calories down to 30,000 calories, corresponding to an almost twofold increase of the diffusion rate at one atomic percent carbon concentration. At higher carbon content the accelerating influence of cobalt is smaller. This property of cobalt is unusual especially in view of the fact that both manganese and nickel are known to have practically no influence on the diffusion of carbon. Similar experiments with tungsten-iron and molybdenum-iron alloys indicate that these two elements decrease the diffusion rate of carbon. The change of diffusion rates, while well measurable, are too small to explain changes in other reactions.

14. Equilibrium Between the Alpha- and Gamma-Phases of Pure Iron. R. S. WEHNER AND WHEELER P. DAVEY, *Pennsylvania State College.*—During experiments made by A. Wangsgard to determine the A_3c point in pure iron, it was noticed that both alpha- and gamma-iron could be found together between the A_3c and the A_3r

points. This was contrary to the current ideas of metallurgists. A careful examination was therefore made of the structure of pure iron (from iron carbonyl, kindly supplied by Professor R. Mehl), between the A_3c and the A_3r points, using an x-ray spectrometer so built that the specimen was kept in a hydrogen atmosphere in a furnace whose temperature could be automatically kept constant to within 0.25° at any desired temperature in the neighborhood of 910°C. It was found that when pure iron was cooled below the A_3c point, it contained both alpha- and gamma-phases over a temperature range of several degrees. Both phases were kept under observation over a period of two hours with readings of temperature, angle of x-ray diffraction, and intensity of diffracted beam, all measured at one minute intervals. It is evident that alpha- and gamma-iron can exist in equilibrium with each other at all temperatures between the A_3c and A_3r points. This is consistent with the phase rule.

15. Temperature Rise in Rubber on Fast Stretching. R. L. ANTHONY AND S. L. DART, *University of Notre Dame.*—The rise in temperature on fast stretching of rubber was first investigated quantitatively by Joule. The thermodynamic relationship of this effect to other thermoelastic phenomena was established by Kelvin. Later investigations have yielded widely varied results. In particular, previous results obtained for the temperature rise accompanying adiabatic stretching are much too small, as may be checked by simple sensory observations. Employing a galvanometer of period 1/10 sec., and sensitivity 10^{-7} amp./mm, the authors have obtained values of this temperature rise of the expected order of magnitude. For example, an accelerated latex vulcanizate gave a temperature rise of 14.7°C at 600 percent extension. The change in temperature was studied as a function of both extension and retraction. These investigations show that at least a part of the disagreement between earlier workers was due to differences in the samples studied and also to heat losses resulting from long galvanometer recording times. The variety of samples studied, as well as the range of extensions employed, make this investigation more comprehensive than previous work.

16. Equation of State of Synthetic Rubbers. L. E. PETERSON AND EUGENE GUTH, *University of Notre Dame.*—The equations of state of several representative synthetic rubbers have been obtained experimentally for the first time. Comparing the results so obtained with the general statistical theory of rubber elasticity developed by James and Guth the applicability of the theory to synthetic rubber was checked and its usefulness thereby extended. The equation of state, i.e., the relationship between the stress as a function of strain and temperature, was obtained by employing a relaxation method. The synthetics investigated exhibited plastic flow and permanent set to a greater degree than natural rubber. Nevertheless, they displayed the same general features of stress-temperature behavior and also a thermoelastic inversion point in general accordance with the theory. By the application of thermodynamics, the experimental equation of state was resolved into two additive components—the internal energy and entropy contributions. The entropy component agreed with the theoretical curve and accounted for the major portion of the stress in each case.

17. Theory of X-Ray Diffraction in Mosaic Crystals. W. H. ZACHARIASEN, *University of Chicago.*—A great many crystals are neither so perfect that the x-ray diffraction data can be interpreted by means of the dynamical theory, nor so imperfect that the Darwin theory of the ideal mosaic crystal is valid. A general theory of x-ray diffraction applicable to mosaic crystals of this intermediate type has been developed by the writer. Solutions have been obtained only for mosaic crystals which are in the form of plane parallel plates since the boundary conditions are difficult to handle for other geometrical shapes. The expression for the diffraction pattern $\mathfrak{P}$ is given in terms of the thickness t of the constituent blocks, the distribution function W for the orientations of these blocks, and the diffraction pattern P of a single block. The integrated reflecting power $\mathfrak{R}$ cannot be expressed in simple form unless the half-width of the distribution function W is large compared to the half width of the diffraction pattern P. If this condition is fulfilled one finds for the symmetrical Bragg case and thick crystal plate

$$\mathfrak{R}=[R/1-\exp(-2\mu t/\gamma)],$$

where R is the integrated reflecting power of a single block (as known from the dynamical theory), μ the linear absorption coefficient, and γ the direction cosine of the incident beam. This result is identical with that of Darwin for very small block size, but as t increases $\mathfrak{R}$ approaches the perfect crystal value.

18. Morphic Double Refraction in Presence of Strong Intrinsic Anisotropy. WILFRIED HELLER, *University of Minnesota.*—Morphic double refraction in dispersed systems of oriented intrinsically isotropic anisometric ultramicroscopic particles disappears if the refractive indices of medium and particles (n_m; n_p) become equal. The same holds (Ambronn) for particles with weak intrinsic double refraction (mean index $n_p \sim n_\alpha \sim n_\gamma$). The case of strong intrinsic anisotropy has now been considered using tartrazine (n_α: 1.49; n_γ: >1.8) and magnetic orientation. Morphic double refraction decreased with increasing n_m without any indication of reversal when $n_m = n_\alpha$, or $= n_p$ (1.59), or $=1.63$ (the highest n_m investigated. All data for 5790A). Morphic double refraction appeared therefore to reach a zero value only if $n_m = n_\gamma \cdot n_\gamma$ was the refractive index perpendicular to the rod axis of the acicular crystals. The crystal rods were oriented perpendicular to the direction of the field. The direction of n_γ coincided therefore with the direction of the symmetry axis of revolution of the anisotropic dispersed system. This result suggests the rule: morphic double refraction disappears if the periodicity of the refractive index is suppressed parallel to the symmetry axis of revolution (extraordinary direction) of a morphically anisotropic dispersed system. Ambronn's above rule appears as an implicit approximation.

19. The Localization Phenomenon in G-M Counters. M. H. WILKENING AND W. R. KANNE, *Illinois Institute of Technology.*—Localization of the discharge in fast counters has been further investigated. Splitting the cathode will localize the discharge, if the separation is sufficiently great, simply by reducing the field intensity in that portion of the counters to threshold values or below. A similar stopping of the discharge spread along the wire has been effected by placing insulating materials of varying geometry and position in the counter. A bead on the wire or a ring fitted into the cylinder are both effective arrangements. The insulating materials reduce the field intensity by the accumulation of surface charges. The localization phenomenon was not observed when slow counter fillings such as pure argon or hydrogen were used. In these experiments the efficiency of localization was found to depend on (1) geometry and nature of the localizing device, (2) overvoltage at which the tube was operated, and (3) concentration and kind of gas filling used. The results of these investigations are consistent with the theory that photons are the chief agents in producing new ions for the spread of the discharge along the wire. A strong absorption of these photons by the gas or vapor in fast counters is implied. The effect of various gases in this respect and the relation to fast counter action has been studied.

20. Construction of Surfaces of Constant Normal Separation. H. M. PARKER, *Tumor Institute of Swedish Hospital, Seattle.*—A surface generated from a given surface by the motion of the end of a normal of constant length traversing the surface is required in the construction of radium applicators. A modified copying machine using a universal link whose length is the required normal separation will cut such surfaces in wood, dental compositions, and plastics. Accuracy in the separation and easy correlation of corresponding points in the two surfaces are the advantages over previous hand methods.

21. $\Delta_1 F$ Values from Some Chlorine Dioxide Bands. JESSE B. COON, *Indiana University.*—Q branches have been previously reported in the sub-bands of four different bands of the violet absorption spectrum of ClO_2. Some P and R branches have now been identified in three of the bands. The $\Delta_1 F''$ values are the same for each band as would be expected since these bands have a common lower vibration state. It is found that within a given band all the $\Delta_1 F$'s are the same for one sub-band as for another. The values of B' and B'' calculated from the $\Delta_1 F$'s on the basis of the numbering of the lines are found to be constant throughout a given sub-band. The value of $B'-B''$ from the $\Delta_1 F$'s agree with the same constants found from second differences in the Q branches except for a small difference which remains constant for all bands. On the basis of $B''=0.306$ cm^{-1} from $\Delta_1 F''$'s, $B'-B''$, and $C'-C''$ previously reported, and the Cl—O distance for the lower state of 1.53A from electron diffraction, the angles for the lower and upper states are found to be 107° and 85°, respectively. But asymmetric top calculations show these small angles to be inconsistent with the observed spectrum. If the electron diffraction result is discarded and the value of 122° for the angle of the lower state is taken from vibration analysis, the Cl—O distance for the lower state turns out to be 1.44A and the angle of the upper state about 116°. Or, using 1.53 and not 0.306 one gets a possible model.

22. A Vibrational Analysis of the Near Ultraviolet System of CS_2. LEONARD N. LIEBERMANN, *University of Kansas.*—Nine progressions in the long wave-length part (3400–3800A) of the λ3100 system of CS_2 have been found with vibrational interval 270 cm^{-1}. The interval 270 cm^{-1} has been previously identified with the deformation frequency, ν_2', in the excited state.[1] The identification of combination bands of the type $V_1'+V_2'$ shows that the symmetrical valence frequency, ν_1' is about 620 cm^{-1}. The intensity distribution of these bands is that which is to be expected from the Franck-Condon principle if the molecule becomes bent in the excited state. Several progressions of the type $V_1'V_2'O\leftarrow 030$, are pseudo $\Pi\rightarrow\Pi$ transitions, having angular momentum about the symmetry axis with $K=1$. This energy of rotation is found to produce a shift of 25 cm^{-1} in the excited states of these bands. Using this value in a formula relating the rotational energy and the apex angle, it is found that the molecule is bent to 160° in the excited state. The absence of strong bands in this region involving the anti-symmetrical frequency is in agreement with the vibrational analysis. Substitution of the values $\nu_1'=620$ cm^{-1}, $\nu_2'=270$ cm^{-1}, and $2\alpha=160°$ in a formula based on a valence force model indicates that $\nu_3'=1380$ cm^{-1}.

[1] L. N. Liebermann, Phys. Rev. **60**, 496 (1941).

23. Hyperfine Structure in the Band Spectrum of HgH. S. MROZOWSKI, *University of Chicago.*—The structure of the lines in the mercury hydride spectrum was investigated in the regions λ4300–3800 and λ3200–2600 by means of a Fabry-Perot etalon and a large Hilger prism spectrograph. Former investigations have shown that the complex structure of these lines is caused by the existence of several isotopes of mercury and can be very well explained by the presence of a normal isotope effect and a nuclear isotope shift. The existence of a hyperfine structure splitting for the isotopic molecules $Hg^{199}H$ and $Hg^{201}H$ was considered at that time very plausible but could not be proved.* The present experiments carried out with a higher resolving power (roughly one million) gave for the first time a clear proof of the presence of a hyperfine structure in a band spectrum. Differences in the structure (number of components) and in the intensity distribution between lines belonging to the Q branches on the one hand, and lines belonging to the P and R branches on the other hand were detected and studied quantitatively. The results can be explained only by the assumption of a splitting of lines belonging to each of the odd isotopes of mercury into at least two hyperfine structure components; the value of the splitting being different for the two types of lines (*a*) Q, (*b*) P and R.

* Cf. S. Mrozowski, Phys. Rev. **58**, 332 (1940) and the references to the older work there.

24. Quantum Yield of Diacetyl Fluorescence. G. M. ALMY AND P. R. GILLETTE, *University of Illinois.*—The quantum yield of fluorescence of diacetyl, excited by radiation of λ4047 and λ4358, has been measured and found to be 0.145±0.03. It is approximately independent of pressure. On the other hand, the yield with excitation of λ3650, as first observed by Henriques and Noyes,[1] increases apparently from zero at zero pressure to nearly the value obtained for the longer wave-length excitations at a pressure of 5 cm Hg. This marked difference in pressure effect for different energies of excitation is explained by assuming that predissociation occurs at a level between those reached upon λ3650 and λ4047 excitations. By removing vibrational energy collisions can save for fluorescence a molecule excited by λ3650, but do not play this role in the case of molecules with excitation energy below the predissociation limit. The observed properties of diacetyl fluorescence can be explained in terms of a model involving a metastable state just below the state reached on absorption. Such a state, electronically metastable, has been predicted by McMurry[2] who estimates, however, that the probabilities of transition from both states are largely due to electronic-vibrational coupling.

[1] Henriques and Noyes, J. Am. Chem. Soc. **62**, 1038 (1940).
[2] McMurry, J. Chem. Phys. **9**, 241 (1941).

25. Raman Spectra of Some Diacetylenes. ARNOLD G. MEISTER, FORREST F. CLEVELAND, AND M. J. MURRAY, *Illinois Institute of Technology.*—Raman frequencies, intensities and depolarization factors have been obtained for 2,4-hexadiyne, 3,5-octadiyne, 4,6-decadiyne, 5,7-dodecadiyne, and 6,8-tetradecadiyne. Relative intensities and depolarization factors were obtained by use of a Gaertner microdensitometer. Comparison of the results for 2,4-hexadiyne ($CH_3-C\equiv C-C\equiv C-CH_3$) with Crawford's analysis of the Raman and infra-red spectra of 2-butyne ($CH_3-C\equiv C-CH_3$) indicates that the lines observed at 1020, 1381, 2847, 2915, and 2955 cm^{-1} originate from vibrations of the CH_3 group. Lines observed near 485 and 2260 cm^{-1} for 2,4-hexadiyne appear also in the spectra of the other four compounds and probably originate from vibrations of the $R-C\equiv C-C\equiv C-R$ group. There was also some indication of a very weak line near 993 in all of the compounds and lines were observed near 1255 and 956 for all except 5,7-dodecadiyne and 4,6-decadiyne, respectively. Frequencies near 530, 1225, 1295, 1328, and 1450 cm^{-1} were observed for all except 2,4-hexadiyne. In the triple bond region, three lines were observed at 2224(26), 2263(1000), and 2308(3) for 2,4-hexadiyne, but only a single strong line near 2256 for the other four compounds. A line was observed near 2960 for all the compounds except 3,5-octadiyne for which it was observed at 2982 cm^{-1}.

26. Raman Spectra of Some Ethane-Like Molecules. DWIGHT T. HAMILTON, FORREST F. CLEVELAND, AND M. J. MURRAY, *Illinois Institute of Technology.*—In continuing a study of ethane-like molecules, the Raman spectra of several solutions of C_2Cl_6 and C_2Br_6 have been obtained. Displacements in cm^{-1}, relative intensities and depolarization factors for C_2Cl_6 are: 162(v.w.)P, 223(450)0.80, 340(372)0.86, 431(1000)0.15, 859(219)0.81, 975(33)0.35; for C_2Br_6: 139(530)0.47, 204(780)0.83, 255(1000)0.13, 768(462)0.70. Relative intensities and depolarization factors were obtained by use of a Gaertner microdensitometer. The fundamental frequencies of C_2Cl_6 were calculated using Stitt's[1] modified valence force type potential function for ethane, with the force constants $K_C=4.00$, $K_{Cl}=2.00$, $K_\alpha=0.75$, $K_\beta=0.35$, $K_{\alpha\beta}=-0.65$, $K_{C\gamma}=-1.36$ in units of 10^5 dynes/cm. With this set of force constants Stitt's equations give the $\Delta\nu$ values 869, 341, 209 for E_g; 973, 310, 282 for A_{1g}; 869, 321, 100 for E_u; 1001, 310 for A_{2u}. Were additional data at hand, Stitt's nine-constant potential function could probably be used to give better agreement between calculated and observed A_{1g} frequencies, and perhaps better establish the above calculated frequencies which overlap at ~315 and 869. Also, if further investigation should reveal that certain of the observed frequencies are overlapping or perturbed fundamentals, an adjustment of the above force constants would be necessary, which might also lead to better agreement between calculated and observed frequencies.

[1] Fred Stitt, J. Chem. Phys. **7**, 297 (1939).

27. Raman Spectra of Some Octenes and Octynes. FORREST F. CLEVELAND, *Illinois Institute of Technology.*—Raman frequencies, relative intensities and depolarization factors have been obtained for 1-octene, *cis*+*trans* 2-octene, 3-octene, 4-octene, 4-octyne, and 1-octyne. Some of the spectrograms were made with a Hilger E-518 spectrograph. Sharp lines could be measured to the nearest cm^{-1} while the over-all accuracy was approximately 3 cm^{-1}. The speed of the Hilger spectrograph was such that, with a slit width of 0.08 mm and with Agfa Superplenachrome Press film, a spectrogram of CCl_4 upon which it was possible to measure frequencies for 5 Stokes and 3 anti-Stokes lines could be obtained in 1 min. In the earlier work, trouble was experienced with motion of the film during the long exposures, with consequent broadening or doubling of the lines. A change to Eastman 103-J spectroscopic plates eliminated this difficulty. The relative intensities and depolarization factors were obtained by use of a Gaertner microdensitometer. The density of the line D_L and the density of the background D_B were obtained and the corresponding intensities I_L and I_B were read from a previously prepared density-intensity table. The true intensity of the line was taken as (I_L-I_B). Comparison of the relative intensities for 4-octyne with the estimated intensities previously obtained in this laboratory indicated that the so-called "estimated intensities" are really estimates of the densities rather than of the intensities of the lines.

28. The Measurement of Photographic Densities by the Scatter of X-Rays. J. C. M. BRENTANO, *Northwestern University.*—The photographic measurement of the total radiation received on an area with uneven density distribution by ordinary absorption densitometry requires a point to point evaluation based on a blackening curve. When use is made of a linear relation the measurement is

simplified. This is done in a scatter method in which the photographic effect is measured by the scattering of light from the silver grains. The amount scattered is proportionate to their number and when the reciprocity law is satisfied (with x-rays), the grain number—within a certain density range—is with good approximation proportionate to the radiation received. An area of uneven density as represented by a spot of an x-ray diffraction pattern can then be evaluated as a whole. By making use of the scattering of x-rays in preference to that of visible light, certain limitations can be avoided and higher densities can be evaluated.

29. Production, Concentration, and Decomposition of Ozone by Ultraviolet Light. ARTHUR W. EWELL, *Worcester Polytechnic Institute.**—With the increasing use of bactericidal ultraviolet lamps it has become very desirable to have more information about the accompanying production of ozone—the only feasible agent for protecting surfaces not exposed to direct or scattered radiation. A low pressure mercury arc lamp of the type of the 30-inch Westinghouse Sterilamp gives an amount of ozone of the order of 1/100th gram per hour. A gentle air motion increases the yield. All the ozone is produced within a few feet of the lamp. The rate of decomposition of the ozone after the lamps are turned off is faster the greater the surfaces compared with the volume, the higher the temperature, the higher the humidity, and the more 2537 radiation present. The most important factor, the equilibrium ozone concentration, in an enclosure of several cubic meters is proportional to the ozone produced, inversely proportional to the volume, reduced to about one-third when the relative humidity changes from a few percent to near saturation and to about one-half when the temperature is raised from 7° to 32°C. In the case of the Westinghouse Sterilamp, it is approximately 30 percent less if the accompanying 2537 radiation is doubled.

* Consultant, Westinghouse Electric & Manufacturing Company.

30. An Indirect Detection of Absorption Bands in Strongly Light Scattering Dispersed Systems. WILFRIED HELLER AND ETIENNE VASSY, *University of Minnesota.*—Strong light absorption due to scattering may "wash out" or completely hide bands of consumptive ("true") absorption. Such bands may then be detected and defined by an indirect method. The relation $-\log k = c + n \log \lambda$ (k: absorption coefficient; c: a constant) governs the absorption curve if nothing but the wave-length is varied. In absence of consumptive absorption, $n = 4$ in the region of Rayleigh scattering. As higher electric partial waves enter, n decreases. In no instance can n assume values >4. However, in presence of consumptive absorption, n may become >4 and it will vary strongly with λ. The differential analysis of the slope of curves drawn according to the above relation may therefore often permit to detect and to delimitate hidden or barely visible bands of consumptive absorption. The method has been applied for detecting in iron oxide sols the existence of strong consumptive absorption below 5500A. The absorption spectra gave no direct indication of it since they were completely dominated by conservative absorption.

AUTHOR INDEX TO ABSTRACTS OF PAPERS PRESENTED AT THE CHICAGO MEETING

Adams, G. D. and R. K. Clark—No. 7
Almy, G. M. and P. R. Gillette—No. 24
Anthony, R. L. and S. L. Dart—No. 15

Baldwin, G. C. and H. W. Koch—No. 3
Brentano, J. C. M.—No. 28

Clark, R. K.—see Adams, G. D.
Cleveland, Forrest, F.—No. 27
——— see Hamilton, Dwight T.
——— see Meister, Arnold G.
Coon, Jesse B.—No. 21
Copeland, Paul L.—No. 11
—— see Kennedy, William R.

Dart, S. L.—see Anthony, R. L.
Davey, Wheeler P.—see Wehner, R. S.

Ewell, Arthur W.—No. 29

Gamertsfelder, G. R.—No. 5
Gillette, P. R.—see Almy, G. M.
Guth, Eugene—see Peterson, L. E.

Hamilton, Dwight T., Forrest F. Cleveland, and M. J. Murray—No. 26
Heller, Wilfried—No. 18
—— **and Etienne Vassy**—No. 30

Iona, Mario, Jr.—see Schein, Marcel
—— **and Marcel Schein**—No. 9

Kanne, W. R.—see Wilkening, M. H.
Kennedy, William R. and Paul L. Copeland—No. 12
Koch, H. W.—see Baldwin, G. C.
Kurbatov, J. D.—see Weimer, Katherine E.
—— see Zumstein, R. V.

Liebermann, Leonard N.—No. 22

Meister, Arnold G., Forrest F. Cleveland, and M. J. Murray—No. 25
Mrozowski, S.—No. 23
Muehlhause, C. O.—No. 6
Murray, M. J.—see Hamilton, Dwight T.
—— see Meister, Arnold G.

Nereson, Norris—see Rossi, Bruno

Parker, H. M.—No. 20
Peterson, L. E. and Eugene Guth—No. 16
Pool, M. L.—see Weimer, Katherine E.
—— see Zumstein, R. V.

Rossi, Bruno and Norris Nereson—No. 10

Schein, Marcel—see Iona, Mario, Jr.
—— **and Mario Iona, Jr.**—No. 8
Smoluchowski, R.—No. 13

Vassy, Etienne—see Heller, Wilfried

Waldman, Bernard and Marcellus L. Wiedenbeck—No. 4
Wehner, R. S. and Wheeler P. Davey—No. 14
Weimer, Katherine E., M. L. Pool, and J. D. Kurbatov—No. 2
Wiedenbeck, Marcellus L.—see Waldman, Bernard
Wilkening, M. H. and W. R. Kanne—No. 19

Zachariasen, W. H.—No. 17
Zumstein, R. V., J. D. Kurbatov, and M. L. Pool—No. 1